

AD-752 582

REPORT ON ELECTRONIC AND IONIC REACTIONS  
IN ATMOSPHERIC GASES

R. H. Neynaber, et al

Gulf Radiation Technology

Prepared for:

Defense Nuclear Agency

July 1972

DISTRIBUTED BY:

**NTIS**

National Technical Information Service  
U. S. DEPARTMENT OF COMMERCE  
5285 Port Royal Road, Springfield Va. 22151

AD 752582



DNA 2944F

## GULF RADIATION TECHNOLOGY

Gulf-RT-A12209

### REPORT ON ELECTRONIC AND IONIC REACTIONS IN ATMOSPHERIC GASES

---

R. H. Meynaber, J. A. Rutherford,  
and D. A. Vroom

Prepared under  
Contract DNA001-72-C-0254  
for the  
Defense Nuclear Agency



Approved for public release; distribution unlimited.

NATIONAL TECHNICAL  
INFORMATION SERVICE

July 1972

GULF RADIATION TECHNOLOGY  
A DIVISION OF GULF ENERGY & ENVIRONMENTAL SYSTEMS COMPANY  
P.O. BOX 608, SAN DIEGO, CALIFORNIA 92112

118

UNCLASSIFIED

Security Classification

## DOCUMENT CONTROL DATA - R &amp; D

(Security classification of title, body of abstract and indexing annotation must be entered when the overall report is classified)

## 1. ORIGINATING ACTIVITY (Corporate author)

Gulf Energy & Environmental Systems Company  
P. O. Box 81608  
San Diego, California 92138

## 2a. REPORT SECURITY CLASSIFICATION

Unclassified

## 2b. GROUP

## 3. REPORT TITLE

REPORT ON ELECTRONIC AND IONIC REACTIONS IN ATMOSPHERIC GASES

## 4. DESCRIPTIVE NOTES (Type of report and inclusive dates)

Final Report

## 5. AUTHOR(S) (First name, middle initial, last name)

R. H. Neynaber, J. A. Rutherford, and D. A. Vroom

## 6. REPORT DATE

July 1972

## 7a. TOTAL NO. OF PAGES

150

## 7b. NO. OF REFS

19

## 8a. CONTRACT OR GRANT NO.

DNA001-72-C-0254

## b. PROJECT NO.

NWED: XA.H

## c. Task &amp; Subtask: D010

## d. Work Unit: 34

## 9a. ORIGINATOR'S REPORT NUMBER(S)

Gulf-RT-A12209

## 9b. OTHER REPORT NO(S) (Any other numbers that may be assigned this report)

DNA 2944F

## 10. DISTRIBUTION STATEMENT

Approved for public release; distribution unlimited.

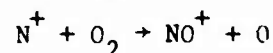
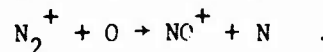
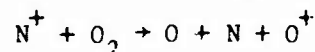
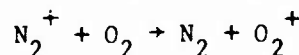
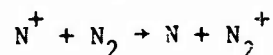
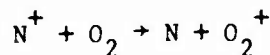
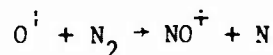
## 11. SUPPLEMENTARY NOTES

## 12. SPONSORING MILITARY ACTIVITY

Director  
Defense Nuclear Agency  
Washington, D. C. 20305

## 13. ABSTRACT

The effect of addition of internal energy to the ion or neutral reactant in an ion-neutral process has been investigated. Changes in the cross section for certain processes are reported and a change in the state of excitation of the final product can in some cases be postulated. The following reactions have been considered:



Where the cross section was found to increase with addition of internal energy to either the ion or the neutral, an approach to near resonance was, in some cases, found to have occurred. In such cases one or the other of the product particles may be produced in an excited state. When the internal energy change is small compared to the energy defect for the reaction, little or no change in the cross section is observed.

Ia

DD FORM 1473

UNCLASSIFIED

Security Classification

**Security Classification**

### KEY WORDS

LINK B

LINK C

WT

80

100

DO

—

### Crossed Beams

Ib

**Security Classification**



DNA 2944F

## **GULF RADIATION TECHNOLOGY**

Gulf-RT-A12209

### **REPORT ON ELECTRONIC AND IONIC REACTIONS IN ATMOSPHERIC GASES**

---

This work was supported by the Defense Nuclear Agency  
under NWED; Subtask HD010-34

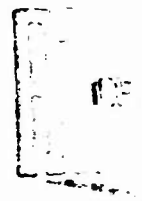
**Work done by:**

A. E. Kristensen  
J. K. Layton  
R. H. Neynaber  
J. A. Rutherford  
D. A. Vroom

**Report written by:**

R. H. Neynaber  
J. A. Rutherford  
D. A. Vroom

Prepared under  
Contract DNA001-72-C-0254  
for the  
Defense Nuclear Agency



Approved for public release; distribution unlimited.

Gulf Radiation Technology  
Project 0454

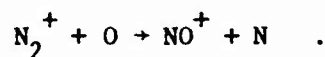
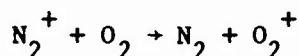
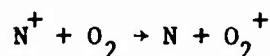
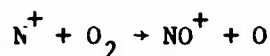
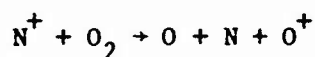
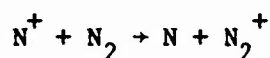
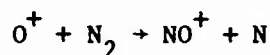
July 1972

**GULF RADIATION TECHNOLOGY  
A DIVISION OF GULF ENERGY & ENVIRONMENTAL SYSTEMS COMPANY  
P O BOX 608, SAN DIEGO, CALIFORNIA 92112**

11

# ABSTRACT

The effect of addition of internal energy to the ion or neutral reactant in an ion-neutral process has been investigated. Changes in the cross section for certain processes are reported and a change in the state of excitation of the final product can in some cases be postulated. The following reactions have been considered:



Where the cross section was found to increase with addition of internal energy to either the ion or the neutral, an approach to near resonance was, in some cases, found to have occurred. In such cases one or the other of the product particles may be produced in an excited state. When the internal energy change is small compared to the energy defect for the reaction, little or no change in the cross section is observed.

## CONTENTS

|     |                                                                                                         |     |
|-----|---------------------------------------------------------------------------------------------------------|-----|
| 1.  | INTRODUCTION . . . . .                                                                                  | 1   |
| 2.  | EXPERIMENTAL METHODS . . . . .                                                                          | 5   |
| 2.1 | Primary and Secondary Ion Systems . . . . .                                                             | 5   |
| 2.2 | Neutral Beam Formation and Measurement . . . . .                                                        | 8   |
| 2.3 | Extrapolation Procedure . . . . .                                                                       | 11  |
| 3.  | RESULTS AND DISCUSSION . . . . .                                                                        | 15  |
| 3.1 | Reaction of $O^+$ with $N_2$ to Form $NO^+$ . . . . .                                                   | 15  |
| 3.2 | Charge-Transfer Reaction of $N^+$ with $N_2$ . . . . .                                                  | 16  |
| 3.3 | Reactions of $N^+$ with $O_2$ . . . . .                                                                 | 22  |
| 3.4 | Charge Transfer from $N_2^+$ to $O_2$ . . . . .                                                         | 29  |
| 3.5 | Charge Transfer Between $H^+$ and $O$ . . . . .                                                         | 36  |
| 3.6 | Reaction of $N_2^+$ with $O$ to give $NO^+$ . . . . .                                                   | 37  |
|     | REFERENCES . . . . .                                                                                    | 43  |
|     | APPENDIX A - FORMATION OF MAGNESIUM IONS BY CHARGE TRANSFER . . . . .                                   | 45  |
|     | APPENDIX B - EFFECT OF METASTABLE $O^+(^9D)$ ON REACTIONS OF $O^+$<br>WITH NITROGEN MOLECULES . . . . . | 57  |
|     | APPENDIX C - FORMATION OF SODIUM IONS BY CHARGE TRANSFER . . . . .                                      | 63  |
|     | APPENDIX D - FORMATION OF CALCIUM IONS BY CHARGE TRANSFER . . . . .                                     | 71  |
|     | APPENDIX E - FORMATION OF IRON IONS BY CHARGE TRANSFER . . . . .                                        | 89  |
|     | APPENDIX F - NEGATIVE ION REACTIONS WITH NEUTRAL OZONE . . . . .                                        | 103 |

Preceding page blank

## ILLUSTRATIONS

### Figure

|    |                                                                                                                                                                                                                           |    |
|----|---------------------------------------------------------------------------------------------------------------------------------------------------------------------------------------------------------------------------|----|
| 1  | Crossed ion and neutral beam apparatus . . . . .                                                                                                                                                                          | 6  |
| 2  | Reaction cross section for $O^+ + N_2 \rightarrow NO^+ + N$ as a function of the energy in the center of mass system . . . . .                                                                                            | 17 |
| 3  | Charge-transfer cross sections for $N^+$ ions incident on neutral nitrogen molecules as a function of the energy of the incident ion . . . . .                                                                            | 20 |
| 4  | Charge-transfer cross sections for $N^+$ ions incident on neutral nitrogen molecules without vibrational excitation and on neutral argon atoms as a function of the energy in the center of mass of each system . . . . . | 21 |
| 5  | Reaction cross section for $N^+$ ions incident on $O_2$ to form $O^+$ as a function of the energy in the center of mass and of the incoming ion energy . . . . .                                                          | 24 |
| 6  | Reaction cross sections for $N^+$ ions incident on $O_2$ to form $O_2^+$ and $NO^+$ as a function of the energy in the center of mass and of the incoming ion energy . . . . .                                            | 26 |
| 7  | Charge-transfer cross sections for $N_2^+$ ions incident on neutral oxygen molecules as a function of the energy of the incident ion . . . . .                                                                            | 30 |
| 8  | Dependence of the charge-transfer cross section for $N_2^+ + O_2 \rightarrow N_2 + O_2^+$ upon the ion-source electron energy . . . . .                                                                                   | 32 |
| 9  | Charge-transfer cross sections for $N_2^+$ ions incident on neutral oxygen molecules as a function of the energy of the incident ion . . . . .                                                                            | 33 |
| 10 | Square root of the cross section for the reactions $H^+ + O \rightarrow H + O^+$ and $H^+ + O_2 \rightarrow H + O + O^+$ . . . . .                                                                                        | 38 |
| 11 | Reaction cross section for $N_2^+$ ions incident on neutral O to form $NO^+$ as a function of the energy of the incident ion . . . . .                                                                                    | 41 |



# LIST OF TABLES

## Table

|   |                                                                                                                                         |    |
|---|-----------------------------------------------------------------------------------------------------------------------------------------|----|
| 1 | Calculation of the Population of the Vibrational Levels of Nitrogen as a Function of Temperature . . . . .                              | 9  |
| 2 | Calculation of the Population of the Vibrational Levels of Oxygen as a Function of Temperature . . . . .                                | 10 |
| 3 | Measured Cross Sections for the Reaction $N^+ + N_2 \rightarrow N + N_2^+$ .                                                            | 18 |
| 4 | Measured Cross Sections for the Reaction $N^+ + O_2 \rightarrow O^+ +$<br>Products . . . . .                                            | 25 |
| 5 | Measured Cross Sections for the Reaction $N^+ + O_2 \rightarrow NO^+ + O$ .                                                             | 27 |
| 6 | Measured Cross Sections for the Reaction $N^+ + O_2 \rightarrow N + O_2^+$ .                                                            | 28 |
| 7 | Measured Cross Sections for the Reaction $N_2^+ + O_2 \rightarrow N_2 + O_2^+$<br>when the $O_2$ is not Vibrationally Excited . . . . . | 34 |
| 8 | Measured Cross Sections for the Reaction $N_2^+ + O_2 \rightarrow N_2 + O_2^+$<br>when the $O_2$ is Vibrationally Excited . . . . .     | 35 |
| 9 | Measured Cross Sections for the Reaction $H^+ + O \rightarrow H + O^+$ . .                                                              | 39 |

## 1. INTRODUCTION

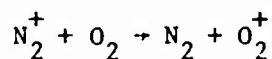
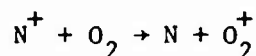
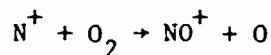
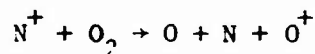
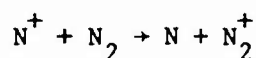
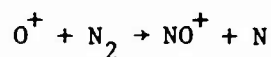
The transmission of radio and radar signals through the atmosphere depends, in large measure, on the free electron density in the ionosphere. The density of these free electrons is a function of both the amount of ionization that is occurring and the magnitude of the rate coefficients for the various mechanisms available for electron loss. In the normal atmosphere, ionization is produced primarily by photoionization processes initiated by solar radiation. During periods of increased solar activity, the amount of ionization and, hence, the free electron density are increased, resulting in degradation of radio and radar equipment performance.

Artificial disturbances of the ionosphere, such as those resulting from nuclear weapons detonation, greatly increase the free electron density. The resultant degradation in radio and radar signals can seriously affect the operation of military communications systems. Since the Nuclear Test Ban Treaty has eliminated atmospheric testing of nuclear weapons, the degree to which artificial disturbances of this nature will influence electromagnetic transmission cannot be ascertained. Therefore, considerable effort has been expended on laboratory and theoretical studies of atmospheric ionization that would be expected from detonating weapons and on the deionization processes that return the atmosphere to normal.

Part of the overall interest in the upper atmospheric process is reflected in the Defense Nuclear Agency (DNA) Reaction Rate Program. This program, which supports research in the study of atmospheric deionization, involves in situ measurements of natural disturbances in the atmosphere (e.g., polar cap absorption events), theoretical studies and laboratory measurements of pertinent reaction rates, cross sections, and other features of the interactions that can occur among electrons, ions, and neutral species in the upper atmosphere. Current progress in the field is reported in the DNA Reaction Rate Handbook.<sup>(1)</sup>

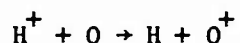
The program under way in the Gulf Radiation Technology (Rad Tech) laboratory (under Contract DNA001-72-C-0254) examines one phase of the deionization problem: reactions of atmospheric ions with neutral species. The primary objective of this phase of the ion-neutral reaction program is the study of charge-transfer and ion-molecule processes. Since the most probable cause of the loss of electrons in the upper atmosphere is dissociative recombination, it is important to know (1) the molecular ions that are present, (2) their cross sections for formation, (3) the effects of internal energy of the reactants on their rate of formation, and (4) the fate of any excess energy that results from their formation. The present program places special emphasis on studies of problems posed by items 3 and 4 above. In the past, these aspects of atmospheric deionization have received very little attention in the energy regime above thermal.

The major goal of the current program was to devise a means for introducing internal energy into the neutral and ionic primary particles and to investigate the effect of this internal energy on the overall reaction probability for formation of certain ionic species and the state of excitation of the final products. Processes that were studied in this manner include:

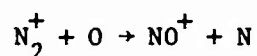


A further program conducted during the past year was the development of a source of oxygen atoms for use in our crossed ion-modulated beam

apparatus. In this study, we used both rf excitation of oxygen containing molecules and thermal dissociation of molecular oxygen to form the O atoms. The degree of dissociation attained in these beams was determined by measuring signals from the following reaction, for which the cross section is known:



Using the O atom beam, the reaction



was studied.

The final task completed during the past year was the co-authorship of a revision of a chapter in the DNA Reaction Rate Handbook entitled "Laboratory Methods of Obtaining Reaction Rate Data."

The following sections of this report describe the apparatus used for the experimental measurements, the results of the measurements, and a discussion of the results. Reprints of papers published during the past year and preprints of papers written for future publication are included as appendices.

## 2. EXPERIMENTAL METHODS

The cross-ion-modulated neutral beam apparatus has been described in the literature.<sup>(2-4)</sup> Thus, only an abbreviated description is given herein. Also included is a brief description of the extrapolation procedure,<sup>(5)</sup> developed in our laboratory, for extending the measured cross-section curves to thermal energies.

### 2.1 PRIMARY AND SECONDARY ION SYSTEMS

Figure 1 shows a schematic of the experimental apparatus. The primary ions are extracted from an electron-bombardment source and mass-analyzed at an energy of 75 eV in a  $180^\circ$  magnetic-mass spectrometer. After analysis, the ions pass through an aperture in an iron plate that shields the magnetic field of the mass analyzer from the succeeding regions of the apparatus. The ions are then retarded or accelerated to the desired collision energy, and pass through a field-free region before intersecting the neutral beam. Collimating apertures ensure that, from purely geometrical considerations, all primary ions pass through the modulated neutral beam. The beam is modulated at 100 Hz by mechanical chopping.

Secondary ions resulting from collisions between the primary ions and neutral species are extracted along the direction of the primary ion beam by an electric field of approximately 2 V/cm. The ions then enter an electric field in which their energy is increased to 1650 eV. Penetration of this accelerating field into the interaction region is reduced by the use of a double-grid structure.

After acceleration, the ions pass through an electrostatic quadrupole lens<sup>(6)</sup> that forms the entrance slit for a  $60^\circ$ -sector magnetic-mass spectrometer. The mass-selected ions impinge on the first dynode of a 14-stage CuBe electron multiplier. For all ions formed by charge transfer or ion-molecule reactions, the most abundant isotope is used when making measurements.

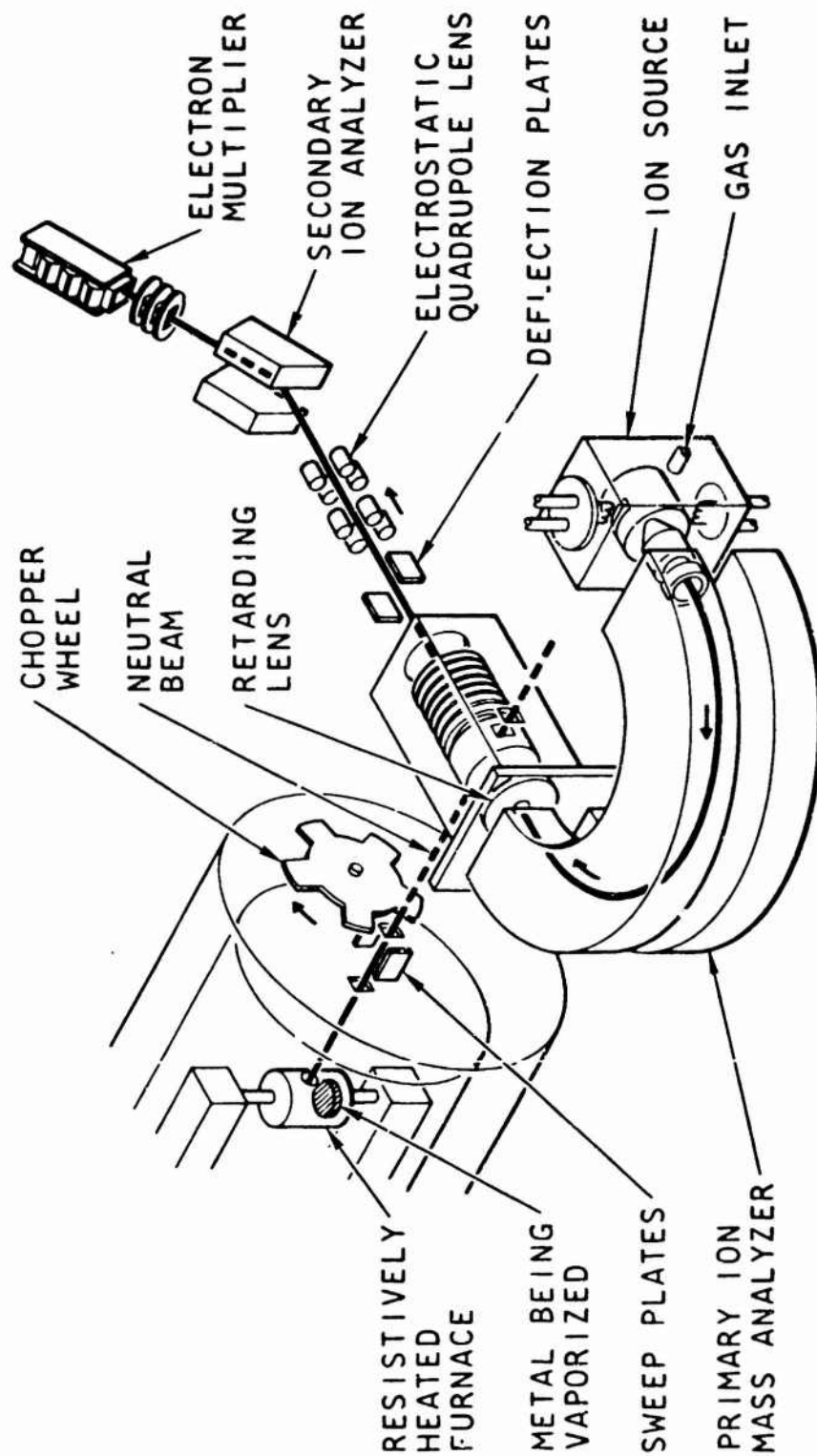


Figure 1. Crossed ion and neutral beam apparatus

The cross sections are corrected for the isotope effect created by collecting only those having this mass. The output from the multiplier passes successively through a preamplifier, a 100-Hz narrow-band amplifier, and a phase-sensitive detector, and is then integrated. The output is presented on a chart recorder.

The primary ion beam intensity is measured at the interaction region with a Faraday cup, which can be moved into the collision region when desired. The primary ion energy is determined from retarding potential measurements. All surfaces at the interaction region and the Faraday cup are coated with alkadag, and the interaction region is normally maintained at 120°C to minimize surface-charging.

Because, in the present work, interest extended to small-collision energies, only weak extraction fields at the collision region were used. As a result, the secondary ions were not collected with 100% efficiency. Obtaining absolute cross sections for production of various secondary ions required, therefore, determination of their overall detection efficiency. This latter consideration was governed by a number of factors, including the multiplier gain and the efficiency of transmission of the secondary ions from the interaction region to the multiplier.

The multiplier-amplifier-recorder gain is measured by modulating the primary ions prior to their entry into the collision region. The ion current signal is first measured with the movable Faraday cup and, after traversing the secondary mass spectrometer multiplier-amplifier system, by the recorder. Primary ion transmission through the second mass spectrometer is 92%. Typical gains for the entire system are of the order of  $10^{15}$  output volts on the recorder per ampere of incoming current. In practice, gains are measured for each product ion.

The major experimental uncertainty is associated with the collection efficiency for the secondary ions. Collection fields large enough to ensure total collection of the secondary ions cannot be used because of the influence these fields exert on the motion of low-energy primary ions. While measurements of the variation of collection efficiency with the strength of the extraction field can readily be made at high primary ion energies, the

results are not necessarily relevant to the low-energy regime, where the dynamics of the ion-neutral process may be different. Interpretations of the present data obtained using weak collection fields is based on the assumption that, for primary ion energies above a few eV, the secondary ions are collected with nearly equal efficiency, and that, as a result, the collection efficiency is independent of both the nature and the energy of the primary ions. This assumption implies that the energy defect in the reaction is not large, since energy not expended in excitation of the products must appear as kinetic energy and, therefore, would influence the collection efficiency.

## 2.2 NEUTRAL BEAM FORMATION AND MEASUREMENT

### 2.2.1 Beams of Stable Gases

Beams of ground state  $N_2$  and  $O_2$  are formed by effusion from a small hole in a room-temperature tungsten or iridium tube containing the gas (Figure 1). Beam density is determined using the cosine law of molecular effusion<sup>(7)</sup> where the pressure in the tungsten source, the area of the aperture in the tube, and distance from the aperture to the interaction region are known factors.

The vibrational energy in the neutral beam can be changed by resistive heating of the tungsten source. Temperatures as high as  $2800^{\circ}K$  have been used for this vibrational excitation, with the temperature being monitored by an optical pyrometer. Tables 1 and 2 summarize the results of calculations of the vibrational population of the ground electronic states of  $N_2$  and  $O_2$ , respectively, as a function of the temperature of the gas. The beam density of the neutral flux due to temperature changes are corrected when effects of vibrational excitation of the neutral species are being studied.

More extensive excitation of  $N_2$  and  $O_2$  molecules used rf techniques. In these studies, the furnace source was replaced by a glass U-shaped discharge tube with a small hole in the bottom of the U-bend. Electrodes attached to the outside of each leg of the U served to introduce the rf power into the gas.



TABLE 1  
CALCULATION OF VIBRATIONAL DISTRIBUTIONS  
FOR NITROGEN

| TEMPERATURE | V=0   | V=1   | V=2   | V=3   | V=4   | V=5   |
|-------------|-------|-------|-------|-------|-------|-------|
| 300.        | 1.000 | .0000 | .0000 | .0000 | .0000 | .0000 |
| 400.        | 1.000 | .0002 | .0000 | .0000 | .0000 | .0000 |
| 500.        | .999  | .0012 | .0000 | .0000 | .0000 | .0000 |
| 600.        | .996  | .0036 | .0000 | .0000 | .0000 | .0000 |
| 700.        | .992  | .0080 | .0001 | .0000 | .0000 | .0000 |
| 800.        | .985  | .0145 | .0002 | .0000 | .0000 | .0000 |
| 900.        | .976  | .0230 | .0006 | .0000 | .0000 | .0000 |
| 1000.       | .966  | .0331 | .0012 | .0000 | .0000 | .0000 |
| 1100.       | .953  | .0444 | .0021 | .0001 | .0000 | .0000 |
| 1200.       | .940  | .0565 | .0035 | .0002 | .0000 | .0000 |
| 1300.       | .925  | .0691 | .0053 | .0004 | .0000 | .0000 |
| 1400.       | .910  | .0818 | .0076 | .0007 | .0001 | .0000 |
| 1500.       | .894  | .0943 | .0102 | .0011 | .0001 | .0000 |
| 1600.       | .878  | .1066 | .0133 | .0017 | .0002 | .0000 |
| 1700.       | .862  | .1185 | .0167 | .0024 | .0004 | .0001 |
| 1800.       | .846  | .1298 | .0204 | .0033 | .0005 | .0001 |
| 1900.       | .830  | .1406 | .0243 | .0043 | .0008 | .0001 |
| 2000.       | .814  | .1507 | .0285 | .0055 | .0011 | .0002 |
| 2100.       | .799  | .1602 | .0328 | .0063 | .0015 | .0003 |
| 2200.       | .783  | .1690 | .0372 | .0083 | .0019 | .0004 |
| 2300.       | .768  | .1772 | .0416 | .0100 | .0024 | .0006 |
| 2400.       | .754  | .1848 | .0461 | .0117 | .0030 | .0009 |
| 2500.       | .739  | .1918 | .0506 | .0136 | .0037 | .0010 |
| 2600.       | .725  | .1982 | .0550 | .0155 | .0044 | .0013 |
| 2700.       | .712  | .2041 | .0594 | .0170 | .0053 | .0016 |
| 2800.       | .699  | .2095 | .0637 | .0197 | .0062 | .0020 |
| 2900.       | .686  | .2144 | .0680 | .0219 | .0071 | .0024 |
| 3000.       | .674  | .2189 | .0721 | .0241 | .0082 | .0028 |
| 3100.       | .662  | .2230 | .0761 | .0263 | .0092 | .0032 |
| 3200.       | .650  | .2267 | .0800 | .0286 | .0104 | .0039 |
| 3300.       | .639  | .2300 | .0838 | .0309 | .0116 | .0044 |
| 3400.       | .629  | .2330 | .0875 | .0332 | .0128 | .0050 |
| 3500.       | .618  | .2357 | .0910 | .0355 | .0140 | .0056 |
| 3600.       | .608  | .2382 | .0944 | .0378 | .0153 | .0063 |
| 3700.       | .598  | .2404 | .0977 | .0401 | .0167 | .0070 |
| 3800.       | .589  | .2423 | .1008 | .0424 | .0190 | .0079 |
| 3900.       | .580  | .2440 | .1038 | .0447 | .0194 | .0085 |
| 4000.       | .571  | .2455 | .1068 | .0463 | .0208 | .0093 |

TABLE 2  
CALCULATION OF VIBRATIONAL DISTRIBUTIONS  
FOR OXYGEN

| TEMPERATURE | V=0  | V=1   | V=2   | V=3   | V=4   | V=5   |
|-------------|------|-------|-------|-------|-------|-------|
| 300.        | .999 | .0005 | .0000 | .0000 | .0000 | .0000 |
| 400.        | .996 | .0035 | .0000 | .0000 | .0000 | .0000 |
| 500.        | .989 | .0109 | .0001 | .0000 | .0000 | .0000 |
| 600.        | .977 | .0227 | .0006 | .0000 | .0000 | .0000 |
| 700.        | .960 | .0383 | .0016 | .0001 | .0000 | .0000 |
| 800.        | .940 | .0560 | .0035 | .0002 | .0000 | .0000 |
| 900.        | .918 | .0749 | .0063 | .0006 | .0001 | .0000 |
| 1000.       | .895 | .0938 | .0102 | .0011 | .0001 | .0000 |
| 1100.       | .871 | .1120 | .0149 | .0020 | .0003 | .0000 |
| 1200.       | .847 | .1292 | .0203 | .0033 | .0005 | .0001 |
| 1300.       | .823 | .1451 | .0263 | .0049 | .0009 | .0002 |
| 1400.       | .799 | .1595 | .0326 | .0069 | .0015 | .0003 |
| 1500.       | .776 | .1726 | .0392 | .0091 | .0022 | .0005 |
| 1600.       | .754 | .1842 | .0459 | .0117 | .0030 | .0008 |
| 1700.       | .733 | .1945 | .0526 | .0145 | .0041 | .0012 |
| 1800.       | .713 | .2035 | .0592 | .0176 | .0053 | .0016 |
| 1900.       | .693 | .2115 | .0657 | .0203 | .0067 | .0022 |
| 2000.       | .675 | .2184 | .0719 | .0241 | .0082 | .0028 |
| 2100.       | .657 | .2243 | .0779 | .0275 | .0098 | .0036 |
| 2200.       | .640 | .2295 | .0836 | .0309 | .0116 | .0044 |
| 2300.       | .624 | .2339 | .0890 | .0344 | .0135 | .0054 |
| 2400.       | .608 | .2377 | .0942 | .0379 | .0154 | .0064 |
| 2500.       | .594 | .2409 | .0990 | .0413 | .0174 | .0075 |
| 2600.       | .580 | .2436 | .1036 | .0447 | .0195 | .0086 |
| 2700.       | .567 | .2458 | .1079 | .0480 | .0216 | .0098 |
| 2800.       | .554 | .2476 | .1120 | .0513 | .0237 | .0111 |
| 2900.       | .542 | .2491 | .1158 | .0545 | .0259 | .0125 |
| 3000.       | .531 | .2503 | .1193 | .0576 | .0281 | .0138 |
| 3100.       | .520 | .2512 | .1227 | .0606 | .0302 | .0152 |
| 3200.       | .510 | .2519 | .1258 | .0635 | .0324 | .0167 |
| 3300.       | .500 | .2524 | .1287 | .0663 | .0345 | .0182 |
| 3400.       | .491 | .2527 | .1314 | .0691 | .0366 | .0196 |
| 3500.       | .482 | .2529 | .1340 | .0717 | .0387 | .0211 |
| 3600.       | .473 | .2528 | .1364 | .0743 | .0408 | .0226 |
| 3700.       | .465 | .2527 | .1386 | .0767 | .0429 | .0242 |
| 3800.       | .457 | .2525 | .1407 | .0791 | .0449 | .0257 |
| 3900.       | .450 | .2522 | .1427 | .0814 | .0469 | .0272 |
| 4000.       | .443 | .2518 | .1445 | .0836 | .0488 | .0287 |

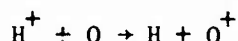
For both the thermal and rf excitation experiments, care was taken to eliminate any charged particles that might be emitted by the source. Electrostatic sweep plates were used for this purpose.

#### 2.2.2 O Atom Beam Sources

Two methods were used to form the O atom beam. The first of these was dissociation of molecules containing oxygen atoms in an rf discharge. Both  $O_2$  and  $CO_2$  were used; both cases resulted in the production of O atoms. The major problem associated with this type of source is the lack of knowledge of other species that may be present in the neutral beam. The rf excitation is not specific and can produce both atoms and molecules in metastable states with unknown concentration.

Thermal dissociation of oxygen in an iridium tube furnace was the second technique used to produce O atoms. Thermal methods of dissociation eliminate the possibility of the presence of excited  $O_2$  and O atoms in the beam, but result in low beam densities ( $\sim 10^9$  atoms/cm<sup>3</sup>) because of the low pressures required in the source for sufficient dissociation.

An ion-probing technique was used to obtain the degree of dissociation present in thermally produced beams. This technique uses the near-resonant asymmetric charge-transfer reaction



The results for this reaction, together with the degree of dissociation in the O atom beam determined using this reaction, are discussed in Section 3.5.

#### 2.3 EXTRAPOLATION PROCEDURE

The lowest ion energies that can be obtained in our apparatus are 1 eV or greater. The charge-exchange processes in the energy range from thermal to several eV is of considerable interest. An extrapolation procedure previously developed in our laboratory was used to obtain cross sections and rate coefficients in this region. This procedure combines the energy dependence of the Rapp and Francis<sup>(8)</sup> resonant charge-transfer theory with the Gioumousis and Stevenson<sup>(9)</sup> complex formation model.

The general formula developed for the total charge-exchange cross section takes into account the probability that charge exchange occurs both when a complex is formed and when it is not. The formula also corrects for nonrectilinear orbit when complex formation does not occur.

The total charge-exchange cross section,  $\sigma$ , is given by

$$\sigma = f\sigma_2 \quad \text{for } 2\sigma_1 \leq \sigma_2 \quad (1)$$

or by

$$\sigma = \left(f - \frac{1}{2}\right)\sigma_2 + \sigma_1 \quad \text{for } 2\sigma_1 > \sigma_2 \quad (2)$$

where  $f$  is the fraction of collisions resulting in complex formation that decays into the charge-exchange channel, and  $\sigma_2$  is the Gioumousis and Stevenson complex formation model cross section,<sup>(9)</sup> represented by

$$\sigma_2 = \pi \left( \frac{2e^2\alpha}{E} \right)^{1/2} \quad (3)$$

where  $e$  is the electronic charge,  $\alpha$  is the polarizability of the neutral, and  $E$  is the barycentric interaction energy. Also,  $\sigma_1$ , which is given by

$$\sigma_1 = \sigma_0 \left[ 1 + \left( \frac{\sigma_2}{4\sigma_0} \right)^2 \right] \quad (4)$$

represents the Rapp and Francis resonant charge-exchange formula modified to take into account the curved orbits of the reactants. The Rapp and Francis formula<sup>(8)</sup> has the form:

$$\sigma_0^{1/2} = A - B \log E \quad (5)$$

where  $A$  and  $B$  are constants.

The extrapolation is carried out by fitting the modified Rapp and Francis formula (Equation 4) to the high-energy portion of the measured data, which is in the region in which complex formation should be negligible.

The calculated curve is then extended to lower energies using the test given by Equations 1 and 2 to evaluate where the measured data deviate from the form of Equation 4. In this manner, the contribution of complex formation is determined, and the calculated curve can be extended to energies below those measured. A computer program has been developed to perform the calculations.

The extrapolation technique was developed by assuming that the relative abundance of the various products emerging from the capture-formed complex is independent of the relative kinetic energy of the reactants; that is,  $f$  remains constant. If this condition is not met, the technique does not yield valid rate coefficients at near-thermal energies. In general, the extrapolation technique is valid if the calculated cross-section curve fits the experimental data to the lowest energy of measurement. This comparison is made for all data given in this report.

### 3. RESULTS AND DISCUSSION

#### 3.1 REACTION OF $O^+$ WITH $N_2$ TO FORM $NO^+$

The reaction of  $O^+$  with  $N_2$  to form  $NO^+$  as a function of the excitation in the  $O^+$  primary ion was studied in a previous phase of the program. The results of this study were published recently, and a reprint is included in this report as Appendix B. Briefly, the results of this study showed that for ground-state atomic oxygen ions ( $O^+ 4S$ ), the reaction to form  $NO^+$  proceeds with a large cross section over the energy range from 1 to 15 eV. Excited ions ( $O^+ 2D$ ), on the other hand, appear to have a very low probability of forming  $NO^+$ .

Study of the reaction of  $O^+$  with  $N_2$  to form  $NO^+$  was extended during the last contract period. The reaction probability was studied as a function of the vibrational energy of the  $N_2$ . Both the thermal and rf discharge methods were employed to excite the  $N_2$ . With the thermal method, it was possible to populate the  $v = 1$  and  $v = 2$  levels of the  $N_2$  to a significant extent. Table 1 gives the calculated  $N_2$  vibrational distribution for 2700°K as being approximately 71% in  $v = 0$ , 20% in  $v = 1$ , and 6% in  $v = 2$ .

The vibrational distribution in the  $N_2$  molecules emerging from the rf source is not easily determined. Methods discussed by Schmeltkopf *et al.*,<sup>(10)</sup> coupled with our ion-probing techniques, can be used to obtain this information. In the present work, however, obtaining this vibrational distribution was not attempted. The rf discharge may also produce  $N_2$  molecules in the metastable ( $A^3\Sigma_u^+$ ) state. We used  $NO^+$  (ionization potential, 9.27 eV) to probe the beam for the presence of this species. Since the  $N_2$  metastable ( $A^3\Sigma_u^+$ ) state has an ionization potential of 9.41 eV, charge exchange with the  $NO^+$  would be expected. No indication of metastable  $N_2$  could be found.

The experimental results for the reaction



Preceding page blank

show an increase in the cross section at low interaction energies (below 5 eV) for both the rf and thermally heated  $N_2$  beam when only  $O^+(^4S)$  particles were present in the ion beam. This increase in cross section with increasing vibrational temperature has also been observed at low-impact energies by Neynaber<sup>(11)</sup> and at thermal energies by Schmeltekopf *et al.*<sup>(10)</sup> One possible explanation for the increase is that the additional energy contained in the neutral reactant assists in the formation of the activated complex necessary for the reaction to proceed.

The experimental results for the reaction of Equation 6 (which is exothermic by 1.1 eV for ground-state particles) are given in Figure 2 for the rf excitation of the  $N_2$ . Both rf-on and rf-off cases are illustrated. The vibrational excitation of the  $N_2$  increases the cross section below 5 eV in the center of mass and decreases it above this energy. As mentioned above, this increase in cross section at low energies is consistent with the experimental results of Neynaber and those of Schmeltekopf and with the theoretical calculations of O'Malley.<sup>(12)</sup>

### 3.2 CHARGE-TRANSFER REACTION OF $N^+$ WITH $N_2$

Preliminary results of a study of the charge-transfer reaction



were discussed in a prior report.<sup>(13)</sup> The charge-transfer cross-section data for ground-state  $N^+$  and  $N_2$  in the  $v = 0$  level are given in Table 3. For convenience, these data are displayed graphically in Figure 3. From the diagram, it can be seen that the cross section is small and decreases with decreasing energy in the region between 4 and 1.5 eV. This behavior is expected since the process is endothermic by approximately 1 eV. The rise in the cross section at about 4 eV probably results from the onset of a second channel for reaction.

The present data are in agreement with the recent studies of Maier and Murad,<sup>(14)</sup> although the cross section discussed herein tends to a somewhat higher absolute value. The peak value (at 8.5 eV in the center of mass)

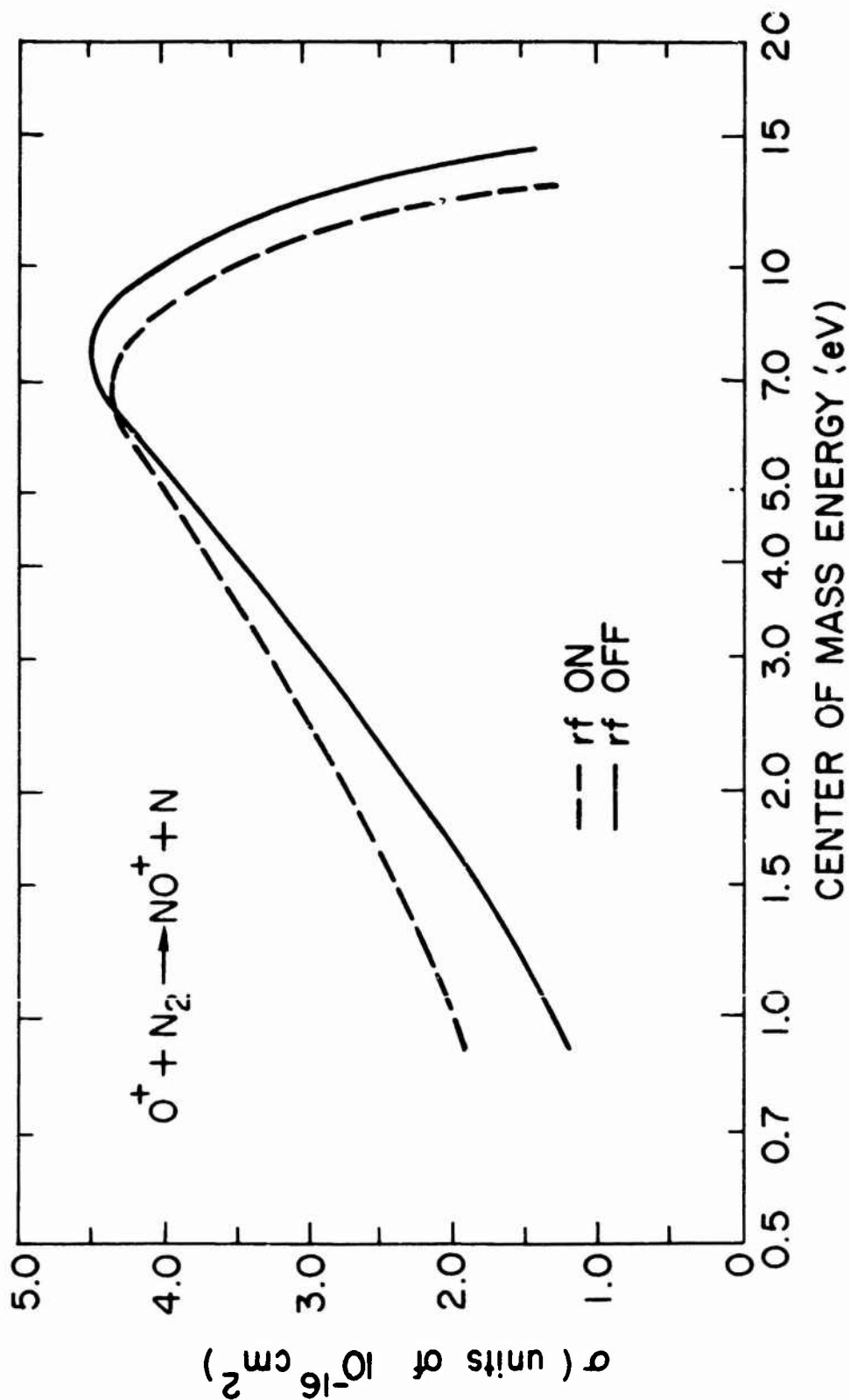


Figure 2. Reaction cross section for  $O^+ + N_2 \rightarrow NO^+ + N$  as a function of the energy in the center of mass system. The solid line gives the cross section for ground-state  $N_2$  (rf off), and the broken line represents the case for vibrationally excited  $N_2$  (rf on)



TABLE 3  
MEASURED CROSS SECTIONS FOR REACTION  $N^+ + N_2 \rightarrow N + N_2^+$   
(Center of Mass and Laboratory Collision Energies Given)

| CM Energy | Cross Section | Lab Energy |
|-----------|---------------|------------|
| 1.00      | 9.856626-18   | 1.50       |
| 1.33      | 1.310120-17   | 2.00       |
| 1.67      | 1.359024-17   | 2.50       |
| 2.00      | 1.843387-17   | 3.00       |
| 2.33      | 1.491769-17   | 3.50       |
| 2.67      | 1.984738-17   | 4.00       |
| 2.87      | 2.412279-17   | 4.30       |
| 3.00      | 2.572015-17   | 4.50       |
| 3.33      | 3.410492-17   | 5.00       |
| 3.67      | 3.764088-17   | 5.50       |
| 4.00      | 5.134206-17   | 6.00       |
| 4.13      | 6.006544-17   | 6.20       |
| 4.33      | 6.679541-17   | 6.50       |
| 4.67      | 8.497850-17   | 7.00       |
| 4.80      | 3.302007-17   | 7.20       |
| 5.00      | 9.093011-17   | 7.50       |
| 5.33      | 1.012502-16   | 8.00       |
| 5.67      | 1.112175-16   | 8.50       |
| 6.00      | 1.287781-16   | 9.00       |
| 6.33      | 1.414603-16   | 9.50       |
| 6.67      | 1.451114-16   | 10.00      |
| 7.00      | 1.577832-16   | 10.50      |
| 7.33      | 1.610895-16   | 11.00      |
| 7.67      | 1.697530-16   | 11.50      |
| 8.00      | 1.753400-16   | 12.00      |
| 8.33      | 1.730909-16   | 12.50      |
| 8.67      | 1.705075-16   | 13.00      |
| 9.33      | 1.680000-16   | 14.00      |
| 10.00     | 1.654025-16   | 15.00      |
| 10.67     | 1.534567-16   | 16.00      |
| 11.33     | 1.353547-16   | 17.00      |
| 12.00     | 1.273806-16   | 18.00      |
| 12.67     | 1.133065-16   | 19.00      |
| 13.33     | 1.123036-16   | 20.00      |
| 14.00     | 1.076039-16   | 21.00      |
| 16.67     | 9.591045-17   | 25.00      |
| 20.00     | 9.377910-17   | 30.00      |
| 26.67     | 9.140131-17   | 40.00      |
| 33.33     | 9.120166-17   | 50.00      |
| 40.00     | 8.710707-17   | 60.00      |
| 46.67     | 3.003411-17   | 70.00      |
| 53.33     | 7.672836-17   | 80.00      |
| 66.67     | 7.764173-17   | 100.00     |
| 80.00     | 7.307463-17   | 120.00     |

Reproduced from  
best available copy.

TABLE 3 (Continued)

| CM Energy | Cross Section | Lab Energy |
|-----------|---------------|------------|
| 100.00    | 7.142880-17   | 150.00     |
| 120.00    | 7.485693-17   | 180.00     |
| 133.33    | 7.637313-17   | 200.00     |
| 166.67    | 7.413368-17   | 250.00     |
| 200.00    | 8.245853-17   | 300.00     |
| 266.67    | 9.311400-17   | 400.00     |
| 333.33    | 9.750695-17   | 500.00     |

derived from our experiments is  $1.7 \times 10^{-16} \text{ cm}^2$ , while the value at the same interaction energy in Reference 14 is  $1.0 \times 10^{-16} \text{ cm}^2$ .

We attempted to introduce the metastable  $\text{N}^+(\text{D})$  into the primary ion beam to observe the effect of this species on the cross section. Although a number of different gases containing N atoms were used to produce the  $\text{N}^+$  beam, no evidence of the metastable could be found. Since several techniques were unsuccessful in producing this species in the laboratory, we conclude that it is not easily formed. As a consequence, it is doubtful if  $\text{N}^+(\text{D})$  is a very common species in the upper atmosphere.

Vibrational excitation of the neutral  $\text{N}_2$  reactant by thermal means appeared to have no effect on the reaction cross section. This behavior is expected since no levels are close enough to cause resonance by vibrational excitation to only the first or second vibrational levels.

Excitation of the  $\text{N}_2$  by rf did, however, produce vibrational levels that were high enough to enhance the reaction cross section at low energies. Figure 4 gives the cross section data for reaction 7 over the energy range from 1 to 20 eV in the center of mass. Both the rf-on and rf-off cases are illustrated. The rf-on data show a larger cross section over the total energy range with the increase being the greatest for low interaction energies. This implies that the vibrationally excited  $\text{N}_2$  reacts more readily in the charge-exchange process. This is probably due to the

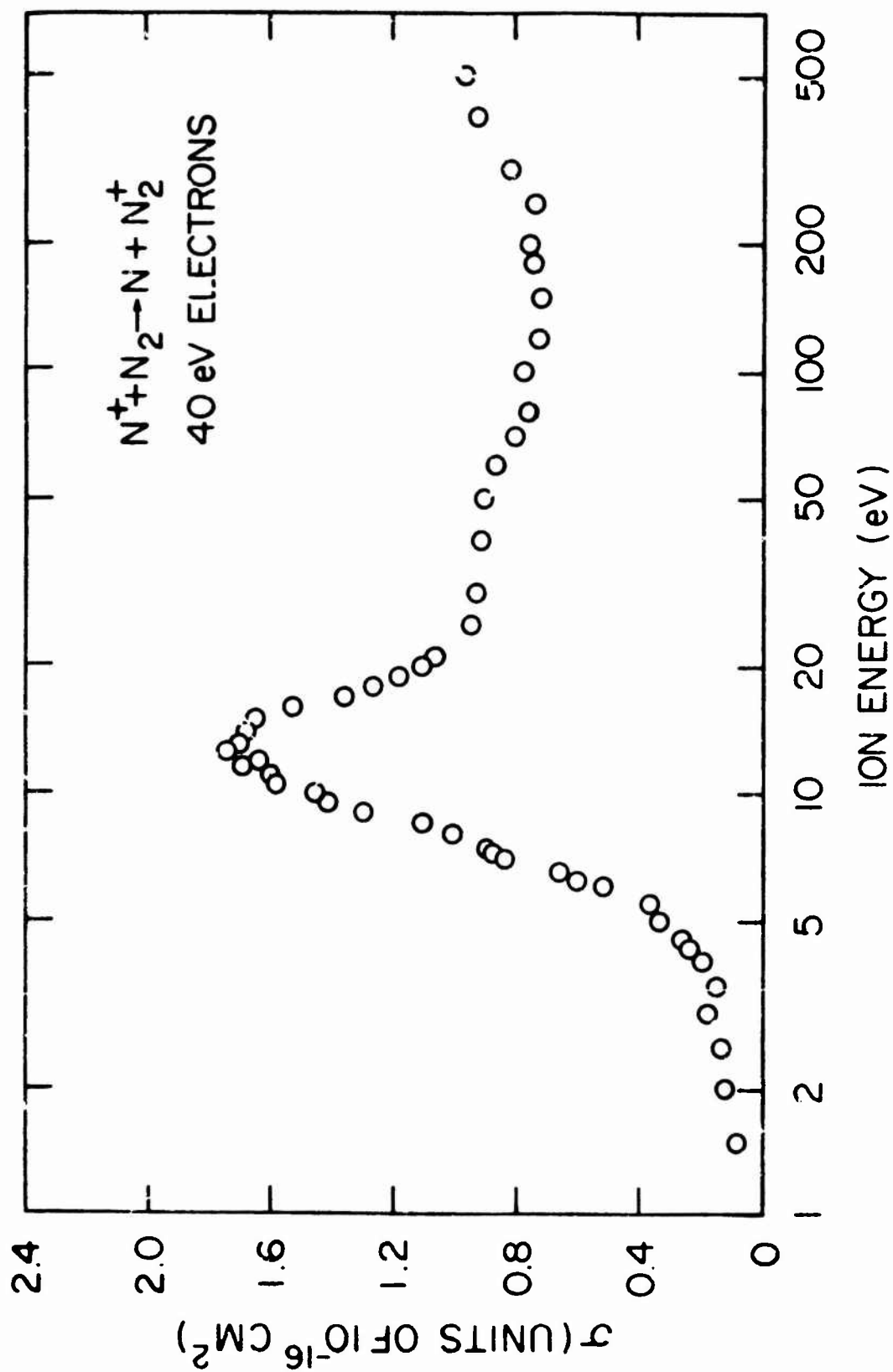


Figure 3. Charge-transfer cross section for  $N^+$  ions incident on neutral nitrogen molecules as a function of the energy of the incident ion

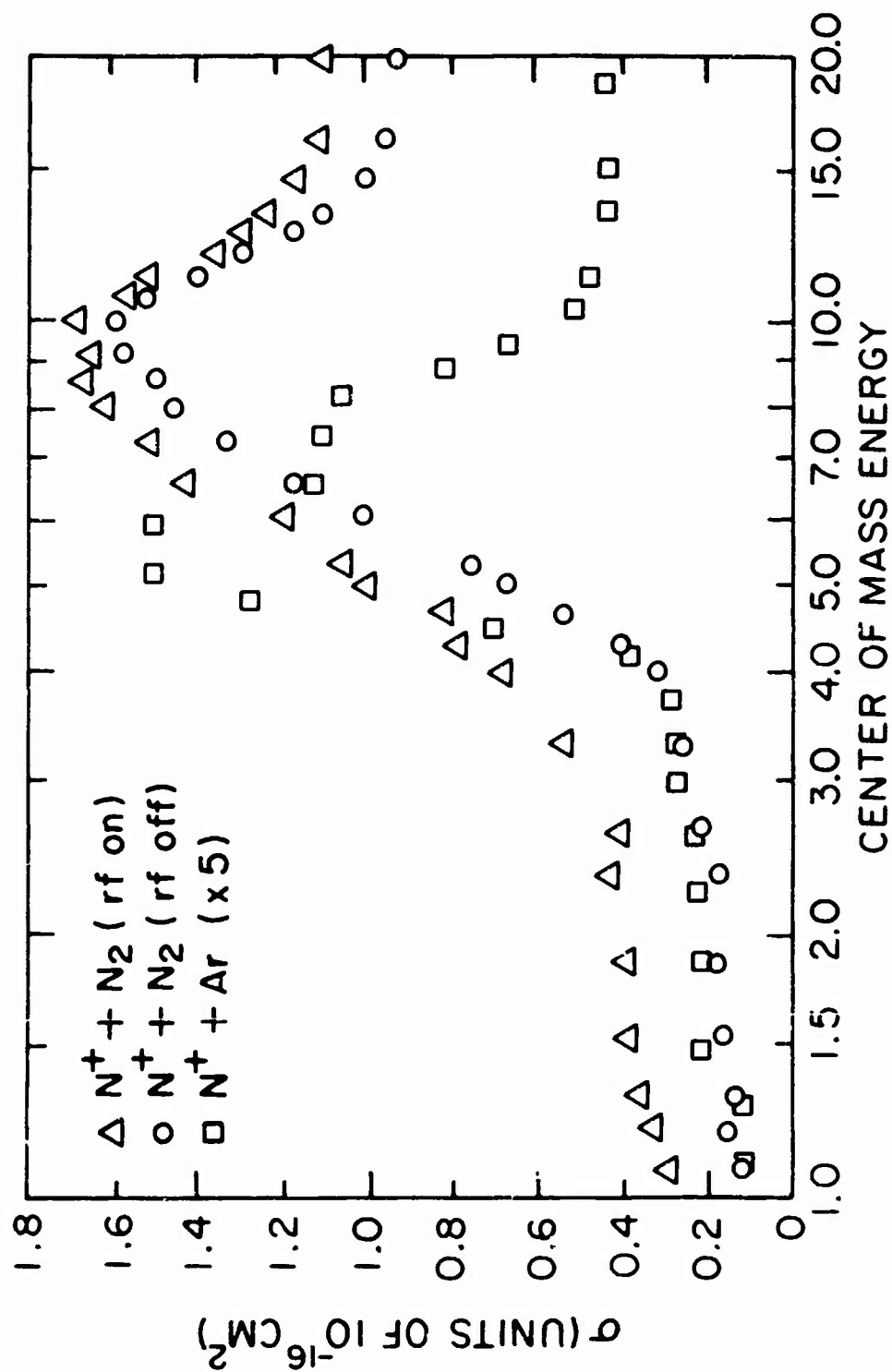


Figure 4. Charge-transfer cross sections for  $N^+$  ions incident on neutral nitrogen molecules without vibrational excitation (rf off), on neutral nitrogen molecules with vibrational excitation (rf on), and on neutral argon atoms as a function of energy in the center of mass of each system

high vibrational excitation in the  $N_2$ , which brings the reaction closer to resonance. The rf-on curve suggests that, for highly vibrationally excited  $N_2$ , a finite cross section for the reaction may exist at thermal energies.

In their study, Maier and Murad<sup>(14)</sup> suggest that the second channel for reaction, which appears at about 3.5 eV in the center of mass (Figure 4), may be due to formation of the  $N_2^+$  product in the A or B excited states. To test this supposition, the reaction



was studied. In this case, Ar replaces the  $N_2$  as the neutral reactant. Since the ionization potential of argon (15.76 eV) is similar to that for  $N_2$  (15.58 eV), a similar reaction threshold can be expected, although the absolute magnitude of the cross section with argon may be smaller since the reaction is about 0.2 eV more endothermic. The cross section for reaction 8 is given in Figure 4 (note the absolute values have been multiplied by a factor of 5 to make the scales comparable). The interesting result of this study is that the onset of the peak for reaction 7 is at about the same energy as that for reaction 8. If a similar mechanism is acting in both cases, it is doubtful if the peak in reaction 7 results from formation of the A or B state of  $N_2^+$ , since similar states do not exist for  $Ar^+$ . Consequently, an alternative explanation for the peak is that the peak may result from formation of the neutral N product in the excited  $^2D$  state. For reaction 7, this process would be expected to have a threshold at about 3.4 eV, which is what we observed. The more pronounced difference between the Ar and  $N_2$  data at higher interaction energies (above 10 eV in Figure 1) may be due to the effects of the ion-molecule reaction reported for reaction 7 by Maier and Murad.<sup>(14)</sup>

### 3.3 REACTIONS OF $N^+$ WITH $O_2$

The present program included studies of the effects of internal energy in the reactants on the following processes involving  $N^+$  and  $O_2$ :



The state of excitation of the reactant  $\text{O}_2$  molecule was altered by passing the gas through an rf discharge. The results with this discharge method were compared with those for no discharge. For all three of the above reactions, no effect due to discharge-induced excitation in the  $\text{O}_2$  could be seen on the reaction cross sections. As discussed above, we attempted to produce a beam of  $\text{N}^+$  with excited states present. Thus far, we have been unable to detect the presence of any excited  $\text{N}^+$  species.

The results for the production of  $\text{O}^+$  are illustrated in Figure 5. Tabular data are given in Table 4. Note that, in the center-of-mass system, the cross section for the production of  $\text{O}^+$  is very small below 1.5 eV, rises slowly to about 4 eV, and then begins to rise rapidly to a peak at about 10 eV. If the production of  $\text{O}^+$  resulted from an ion-molecule reaction in which NO was the other product, the overall process would be exothermic by approximately 2.3 eV for all products in the ground state. Since the cross section appears to be very small at low energies, this does not seem a likely channel for the reaction. Reaction 9, a dissociative charge-transfer process, is endothermic by 4.2 eV. Since our cross-section curve increases sharply above this energy, we postulate that, above 4.2 eV, reaction 9 is the principal process leading to the production of  $\text{O}^+$ .

Cross-section curves for reactions 10 and 11 are given in Figure 6; tabular data for these reactions are given in Tables 5 and 6, respectively. For both these reactions, measured values were obtained at lower interaction energies than previously reported.<sup>(3)</sup> As with reaction 9, these cross sections are not affected by the introduction of excited states in the  $\text{O}_2$  beams. The deposition of the excess energy in these reactions is also of interest. For reaction 10, it is energetically possible to form  $\text{NO}^+$  in an excited state:

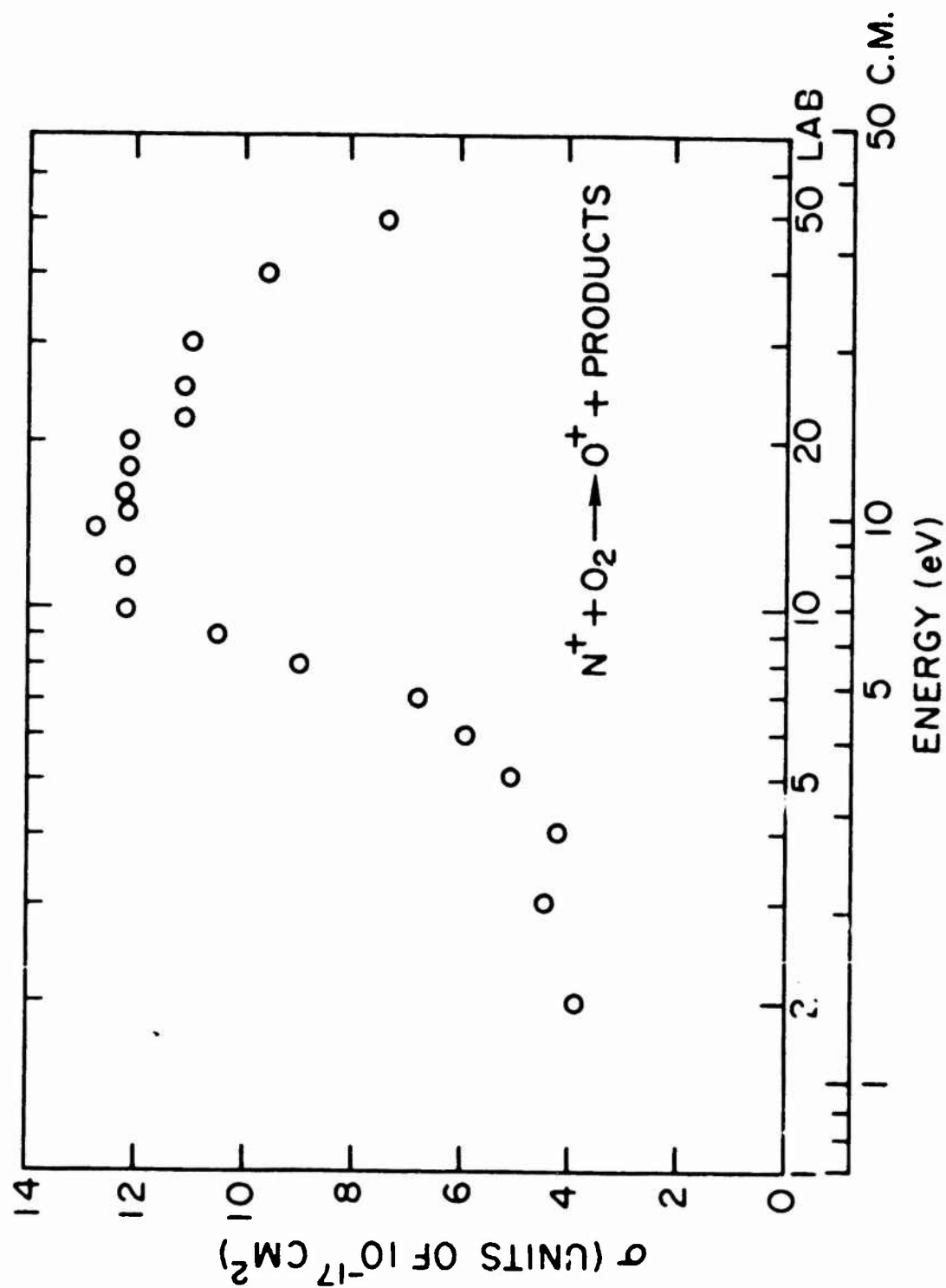



Figure 5. Reaction cross section for  $N^+$  ions incident on  $O_2$  to form  $O^+$  as a function of the energy in the center of mass and of the incoming ion energy

TABLE 4  
MEASURED CROSS SECTIONS FOR THE REACTION  $N^+ + O_2 \rightarrow O^+ + \text{PRODUCTS}$   
(Center of Mass and Laboratory Energies are Given)

| CM ENERGY | CROSS SECTION | LAB ENERGY |
|-----------|---------------|------------|
| 1.39      | 3.902470-17   | 2.00       |
| 2.09      | 4.462452-17   | 3.00       |
| 2.78      | 5.179351-17   | 4.00       |
| 3.48      | 5.041545-17   | 5.00       |
| 4.17      | 5.952657-17   | 6.00       |
| 4.87      | 6.757515-17   | 7.00       |
| 5.57      | 9.055573-17   | 8.00       |
| 6.26      | 1.051696-16   | 9.00       |
| 6.96      | 1.216523-16   | 10.00      |
| 8.35      | 1.197623-16   | 12.00      |
| 9.74      | 1.299593-16   | 14.00      |
| 10.43     | 1.222000-16   | 15.00      |
| 11.13     | 1.220414-16   | 16.00      |
| 12.52     | 1.243058-16   | 18.00      |
| 13.91     | 1.228434-16   | 20.00      |
| 15.30     | 1.114733-16   | 22.00      |
| 17.39     | 1.116015-16   | 25.00      |
| 20.87     | 1.109333-16   | 30.00      |
| 27.83     | 9.582857-17   | 40.00      |
| 34.78     | 7.447742-17   | 50.00      |

Reproduced from  
best available copy. 



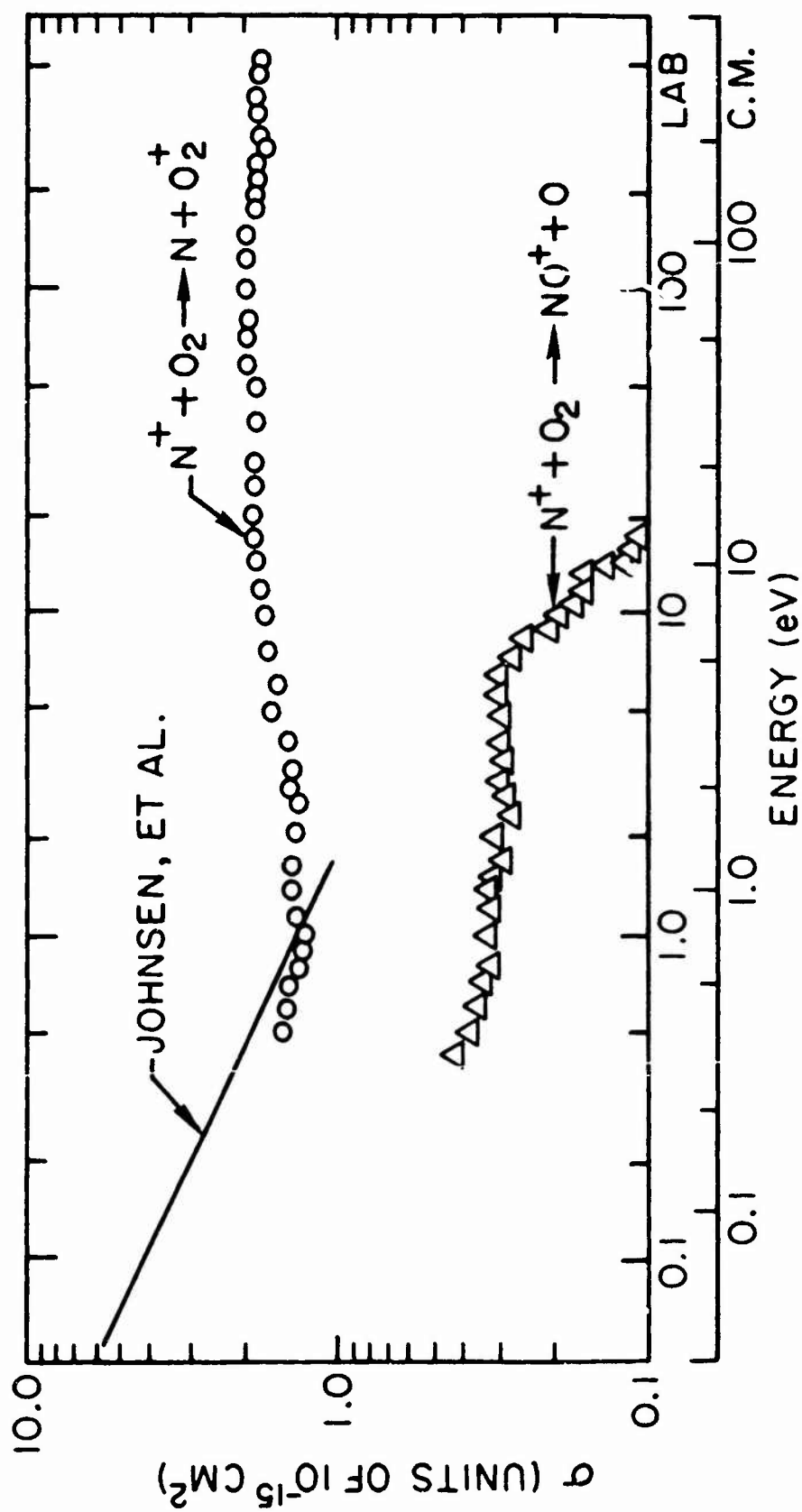


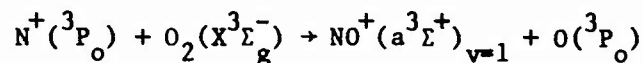
Figure 6. Reaction cross sections for  $\text{N}^+$  ions incident on  $\text{O}_2$  to form  $\text{O}_2^+$  and  $\text{NO}^+$  as a function of the energy in the center of mass and of the incoming ion energy

TABLE 5  
MEASURED CROSS SECTIONS FOR THE REACTION  $N^+ + O_2 \rightarrow NO^+ + O$   
(Center of Mass and Laboratory Energies are Given)

| CM ENERGY | CROSS SECTION | LAB ENERGY |
|-----------|---------------|------------|
| .35       | 3.817911-16   | .50        |
| .42       | 3.641270-16   | .60        |
| .49       | 3.410171-16   | .70        |
| .56       | 3.233833-16   | .80        |
| .70       | 3.292770-16   | 1.00       |
| .83       | 3.199635-16   | 1.20       |
| .97       | 3.210252-16   | 1.40       |
| 1.04      | 3.194420-16   | 1.50       |
| 1.18      | 2.926599-16   | 1.70       |
| 1.32      | 2.874176-16   | 1.90       |
| 1.39      | 3.038658-16   | 2.00       |
| 1.46      | 2.854303-16   | 2.10       |
| 1.67      | 2.777826-16   | 2.40       |
| 1.74      | 2.873479-16   | 2.50       |
| 1.95      | 2.818094-16   | 2.80       |
| 2.09      | 3.062579-16   | 3.00       |
| 2.43      | 2.962250-16   | 3.50       |
| 2.78      | 3.032180-16   | 4.00       |
| 3.13      | 2.958197-16   | 4.50       |
| 3.48      | 3.011178-16   | 5.00       |
| 3.83      | 2.966466-16   | 5.50       |
| 4.17      | 2.945238-16   | 6.00       |
| 4.52      | 2.995644-16   | 6.50       |
| 4.87      | 2.752021-16   | 7.00       |
| 5.22      | 2.757627-16   | 7.50       |
| 5.57      | 2.459636-16   | 8.00       |
| 5.91      | 2.529303-16   | 8.50       |
| 6.26      | 2.225541-16   | 9.00       |
| 6.61      | 2.324470-16   | 9.50       |
| 6.96      | 1.922576-16   | 10.00      |
| 7.65      | 1.724517-16   | 11.00      |
| 8.35      | 1.573534-16   | 12.00      |
| 9.04      | 1.598388-16   | 13.00      |
| 9.74      | 1.396656-16   | 14.00      |
| 10.43     | 1.275112-16   | 15.00      |
| 11.13     | 1.185548-16   | 16.00      |
| 11.83     | 1.245916-16   | 17.00      |
| 12.52     | 1.001052-16   | 18.00      |
| 13.22     | 1.089535-16   | 19.00      |
| 13.91     | 9.300975-17   | 20.00      |
| 15.30     | 9.685736-17   | 22.00      |
| 17.39     | 7.837500-17   | 25.00      |
| 18.78     | 7.036207-17   | 27.00      |
| 20.87     | 6.458064-17   | 30.00      |
| 22.96     | 6.830645-17   | 33.00      |
| 24.35     | 6.803421-17   | 35.00      |
| 27.83     | 5.329572-17   | 40.00      |

TABLE 6  
MEASURED CROSS SECTIONS FOR THE REACTION  $N^+ + O_2 \rightarrow N + O_2^+$   
(Center of Mass and Laboratory Energies are Given)

| CM ENERGY | CROSS SECTION | LAB ENERGY |
|-----------|---------------|------------|
| .42       | 1.433484-15   | .60        |
| .49       | 1.426070-15   | .70        |
| .56       | 1.376669-15   | .80        |
| .63       | 1.303575-15   | .90        |
| .70       | 1.321385-15   | 1.00       |
| .83       | 1.351571-15   | 1.20       |
| 1.10      | 1.414623-15   | 1.70       |
| 1.46      | 1.384615-15   | 2.10       |
| 1.81      | 1.370769-15   | 2.60       |
| 2.09      | 1.473945-15   | 3.00       |
| 2.30      | 1.383922-15   | 3.30       |
| 2.43      | 1.447268-15   | 3.50       |
| 2.78      | 1.462154-15   | 4.00       |
| 3.48      | 1.644788-15   | 5.00       |
| 4.17      | 1.583348-15   | 6.00       |
| 5.57      | 1.676448-15   | 8.00       |
| 6.96      | 1.734053-15   | 10.00      |
| 8.35      | 1.791855-15   | 12.00      |
| 10.43     | 1.826219-15   | 15.00      |
| 12.52     | 1.911312-15   | 18.00      |
| 13.91     | 1.929690-15   | 20.00      |
| 17.39     | 1.859220-15   | 25.00      |
| 20.97     | 1.863529-15   | 30.00      |
| 27.83     | 1.795550-15   | 40.00      |
| 34.78     | 1.708684-15   | 50.00      |
| 41.74     | 2.015937-15   | 60.00      |
| 48.70     | 2.005171-15   | 70.00      |
| 55.65     | 1.954751-15   | 80.00      |
| 57.04     | 1.958242-15   | 82.00      |
| 69.57     | 2.033066-15   | 100.00     |
| 83.48     | 1.985294-15   | 120.00     |
| 104.35    | 1.962081-15   | 150.00     |
| 125.22    | 1.925192-15   | 180.00     |
| 139.13    | 1.960773-15   | 200.00     |
| 153.04    | 1.791855-15   | 220.00     |
| 173.91    | 1.915747-15   | 250.00     |
| 194.70    | 1.697376-15   | 280.00     |
| 208.70    | 1.923336-15   | 300.00     |
| 243.48    | 1.810717-15   | 350.00     |
| 278.26    | 1.300000-15   | 400.00     |
| 313.04    | 1.778072-15   | 450.00     |
| 347.83    | 1.742425-15   | 500.00     |



This process is nearly energy-resonant and may well be the favored path since it does not require the 6-eV exothermicity of the reaction path leading to ground-state products to be transformed into kinetic energy.

The charge-transfer reaction 11, exhibits a large cross section over the entire energy range studied. Previous publications<sup>(2,15)</sup> show that such behavior in charge-transfer processes is indicative of a near-resonant reaction path. For reaction 11, near-resonance can be obtained by a mechanism such as

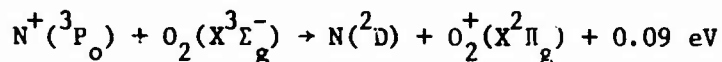


Figure 6 also includes the recent data of Johnson, Brown, and Biondi,<sup>(16)</sup> who have studied reactions 10 and 11 using drift-tube mass spectrometer techniques. They obtained a total rate constant for both reactions of  $5 \times 10^{-10} \text{ cm}^3/\text{sec}$  over the entire range from thermal to 1 eV. Comparison of the sum of our two reaction cross sections with the cross section obtained from their rate coefficients in the range of overlap shows good agreement.

### 3.4 CHARGE TRANSFER FROM $\text{N}_2^+$ TO $\text{O}_2$

In earlier studies of the charge-transfer reaction



in our laboratory,<sup>(3)</sup> the effects of vibrational excitation of the  $\text{O}_2$  on the reaction cross section was not examined.

In a previous report,<sup>(13)</sup> we described a reinvestigation of this reaction in which special attention was given to the change in cross section as a function of the state of vibrational excitation of the  $\text{N}_2^+$  primary ion. The results of this study are given in Figure 7. Two cases are represented:

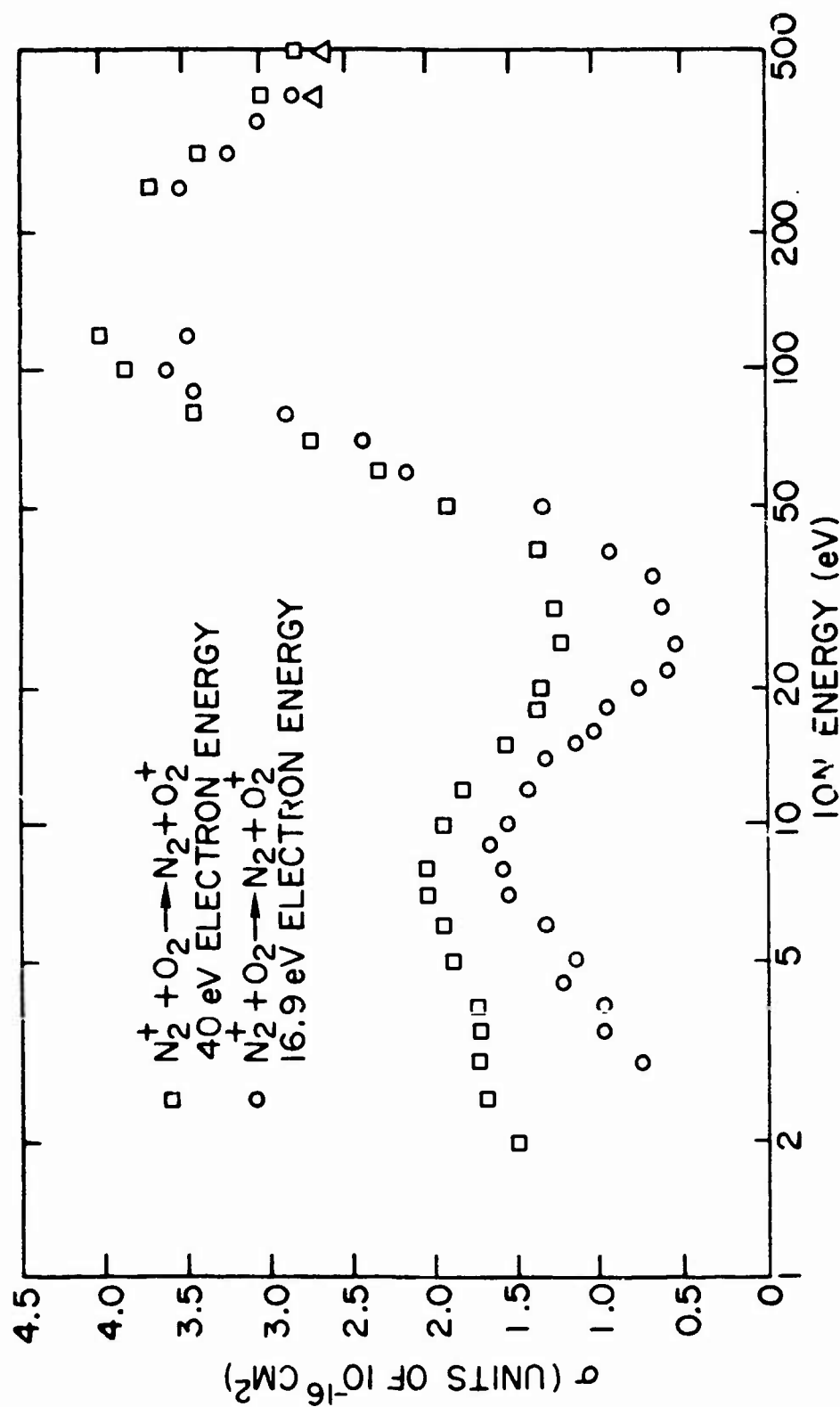
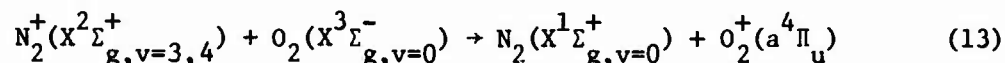


Figure 7. Charge-transfer cross sections for  $N_2^+$  ions incident on neutral oxygen molecules as a function of the energy of the incident ion. The cross sections for  $N_2^+$  formed at two primary ion-source electron energies are shown. The differences in the curve reflect the different vibrational distributions present in the primary ion.

(1) very low electron energies (16.9 eV) in the primary ion source, and  
 (2) higher electron energies (40 eV). A brief discussion of these results is given to assist in interpreting the newer results in which the  $O_2$  is vibrationally excited. Comparison of the two  $N_2^+$  curves in Figure 7 reveals that the results obtained for high ion energies (above 50 eV) are similar. Below 50 eV, however, the cross section for  $N_2^+$  ions with very little vibrational excitation (those ions formed by 16.9-eV electrons) is less than that for ions with appreciable vibrational energy. Franck-Condon calculations indicated that, below the onset of the  $N_2^+(A^2\Pi_u)$  state ( $\sim 16.9$  eV), all direct ionization of  $N_2$  produces ions in the zeroth and first vibrational levels of the ionic ground state.

The probable reason for the difference in the two curves shown in Figure 7 is that, if sufficient energy is available internally in the  $N_2^+$  ion, formation of the  $O_2^+(a^4\Pi_u)$  state is possible. This process, which is nearly resonant, can be represented as



The importance of the vibrational excitation of the  $N_2^+$  in the charge transfer is further demonstrated by examining the primary ion-source electron-energy dependence of the cross section for 10-eV  $N_2^+$  ions on  $O_2$ . This dependence (Figure 8) indicates that the cross section for the process changes rapidly for electron energies between 16 and 19 eV. At these energies, higher vibrational levels of the ground ionic state are probably being filled by cascade from the  $N_2^+(A^2\Pi_u)$  state.

The results of the experiments in which vibrational energy was added to the neutral  $O_2$  also showed an increase in cross section. Figure 9 is a plot of the data for cold and hot  $O_2$ . Tabular data are given in Tables 7 and 8, respectively. Note that, for both reactions, the vibrational excitation of the  $N_2^+$  was kept low ( $v = 0,1$ ) by the use of 16.9-eV electrons to form the ion. The effect in the present case, therefore, is that due to vibrationally excited  $O_2$  alone. For these experiment, the  $O_2$  gas was heated

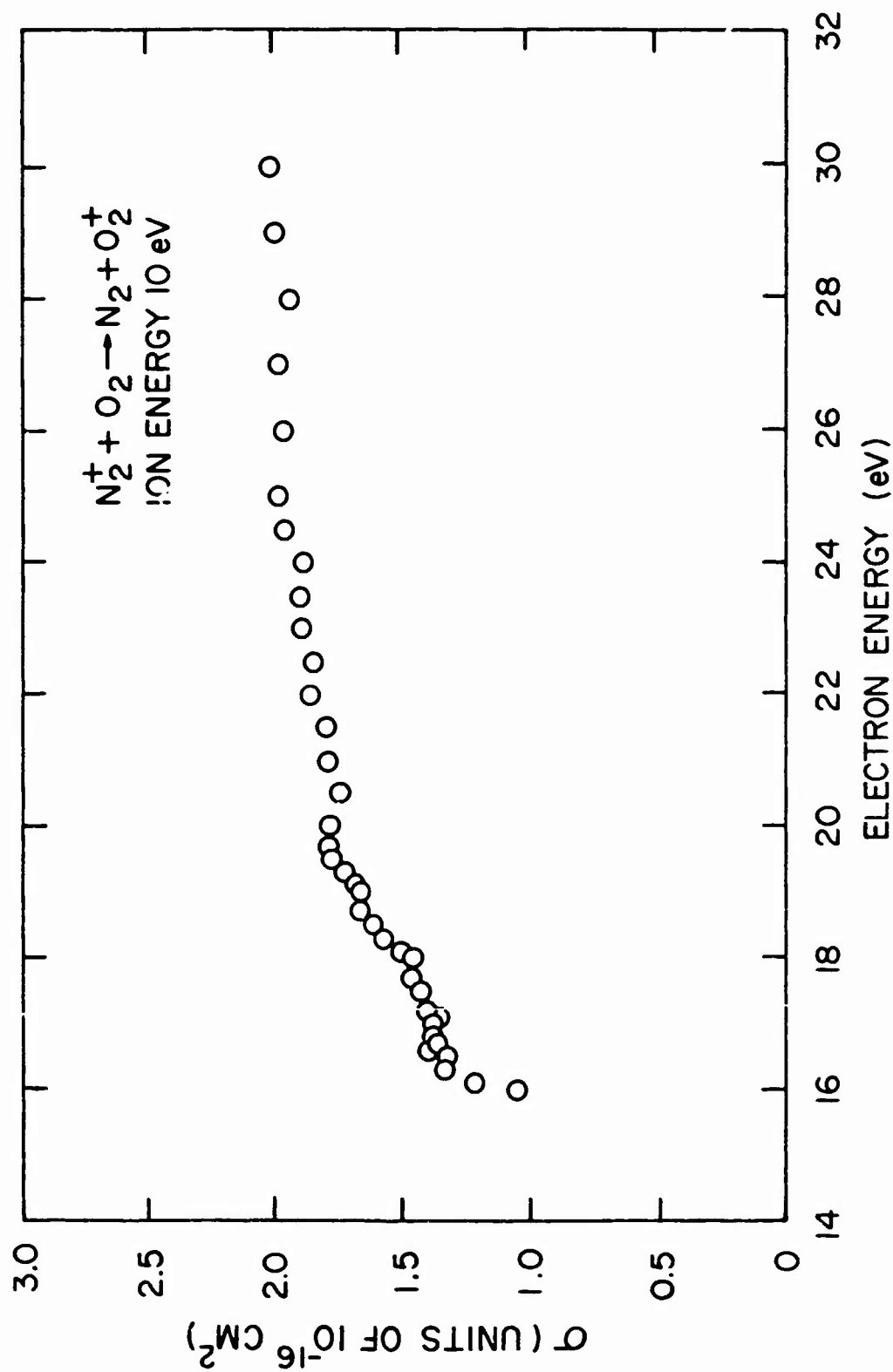


Figure 8. Dependence of the charge-transfer cross section for  $N_2^+ + O_2 \rightarrow N_2 + O_2^+$  upon the ion-source electron energy. The  $N_2^+$  had a kinetic energy of 10 eV.

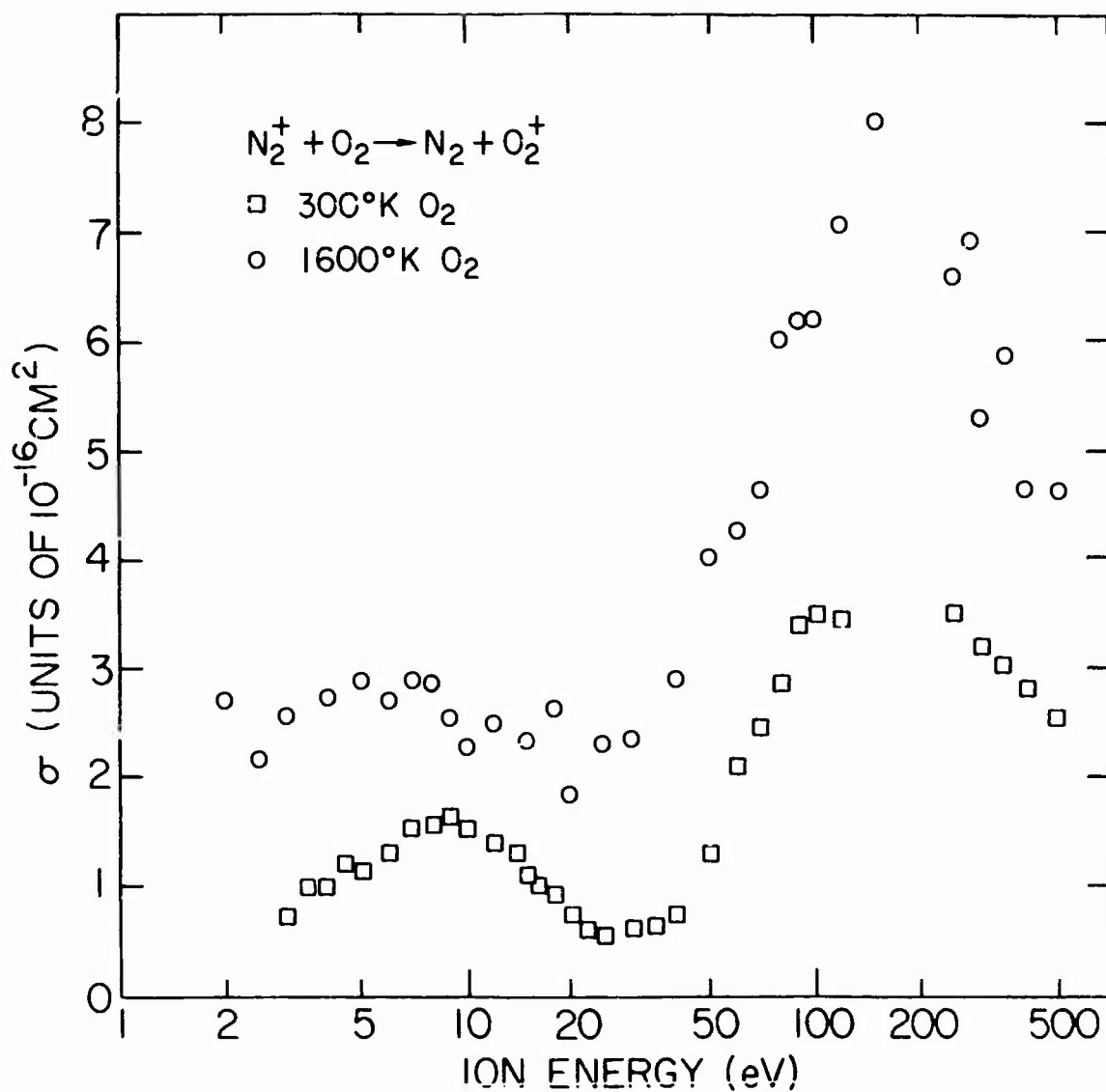


Figure 9. Charge-transfer cross sections for  $N_2^+$  ions incident on neutral oxygen molecules as a function of the energy of the incident ion. The lower set of data represents the cross section for neutral  $O_2$  with no vibrational excitation, while the upper curve gives the cross section when vibrational excitation is present in the  $O_2$ .



TABLE 7  
 MEASURED CROSS SECTIONS FOR THE REACTION  $N_2^+ + O_2 \rightarrow N_2 + O_2^+$   
 WHEN THE  $O_2$  IS NOT VIBRATIONALLY EXCITED  
 (Center of Mass and Laboratory Energies are Given)

| CM ENERGY | CROSS SECTION | LAB ENERGY |
|-----------|---------------|------------|
| 1.60      | 7.331371-17   | 3.00       |
| 1.87      | 9.928161-17   | 3.50       |
| 2.13      | 9.819004-17   | 4.00       |
| 2.40      | 1.216987-16   | 4.50       |
| 2.67      | 1.143727-16   | 5.00       |
| 3.20      | 1.319755-16   | 6.00       |
| 3.73      | 1.534599-16   | 7.00       |
| 4.27      | 1.575374-16   | 8.00       |
| 4.90      | 1.642693-16   | 9.00       |
| 5.33      | 1.503314-16   | 10.00      |
| 6.40      | 1.415544-16   | 12.00      |
| 7.47      | 1.319301-16   | 14.00      |
| 8.00      | 1.126787-16   | 15.00      |
| 8.53      | 1.035354-16   | 16.00      |
| 9.60      | 9.197460-17   | 18.00      |
| 10.67     | 7.419408-17   | 20.00      |
| 11.73     | 5.957962-17   | 22.00      |
| 13.33     | 5.524839-17   | 25.00      |
| 16.00     | 6.000698-17   | 30.00      |
| 18.67     | 6.223530-17   | 35.00      |
| 21.33     | 7.327460-17   | 40.00      |
| 26.67     | 1.323355-16   | 50.00      |
| 32.00     | 2.135104-16   | 60.00      |
| 37.33     | 2.463109-16   | 70.00      |
| 42.67     | 2.975438-16   | 80.00      |
| 49.00     | 3.425431-16   | 90.00      |
| 53.33     | 3.604567-16   | 100.00     |
| 64.00     | 3.453055-16   | 120.00     |
| 133.33    | 3.523972-16   | 250.00     |
| 160.00    | 3.200400-16   | 300.00     |
| 186.67    | 3.053421-16   | 350.00     |
| 213.33    | 2.300000-16   | 400.00     |
| 266.67    | 2.569073-16   | 500.00     |

Reproduced from  
 best available copy.



TABLE 8  
MEASURED CROSS SECTIONS FOR THE REACTION  $N_2^+ + O_2 \rightarrow N_2 + O_2^+$   
WHEN THE  $O_2$  IS VIBRATIONALLY EXCITED  
(Center of Mass and Laboratory Energies are Given)

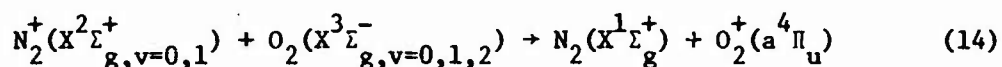
| CM ENERGY | CROSS SECTION | LAB ENERGY |
|-----------|---------------|------------|
| 1.07      | 2.761325-16   | 2.00       |
| 1.33      | 2.175822-16   | 2.50       |
| 1.60      | 2.601526-16   | 3.00       |
| 2.13      | 2.754557-16   | 4.00       |
| 2.67      | 2.907248-16   | 5.00       |
| 3.20      | 2.710317-16   | 6.00       |
| 3.73      | 2.919115-16   | 7.00       |
| 4.27      | 2.993629-16   | 8.00       |
| 4.80      | 2.569162-16   | 9.00       |
| 5.33      | 2.270422-16   | 10.00      |
| 6.40      | 2.497465-16   | 12.00      |
| 8.00      | 2.341373-16   | 15.00      |
| 9.60      | 2.660651-16   | 19.00      |
| 10.67     | 1.962456-16   | 20.00      |
| 13.33     | 2.322023-16   | 25.00      |
| 16.00     | 2.373024-16   | 30.00      |
| 21.33     | 2.919115-16   | 40.00      |
| 26.67     | 4.032987-16   | 50.00      |
| 32.00     | 4.257042-16   | 60.00      |
| 37.33     | 4.651597-16   | 70.00      |
| 42.67     | 6.019260-16   | 80.00      |
| 48.00     | 7.192671-16   | 90.00      |
| 53.33     | 6.203187-16   | 100.00     |
| 64.00     | 7.095070-16   | 120.00     |
| 80.00     | 8.032155-16   | 150.00     |
| 133.33    | 6.634351-16   | 250.00     |
| 149.33    | 6.930009-16   | 280.00     |
| 160.00    | 5.321003-16   | 300.00     |
| 186.67    | 5.757143-16   | 350.00     |
| 213.33    | 4.650000-16   | 400.00     |
| 266.67    | 4.697420-16   | 500.00     |

Reproduced from  
best available copy.



to approximately 1600°K in an iridium furnace (no dissociation of the O<sub>2</sub> occurs at this temperature).

Examination of Figure 9 shows that there is an increase in the charge-transfer cross section for vibrationally excited O<sub>2</sub> over the total energy range studied. The reason for the change is probably identical to that for adding vibrational energy to the N<sub>2</sub><sup>+</sup> ions. The heated O<sub>2</sub> gas has some particles in high enough vibrational levels that the reaction becomes near-resonant for formation of the O<sub>2</sub><sup>+</sup> in the excited (a<sup>4</sup>Π<sub>u</sub>) state. This reaction can be written as



Vibrational excitation of the O<sub>2</sub> may be more effective than similar excitation in N<sub>2</sub><sup>+</sup> (compare Figures 7 and 9) because the O<sub>2</sub> excitation not only decreases the energy defect of the reaction, but also improves the Franck-Condon overlap between the ground-neutral and excited-ion states.

### 3.5 CHARGE TRANSFER BETWEEN H<sup>+</sup> AND O

The charge-transfer reaction



was studied to evaluate the operation of our O atom sources and for use in determining the degree of dissociation present in the O beam arising from either rf or thermal dissociation. Reaction 15 is particularly suited for these tasks because it is accidentally resonant, making it easy to study. Furthermore, cross sections for this reaction at both thermal<sup>(17)</sup> and high energies<sup>(18)</sup> have been derived from earlier studies. These earlier measurements allow comparison of our results with others to check our degree of dissociation.

Care must be taken when using reaction 15 for probing the O atom beam since the competing endothermic reactions



and



can appreciably affect the measured cross-section curve. The first of these competing reactions can only occur with the absorption of 5.1 eV of kinetic energy from the system, while the second requires only 0.7 eV.

Our investigations using the O atom beam produced by thermal dissociation of  $\text{O}_2$  show that the cross section for reaction 15 is larger than that of reaction 16, and that any effects from this reaction can easily be subtracted from the overall curve measured for production of  $\text{O}^+$ . Figure 10 is a plot of the cross sections for reactions 15 and 16. Reaction 17 was found to be insignificant. All the data shown in Figure 10 were obtained using the thermal dissociation method. The degree of dissociation was approximately 20%. Tabular data for reaction 15 are given in Table 9.

Using the rf discharge technique met with less success. Both  $\text{O}_2$  and  $\text{CO}_2$  were used in attempts to produce O atoms. Although higher beam densities were obtained using this technique, interpretation of the data proved difficult perhaps because of the presence of metastable species in the beam.

Our success in measuring cross sections for the reaction of Equation 15 using O atoms produced by thermal dissociation has allowed us to attempt measurements of other reactions involving O atoms. The following subsection gives a report on one of these processes.

### 3.6 REACTION OF $\text{N}_2^+$ WITH O TO GIVE $\text{NO}^+$

The ion-molecule reaction



has been studied in the energy range from 1 to 4 eV in the laboratory system. Two difficulties were encountered during the measurements. The first was the low density of O atoms in the beam coming from the iridium furnace. The

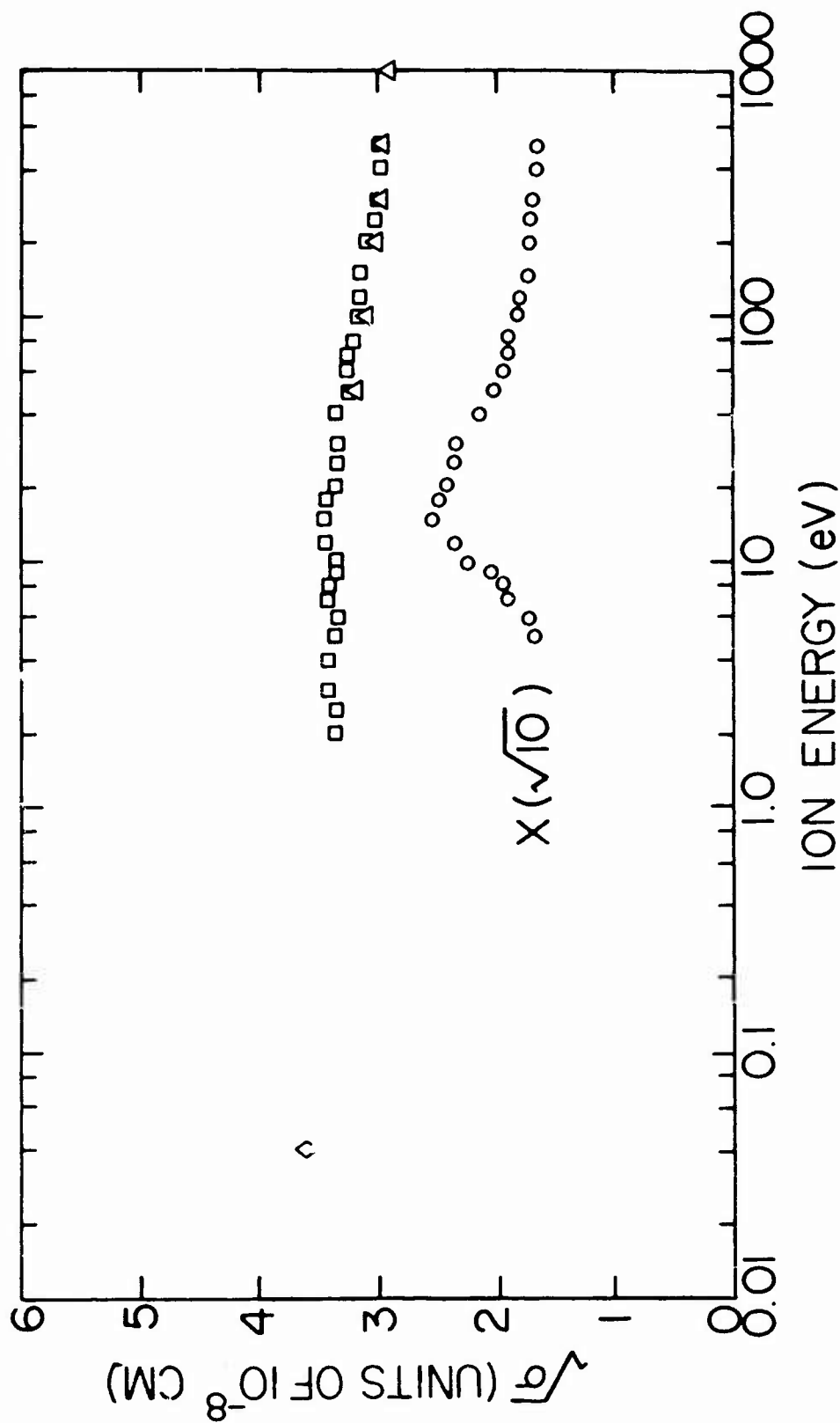


Figure 10. Square root of the cross section for the reactions  $\text{H}^+ + \text{O} \rightarrow \text{H} + \text{O}^+$  ( $\square$ ) and  $\text{H}^+ + \text{O}_2 \rightarrow \text{H} + \text{O}$  ( $\circ$ ). The latter cross section was increased by a factor of 10 before the square root was taken. The data of Fehsenfeld et al. ( $\diamond$ ) and Stebbings et al. ( $\Delta$ ) for the first reaction are shown for comparison.

TABLE 9  
MEASURED CROSS SECTION FOR THE REACTION  $H^+ + O \rightarrow H + O^+$   
(Center of Mass and Laboratory Energies are Given)

| CM ENERGY | CROSS SECTION | LAB ENERGY |
|-----------|---------------|------------|
| 1.98      | 1.150000-15   | 2.00       |
| 2.35      | 1.140000-15   | 2.50       |
| 2.82      | 1.170000-15   | 3.00       |
| 3.76      | 1.190000-15   | 4.00       |
| 4.71      | 1.140000-15   | 5.00       |
| 5.65      | 1.120000-15   | 6.00       |
| 6.59      | 1.170000-15   | 7.00       |
| 7.53      | 1.170000-15   | 8.00       |
| 8.47      | 1.120000-15   | 9.00       |
| 9.41      | 1.150000-15   | 10.00      |
| 11.29     | 1.200000-15   | 12.00      |
| 14.12     | 1.210000-15   | 15.00      |
| 16.94     | 1.200000-15   | 18.00      |
| 19.82     | 1.150000-15   | 20.00      |
| 23.53     | 1.130000-15   | 25.00      |
| 28.24     | 1.130000-15   | 30.00      |
| 37.65     | 1.140000-15   | 40.00      |
| 47.06     | 1.050000-15   | 50.00      |
| 56.47     | 1.000000-15   | 60.00      |
| 65.89     | 1.080000-15   | 70.00      |
| 75.29     | 1.030000-15   | 80.00      |
| 94.12     | 1.010000-15   | 100.00     |
| 112.94    | 1.020000-15   | 120.00     |
| 141.19    | 1.010000-15   | 150.00     |
| 189.24    | 9.710000-16   | 200.00     |
| 235.22    | 9.300000-16   | 250.00     |
| 282.35    | 9.000000-16   | 300.00     |
| 376.47    | 9.000000-16   | 400.00     |
| 470.59    | 9.000000-16   | 500.00     |

second difficulty was noise associated with having the mass of the primary ion beam (28 amu) close to that of secondary ions (30 amu). The resolution of the secondary mass spectrometer employed for the study was sufficient to completely separate the mass 28 peak from the mass 30 peak; nevertheless, a certain amount of dc noise resulting from scattering of the primary mass 28 peak appeared at mass 30. (Note that the magnitude of the product 30 peak is several orders of magnitude less than that of the primary beam at mass 28.)

Figure 11 gives the results obtained for the reaction of Equation 18. The results are compared to a  $1/v$  dependence, where  $v$  is the velocity of the center of mass. The fit to a  $1/v$  dependence is fair, indicating that the reaction may proceed by an ion-dipole mechanism.<sup>(9)</sup>

The cross section for the reaction of Equation 18 is smaller than might be expected for an exothermic ion-molecule reaction. This small cross section may indicate that the products of the reaction cannot easily absorb the excess energy in the reaction (13.0 eV).

Previous measurements of a thermal energy coefficient for the reaction of Equation 18 were performed. Ferguson et al.<sup>(19)</sup> obtained  $k = 2.5 \times 10^{-10}$  cm<sup>3</sup>/sec at 300°K. Extension of our measured data using the  $1/v$  fit shown in Figure 11 results in a rate coefficient of about 1/6 of that reported by Ferguson et al. at the same energy.

Work on reactions involving O atoms is continuing.

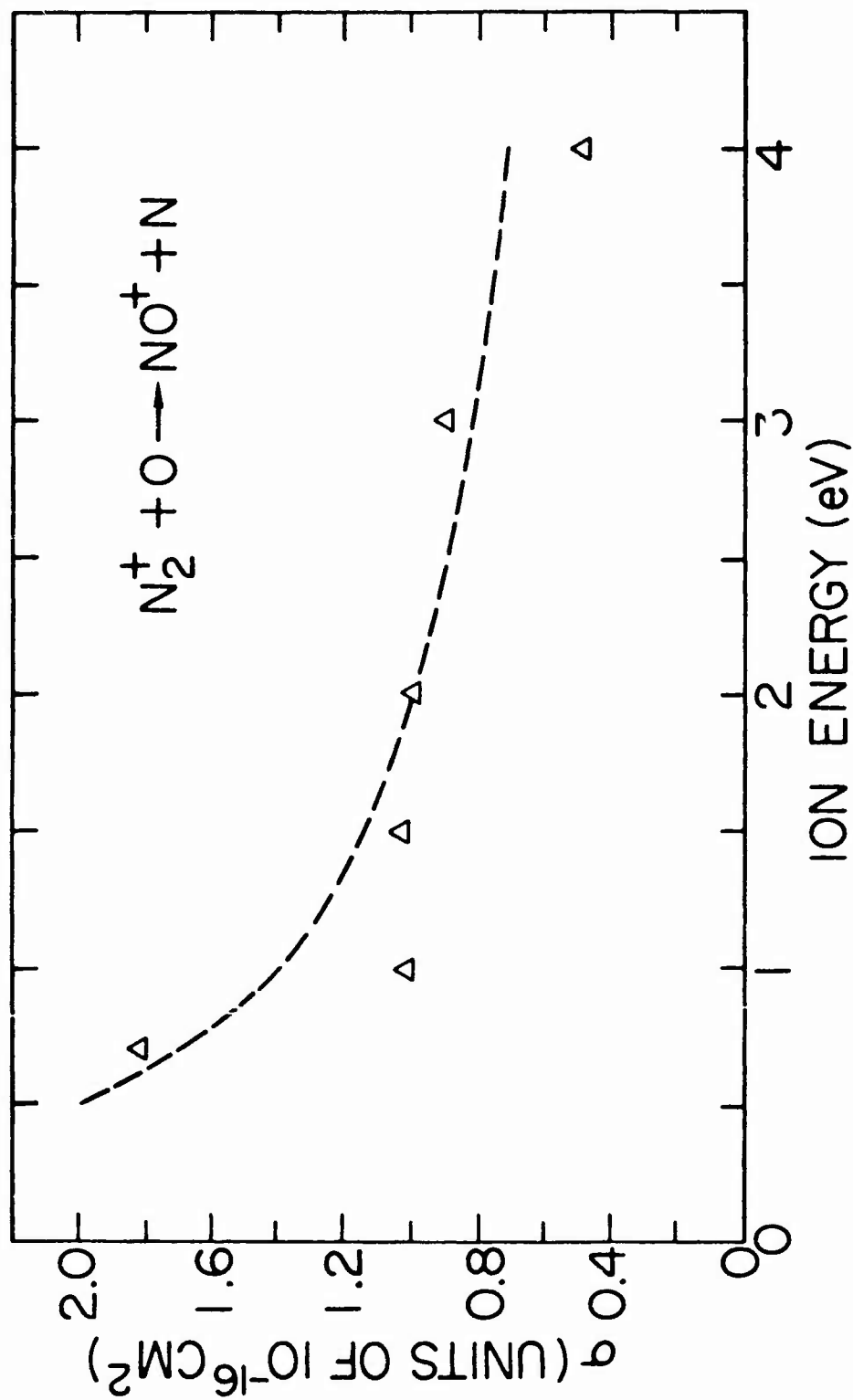


Figure 11. Reaction cross section for  $N_2^+$  ions incident on neutral O to form  $NO^+$  as a function of the energy of the incident ion. The broken line gives a  $1/v$  dependence over the energy range.



## REFERENCES

1. M. H. Bortner, Coordinator, DNA Reaction Rate Handbook, DASA-1948, General Electric Company Missile and Space Division, Philadelphia, Pennsylvania, 1967.
2. J. A. Rutherford, R. F. Mathis, B. F. Turner, and D. A. Vroom, "Formation of Magnesium Ions by Charge Transfer," J. Chem. Phys. 55, 3785 (1971).
3. R. F. Stebbings, B. R. Turner, and J. A. Rutherford, "Low-Energy Collisions Between Some Atmospheric Ions and Neutral Particles," J. Geophys. Res. 71, 771 (1966).
4. B. R. Turner, J. A. Rutherford, and R. F. Stebbings, "Charge Transfer Reactions of Nitric Oxide and Atomic and Molecular Ions of Oxygen and Nitrogen," J. Geophys. Res. 71, 4521 (1966).
5. F. A. Wolf and B. R. Turner, "Energy Dependence of the Charge-Transfer Reaction in Thermal and Low-Electron-Volt Region," J. Chem. Phys. 48, 4266 (1968).
6. C. F. Giese, "Strong Focusing Ion Source for Mass Spectrometers," Rev. Sci. Instr. 30, 260 (1959).
7. M. Knudsen, "Kinetic Theory of Gases," Methuen's Monographs on Physical Subjects, 3rd ed., Methuen & Co. Ltd., London, 1950.
8. D. Rapp and W. E. Francis, "Charge Exchange Between Gaseous Ions and Atoms," J. Chem. Phys. 37, 2631 (1962).
9. G. Gioumousis and D. P. Stevenson, "Reactions of Gaseous Molecule Ions with Gaseous Molecules; V. Theory," J. Chem. Phys. 29, 294 (1958).
10. A. L. Schmeltekopf, E. E. Ferguson, and F. C. Fehsenfeld, "Afterglow Studies of the Reactions  $\text{He}^+$ ,  $\text{He}(2^3\text{S})$ , and  $\text{O}^+$  with Vibrationally Excited  $\text{N}_2$ ," J. Chem. Phys. 48, 2966 (1968).
11. R. H. Neynaber, private communication of results obtained using merging beams technique under an ARPA/ONR contract.
12. T. F. O'Malley, "A Simple Model for the High Energy Reaction of  $\text{O}^+$  Ions with  $\text{N}_2$ ," J. Chem. Phys. 52, 3269 (1970).

Preceding page blank

13. R. H. Neynaber, J. A. Rutherford, and D. A. Vroom, "Electronic and Ionic Reactions in Atmospheric Gases," Yearly Technical Summary Report, September 1970 through June 1971, Gulf Radiation Technology Report GULF-RT-A10767, July 1971.
14. W. B. Maier II and E. Murad, "Study of Collisions Between Low Energy  $N^+$  and  $N_2$ : Reaction Cross Sections, Isotopic Compositions, and Kinetic Energies of the Products," J. Chem. Phys. 55, 2308 (1971).
15. J. A. Rutherford, R. F. Mathis, B. R. Turner, and D. A. Vroom, "Formation of Sodium Ions by Charge Transfer," J. Chem. Phys. 56, 4654 (1972).
16. K. Johnson, H. L. Brown, and M. A. Biondi, "Ion-Molecule Reactions Involving  $N_2^+$ ,  $N^+$ ,  $O_2^+$ , and  $O^+$  Ions from 300°K to ~1 eV," J. Chem. Phys. 52, 5080 (1970).
17. F. C. Fehsenfeld and E. E. Ferguson, "Thermal Energy Reaction Rate Constants for  $H^+$  and  $CO^+$  with O and NO," J. Chem. Phys. 56, 3066 (1972).
18. R. F. Stebbings, A. C. H. Smith, and H. Ehrhardt, "Charge Transfer Between Oxygen Atoms and  $O^+$  and  $H^+$  Ions," J. Geophys. Res. 49, 2349 (1964).
19. E. E. Ferguson, F. C. Fehsenfeld, P. D. Goldan, A. L. Schmeltekopf, and H. I. Schiff, "Laboratory Measurement of the Rate of the Reaction  $N_2^+ + O \rightarrow NO^+ + N$  at Thermal Energy," Planet. Space Sci. 13, 823 (1965).

APPENDIX A

FORMATION OF MAGNESIUM IONS BY CHARGE TRANSFER

*Reprinted from:*

THE JOURNAL OF CHEMICAL PHYSICS

VOLUME 53, NUMBER 8

15 OCTOBER 1971

## Formation of Magnesium Ions by Charge Transfer\*

J. A. RUTHERFORD, R. L. MATHIS, B. R. TURNER, AND D. A. VROOM

*Gulf Radiation Technology, A Division of Gulf Energy and Environmental Systems, Incorporated, San Diego, California 92112*

(Received 15 January 1971)

The charge transfer cross sections for several ions in collision with atoms of magnesium to form  $Mg^+$  have been measured in the energy range 1–500 eV. The ions  $O^+$ ,  $N^+$ ,  $N_2^+$ ,  $NO^+$ ,  $O_2^+$ ,  $H_2O^+$ ,  $H_2O_2^+$ ,  $N_2O^+$ , and  $Mg^+$  have been used. The results obtained are analyzed by considering the possibility of resonant or near resonant processes being responsible for the large cross sections obtained for most processes. When the possibility of resonance-type mechanisms does not exist, the cross sections are found to be considerably smaller. The effect of metastable states present in the primary ion beam on the charge transfer cross section is examined. Extrapolation of the measured cross sections to thermal energies has also been performed.

### I. INTRODUCTION

Considerable effort has been devoted to the study of symmetric resonant charge transfer processes in recent years. These studies were, for a large part, prompted by the several theories for resonant charge transfer such as those of Bates,<sup>1</sup> of Rapp and Francis,<sup>2</sup> and of Firsov.<sup>3</sup> More recently, it has been shown that the cross section for asymmetric resonant charge transfer

may have a magnitude and energy dependence similar to those found for the symmetric case.<sup>4</sup> In such cases, it appears that while other reaction channels are often possible, the greatest contribution to the total cross section comes from the channel which results in closest energy resonance between the reactant and product states.

The reactions studied here represent a further test of the above hypothesis since several different reac-

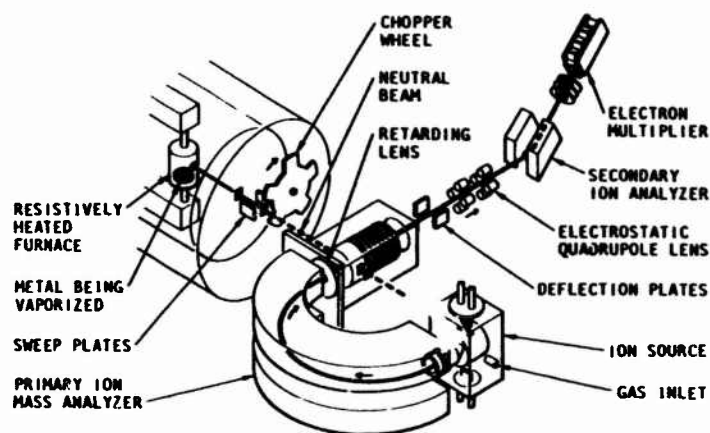


FIG. 1. Crossed ion and neutral beam apparatus.

tions involving the same neutral species are considered. Furthermore, cases where no resonance and near resonance exist are present.

The cross sections obtained also have a practical application with regard to understanding the ionosphere since magnesium is known from rocket studies<sup>5,6</sup> to be among the more prevalent metallic ions in the altitude region ranging from 83 to 112 km. Two properties of these ions result in an atmospheric behavior different from that of the more common  $O_2^+$  and  $NO^+$ . Firstly, they are atomic and hence are not removed by dissociative recombination; secondly, they have ionization potentials below those of all the common atmospheric constituents, and there are, therefore, no neutral species with a significant number density with which these ions may undergo charge transfer. The metallic ions formed in the ionosphere are therefore expected to be long lived.

## II. EXPERIMENTAL

Although the apparatus has been described previously,<sup>7-9</sup> it was felt that the experiment reported here differs sufficiently from past work to warrant a complete description of the machine and a discussion of the experimental procedure.

### A. Primary and Secondary Ion Systems

A schematic of the apparatus is shown in Fig. 1. The primary ions are extracted from an electron bombardment source and mass analyzed at an energy of 75 eV in a  $180^\circ$  magnetic mass spectrometer. After mass analysis, the ions pass through an aperture in an iron plate that shields the magnetic field of the mass analyzer from the succeeding regions of the apparatus. They are then retarded or accelerated to the desired collision energy. The ions next pass through a field-free region before intersecting with the neutral beam. Collimating apertures ensure that, from purely geometrical considerations, all primary ions pass

through the modulated neutral beam (modulated at 100 Hz by mechanical chopping). Secondary ions resulting from collisions between the primary ions and neutrals are extracted along the direction of the primary ion beam by an electric field of approximately 2 V/cm. The ions then enter an electric field where their energy is increased to 1650 eV. Penetration of this accelerating field into the interaction region is reduced by use of a double grid structure. After acceleration, the ions pass through an electrostatic quadrupole lens<sup>10</sup> which forms the entrance slit for the  $60^\circ$  sector magnetic mass spectrometer. The selected ions impinge on the first dynode of a 14-stage CuBe electron multiplier. For magnesium, the most abundant isotope at mass 24 was used when making measurements. The cross sections have been corrected for the isotope effect created by collecting only the 78.6% of the magnesium beam which has mass of 24 amu. The output from the multiplier passes successively through a preamplifier, a 100-Hz narrow-band amplifier, phase-sensitive detector and is then integrated. The output is presented on a chart recorder.

The primary ion beam intensity is measured at the interaction region with a Faraday cup which can be moved into the collision region when desired. The primary ion energy is determined from retarding potential measurements. All surfaces at the interaction region and the Faraday cup are coated with a collidal graphite in alcohol, and the interaction region is normally maintained at a temperature of  $120^\circ\text{C}$  to minimize surface charging.

Because interest in the present work extends down to small collision energies, it was necessary to use only weak extraction fields at the collision region. As a result, the secondary ions were not collected with 100% efficiency. To obtain absolute cross sections for production of various secondary ions, it was necessary, therefore, to determine their over-all detection efficiency. This latter consideration is governed by a

number of factors including the multiplier gain and the efficiency of transmission of the secondary ions from the interaction region to the multiplier.

The gain of the multiplier-amplifier-recorder system is measured by modulating the primary ions prior to their entering the collision region. The ion current signal is first measured with the movable Faraday cup and then, after traversing the secondary mass spectrometer multiplier amplifier system, by the recorder. Transmission of the primary ion through the second mass spectrometer was observed to be 92%. In Table I the system gain for several species of ion impinging upon the multiplier is shown.

The major experimental uncertainty is associated with the collection efficiency for the secondary ions.

TABLE I. System gain for several incident ions.<sup>a</sup>

| Ion mass | Ion species                   | System gain           |
|----------|-------------------------------|-----------------------|
| 1        | H <sup>+</sup>                | $1.0 \times 10^{+12}$ |
| 2        | H <sub>2</sub> <sup>+</sup>   | $1.4 \times 10^{+12}$ |
| 4        | He <sup>+</sup>               | $1.4 \times 10^{+12}$ |
| 12       | C <sup>+</sup>                | $1.5 \times 10^{+12}$ |
| 14       | N <sup>+</sup>                | $1.8 \times 10^{+12}$ |
| 16       | O <sup>+</sup>                | $1.6 \times 10^{+12}$ |
| 18       | H <sub>2</sub> O <sup>+</sup> | $1.7 \times 10^{+12}$ |
| 23       | Na <sup>+</sup>               | $7.7 \times 10^{+12}$ |
| 24       | Mg <sup>+</sup>               | $8.7 \times 10^{+12}$ |
| 28       | N <sub>2</sub> <sup>+</sup>   | $1.0 \times 10^{+12}$ |
| 28       | CO <sup>+</sup>               | $1.1 \times 10^{+12}$ |
| 30       | NO <sup>+</sup>               | $1.0 \times 10^{+12}$ |
| 32       | O <sub>2</sub> <sup>+</sup>   | $1.0 \times 10^{+12}$ |
| 39       | K <sup>+</sup>                | $5.7 \times 10^{+12}$ |
| 40       | Ar <sup>+</sup>               | $6.0 \times 10^{+12}$ |
| 40       | Ca <sup>+</sup>               | $4.7 \times 10^{+12}$ |
| 44       | CO <sub>2</sub> <sup>+</sup>  | $6.7 \times 10^{+12}$ |

<sup>a</sup> For an ion energy of 2.365 V impinging on the multiplier.

The uncertainty arises because collection fields sufficiently large to ensure total collection of the secondary ions cannot be employed due to the influence these fields would exert on the motion of low-energy primary ions. While measurements of the variation of collection efficiency with the strength of the extraction field may readily be made at high primary ion energies, these results are not necessarily relevant to the low-energy regime, where the dynamics of the Mg<sup>+</sup> production may be different. Interpretation of the present data obtained using weak collection fields is therefore based on the assumption that at energies above a few electron volts, the Mg<sup>+</sup> ions are produced by simple electron transfer in collisions involving little momentum transfer and that as a result, the collection efficiency is independent of both the nature and energy of the primary ions. It is implicit in this assumption that the energy defect in the reaction is small, since energy not expended in excitation of the products must appear as

TABLE II. Collection efficiency of secondary ions produced by charge exchange at interaction region.

| Reactants                                   | Cross section <sup>a</sup><br>(10 <sup>-16</sup> cm <sup>2</sup> ) | Secondary ion<br>collection<br>efficiencies <sup>b</sup> (%) |
|---------------------------------------------|--------------------------------------------------------------------|--------------------------------------------------------------|
| N <sub>2</sub> <sup>+</sup> :N <sub>2</sub> | 29.0                                                               | 80                                                           |
| O <sub>2</sub> <sup>+</sup> :O <sub>2</sub> | 15.5                                                               | 68                                                           |
| N <sup>+</sup> :O <sub>2</sub>              | 16.5                                                               | 74                                                           |

<sup>a</sup> The primary ions were produced by bombardment with 40-eV electrons. The ion energy used for these measurements was 400 eV.

<sup>b</sup> Assuming cross sections listed (taken as most representative of those reported in the literature).

kinetic energy and therefore would influence the collection efficiency.

A number of charge transfer reactions for which absolute cross sections had been previously determined were tabulated. Using the same experimental conditions and the detection efficiencies deduced from measurements of the primary beam, as well as the same signal strengths and detector sensitivity, the collection efficiency of our instrument is obtained by comparing our measured cross sections with the best tabulated values. The efficiencies so obtained, and illustrated in Table II, varied by 20%; this may represent a real variation in the collection efficiency or simply reflect the discrepancies in the published cross-section values. In the present work, a collection efficiency of 75% is used in the evaluation of the cross sections from measurements of the neutral beam density, the primary ion beam intensity, the dimensions of the neutral beam at the interaction zone, the system gain, and the recorded signal.

An over-all analysis of all possible systematic errors has been performed. From this study, a possible error of  $\pm 30\%$  is placed on the absolute charge transfer cross sections for the higher reaction energies. This error may increase to as much as a factor 2 at the lowest impact energies.

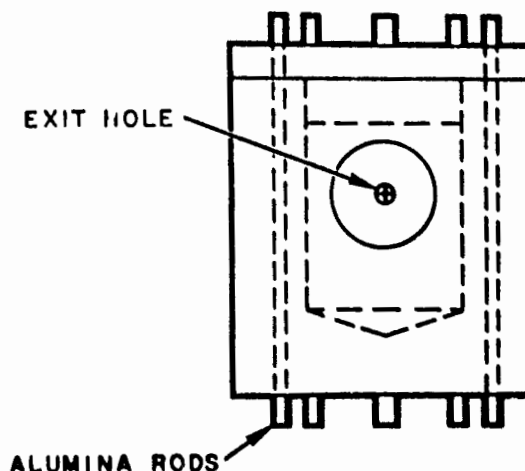


FIG. 2. Neutral beam Knudsen cell furnace.

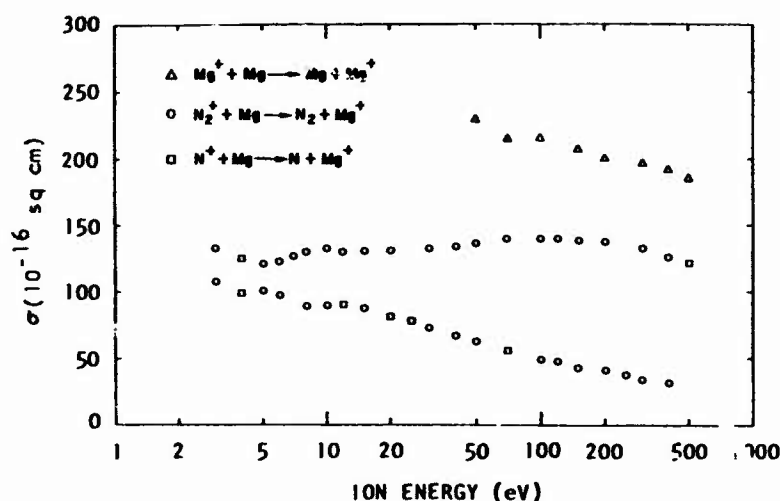


FIG. 3. Charge transfer cross sections for  $Mg^+$ ,  $N_2^+$ , and  $N^+$  ions impinging on neutral Mg as a function of the energy of the incident ion.

### B. Neutral Beam Formation and Measurement

The neutral atom beams originate in a heated molecular effusion source (a Knudsen cell). A sketch of this cylindrically shaped furnace is shown in Fig. 2. Tantalum was used for the construction of the Knudsen cell. The cavity is surrounded by  $\frac{3}{16}$ -in. walls and is heated with a tantalum wire filament which passes through five evenly spaced holes. The heater wires are insulated by hollow alumina tubing. A lid of tantalum is held tightly in place by screws. The temperature is measured with a chromel alumel thermocouple mounted inside the furnace wall. The chromel alumel thermocouple was shown through repeated tests to be reproducible even after having been removed and replaced.

The cosine law of molecular effusion<sup>11</sup> was applied to determine the beam density knowing the equilibrium vapor pressure of the magnesium in the Knudsen cell at a particular temperature. The number density,  $n$ , in the beam at the interaction region is then computed under effusive flow condition to be

$$n = N_0 a / 4\pi r^2, \quad (1)$$

where  $N_0$  is the number density in the furnace,  $a$  is the area of the aperture in the furnace, and  $r$  is the distance from the aperture to the interaction region.

The vapor pressure of magnesium is greater than 1 torr before its melting point is reached. As a consequence, sufficient pressure could be obtained in the Knudsen cell without melting the solid. Magnesium reacts slowly with air, allowing the problem of oxidation to be kept to a minimum.

Calculation of the beam density with Eq. (1) has been used for the preliminary analysis of the data. One difficulty associated with this method is that the temperature must be quite accurately known as the pressure is a sensitive function of the temperature. A small temperature gradient between the location of the

thermocouple and the inside of the chamber could result in a large error in the calculated beam density and thus the cross section. In addition to this, any temperature gradient in the volume of the furnace containing the metal vapor would result in a corresponding uncertainty in the furnace pressure and thus in the neutral beam density.

To ensure that our temperature measurements were accurate and that our oven behaved correctly, a complimentary technique was employed. This method utilized neutron activation analysis to determine the number of atoms deposited into the collector by the neutral beam in a known time period. In the initial attempts to collect the atom beam, a small polyethylene cylinder, was used. It was found that the magnesium atoms did not stick in this collector but scattered away. To overcome this problem, a collector consisting of a polyethylene bag attached to the end of the polyethylene cylinder was used. This assembly was located so that all the beam passing through the collision region entered the collector. Commercially available "Baggies" were chosen as the type of polyethylene bags since they were found to be both free of contamination and thin walled. After the deposition of approximately 100  $\mu$ g of magnesium, the bag was removed and sent to Gulf Radiation Technology Neutron Activation Analysis Facility for measurement. This method gave results in close agreement with the density calculated from the molecular effusion considerations. It is interesting that even though magnesium is a condensible beam, several reflections were required before total sticking to a room-temperature surface could be achieved.

### III. RESULTS

The cross sections for charge transfer between neutral magnesium and the nine ions investigated were determined over the energy range 1–500 eV. These cross sections are presented here in graphical form

FIG. 4. Charge transfer cross sections for  $N_2O^+$ ,  $H_2O^+$ , and  $NO^+$  ions impinging on neutral Mg as a function of the energy of the incident ion.

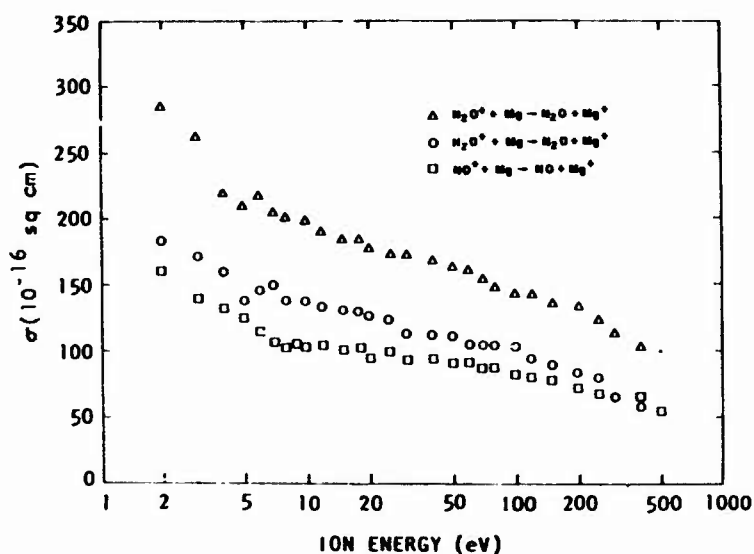


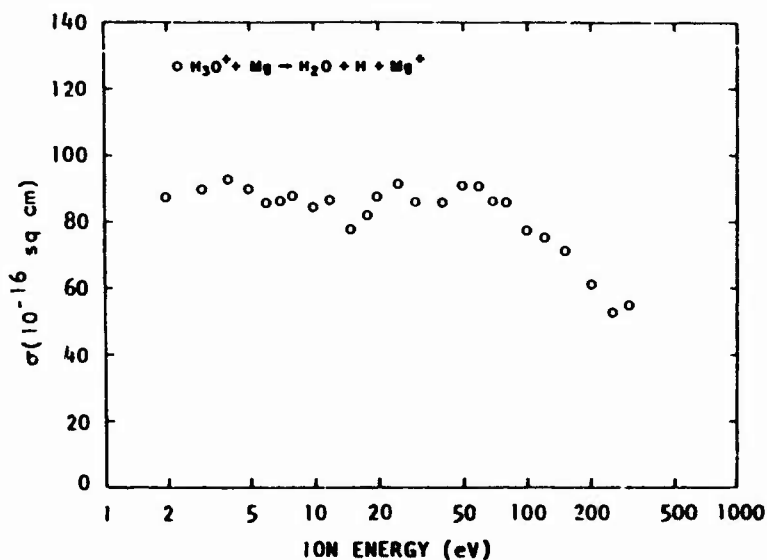
TABLE III. Recombination energies and relevant energies of reactants and products cited in the text.\*

| Species and ground state     | Excited neutral states and energy above ground state (eV)              | Ground ionic state and ionization potential (eV) | Ion state and energy above ionic ground state (eV) |
|------------------------------|------------------------------------------------------------------------|--------------------------------------------------|----------------------------------------------------|
| $Mg(3s^2, ^1S_0)$            |                                                                        | $(3s, ^1S_{1/2}), 7.644$                         | $(3p, ^3P_{1/2}), 4.419$                           |
| $N_2(X^1\Sigma_g^+), r_{eq}$ | $(B^1\Sigma_u^-), 8.164$<br>$(B^3\Pi_g), 7.353$<br>$(B^3\Pi_g), 7.987$ | $(X^2\Sigma_g^+), 15.580$                        | $(X^2\Sigma_g^+), 0.270$                           |
| $N(2p^2, ^4S_{3/2})$         | $(2p^1, ^2D_{3/2}), 2.382$                                             | $(2p^2, ^2P_0), 14.352$                          |                                                    |
| $O_2(X^2\Sigma_g^-), r_{eq}$ |                                                                        | $(X^3\Pi), 12.063$                               | $(a^4\Pi_u), 4.038$                                |

\* Atomic levels obtained from C. Moore, Natl. Bur. Std. (U. S.) Circ. 467, Vol. 1 (1949). Molecular levels obtained from F. R. Gilmore, "Basic Energy Level and Equilibrium Data for Atmospheric Atoms and Molecules,"

The Rand Corporation, Research Memorandum, R.M. 5201-ARPA, March 1967.

FIG. 5. Charge transfer cross sections for  $H_2O^+$  ions impinging on neutral Mg as a function of the energy of the incident ion.





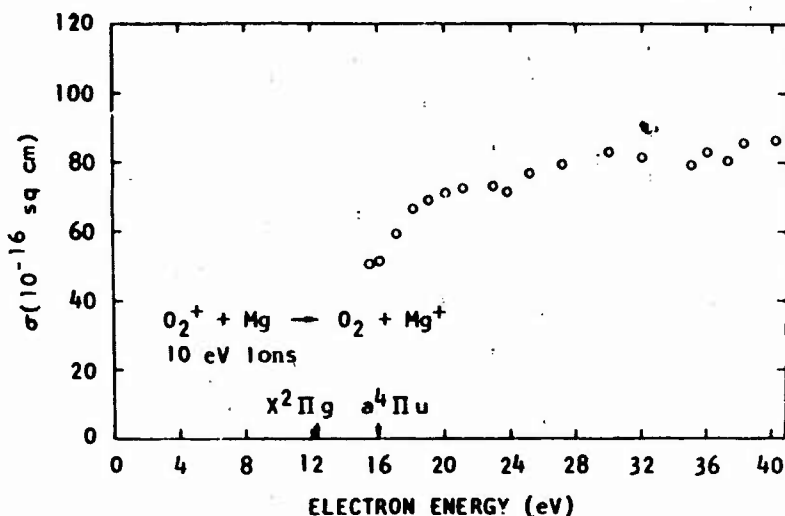


FIG. 6. Dependence of the charge transfer cross section upon the source electron energy for the reaction  $O_2^+ + Mg \rightarrow O_2 + Mg^+$ .

since this type of representation aids the discussion of the data. In general, the reactions have been grouped such that processes which exhibit similar structure and which have comparable cross sections appear in the same figure.

Figure 3 gives the cross section for charge transfer for  $N_2^+$  and  $N^+$  ions incident on neutral magnesium. The symmetric resonant reaction  $Mg^+ - Mg$  is also shown for comparison.

The cross sections for three other ions ( $N_2O^+$ ,  $H_2O^+$ , and  $NO^+$ ) incident on Mg are shown in Fig. 4. Like the previous three reactions, these processes have a large cross section. The smallest cross section observed was that for  $O^+$  on magnesium. The results for  $H_2O^+$  are given in Fig. 5.

Figure 6 illustrates the variation in cross section for charge transfer between  $O_2^+$  and magnesium as the number of excited states present in the primary ion

beam is varied. Data of this type are obtained by changing the energy of the electrons in the primary ion source and measuring the charge transfer cross section at a fixed ion-impact energy (in this case 10-eV ions). When the electron energy is such that no electronically excited ion states can be formed in the  $O_2^+$  beam (less than 16 eV), the cross section for charge transfer is seen to be considerably lower than when excited states are present (electron energies greater than 16 eV). Similar studies involving both  $O^+$  and  $NO^+$ , which have metastable ionic states, showed little dependence of the cross section on primary ion source electron energy. From this we can conclude that the cross sections for charge exchange must be similar for both the ground and metastable ionic states.

The cross sections for charge exchange between the ground state of  $O_2^+$  and the metastable  $O_2^+$  state with Mg are shown in Fig. 7. The curve for the ground

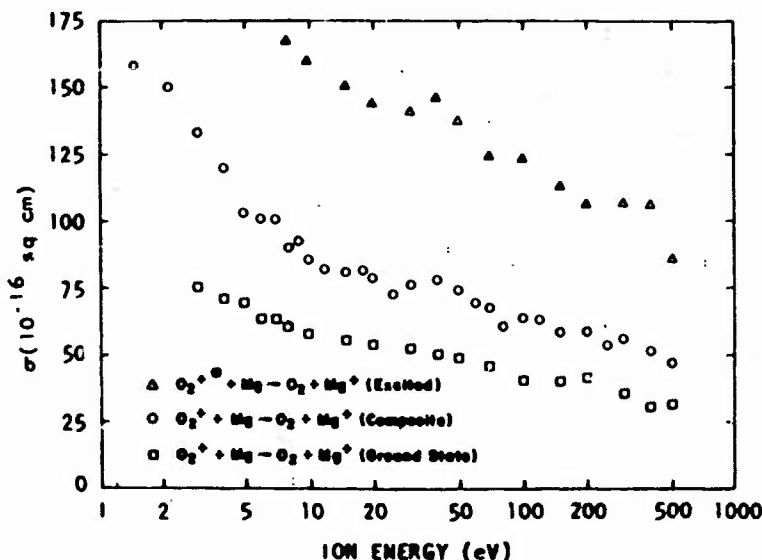


FIG. 7. Charge-transfer cross sections involving excitation for  $O_2^+$  ions with Mg as a function of the incident ion energy. The cross section is shown for ground-state  $O_2^+$  ions, for  $O_2^+$  ions in the mixture of states (composite) which results when 40-eV electrons impinged on  $O_2$  to form the  $O_2^+$ , and for the excited states in the composite alone, i.e., after the contribution of the ground-state ions in the composite has been removed.

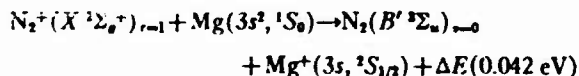
state is obtained using ions formed with 16-eV electrons. The curve for the composite beam of ground and metastable ions is obtained using 40-eV electrons in the ion source. In order to determine the cross section for the excited state, the ratio of the ground to metastable state concentration in the beam must be known. This ratio is determined in a separate experiment using a technique previously developed in this laboratory,<sup>12</sup> which showed that for 40-eV electrons impacting on  $O_2$ , 32% of the ions formed are in metastable states.

#### IV. DISCUSSION

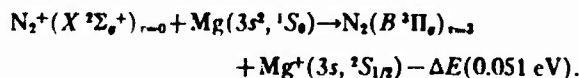
In attempting to interpret the results obtained for the charge transfer reactions, the major difficulty arises in accounting for the excess energy released. In the discussion of the results given below an attempt has been made to correlate the magnitude of the charge transfer cross section with the formation of excited states of the products of the collision. The resultant processes should be considered as only possible mechanisms. Recombination energies and energy levels quoted in the discussion below are given in Table III.

In the symmetric charge transfer process between Mg and  $Mg^+$ , exact resonance must exist and as a consequence a large cross section would be expected. In Fig. 3, the results for this process show that the cross section is indeed large. The slope of the curve is similar to that predicted by Rapp and Francis<sup>2</sup> but the magnitude of the cross section is twice the predicted results. Previous resonant charge transfer measurements for  $Li^+ + Li$ <sup>13</sup> and  $Cs^+ + Cs$ <sup>14</sup> have also been found to give cross sections larger than predicted by the theory.

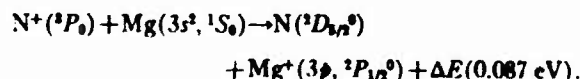
The magnitudes of the cross sections for the reaction of  $N_2^+$  and  $N^+$  on Mg are both similar to that for the symmetric case. Such a result is indicative of a near resonance mechanism for the reaction which would probably leave the  $N_2$  or N in an excited state. Two possible nearly resonant routes for electron capture to form excited  $N_2$  states are



and



The possible mechanisms available for the reaction of  $N^+$  with Mg are less complex since fewer possible states of the product N atom exist in the energy regime of interest. One possible mechanism which is nearly resonant is



This reaction results in both products being left in

excited states. It is interesting to note that if the N neutral formed is in the excited ( $^3D_{3/2}$ ) state the energy released in the neutralization process is 12.15 eV. This energy is very similar to the ionization potential  $O_2$  and the reaction of  $O_2^+$  on Mg might therefore be expected to be similar to that given above. This reaction will be discussed below.

The cross sections for charge exchange of  $N_2O^+$ ,  $H_2O^+$ , and  $NO^+$  in collisions with magnesium can be seen in Fig. 4 to be smoothly increasing with decreasing ion energy. Comparison of these results with those for  $N_2^+$  and  $N^+$  in Fig. 3 shows that the cross sections are of the same order of magnitude, indicating that processes having a small energy defect may again predominate. For the cases of  $N_2O^+$  and  $H_2O^+$ , possible reactions are difficult to determine because of the lack of spectroscopic information available on the location of the excited states of these species.

The reaction of  $NO^+$  with magnesium may be of importance in the upper atmosphere because of the large concentration of  $NO^+$ . As for the reactions discussed above, charge exchange between Mg and  $NO^+$  is exothermic, in this case by 1.61 eV. Electronic levels that will allow near resonance do not exist in either the product ion or neutral, and vibrational excitation of the neutral NO ground state may therefore be expected. Since the internuclear distance in  $NO^+$  is less than in NO, the Franck-Condon transition zone for processes leading to production of NO from  $NO^+$  overlaps many vibrational levels of the neutral product. Such a configuration favors the formation of products with considerable vibration excitation.

The recombination energy for  $H_2O^+$  is about 7 eV,<sup>9</sup> and as a consequence this process would be endothermic for ground-state ions. Figure 5 shows that the measured cross section is both appreciable and exhibits the shape expected for a near resonant process. This observation can be justified by either the presence of excited ions in the primary beam or a slightly higher recombination energy for the  $H_2O^+$ .

The case of  $O^+$  on Mg differs from that for the other atomic ion,  $N^+$ , in that no energy level combination in the secondary neutral or ion will allow near resonance. This fact probably accounts for the low measured cross section. (Data with poor signal-to-noise ratio suggest a cross-section value of less than  $20 \times 10^{-18} \text{ cm}^2$ .)

The results for  $O_2^+$  on Mg, seen in Fig. 7, again indicate that near resonant processes may be important. The cross sections for both the ground and excited states show a rapid increase with decreasing ion energy. If the  $O_2^+$  ground-state species recombines to give  $O_2$  in the ground state, the recombination energy is nearly equal to that for recombination of  $N^+$  ground state to form  $N(^3D_{3/2})$ . This suggests that the mechanisms for the  $O_2^+$  ground state recombination could be

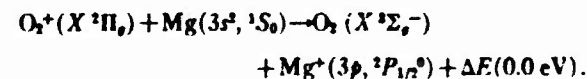


TABLE IV. Calculated cross sections and rate coefficients.

| Reaction                                                                     | 300°K                                                |                                                              | 600°K                                                |                                                              | 1200°K                                               |                                                              |
|------------------------------------------------------------------------------|------------------------------------------------------|--------------------------------------------------------------|------------------------------------------------------|--------------------------------------------------------------|------------------------------------------------------|--------------------------------------------------------------|
|                                                                              | Cross section<br>$\times 10^{20}$<br>cm <sup>2</sup> | Rate coefficient<br>$\times 10^{10}$<br>cm <sup>3</sup> /sec | Cross section<br>$\times 10^{20}$<br>cm <sup>2</sup> | Rate coefficient<br>$\times 10^{10}$<br>cm <sup>3</sup> /sec | Cross section<br>$\times 10^{20}$<br>cm <sup>2</sup> | Rate coefficient<br>$\times 10^{10}$<br>cm <sup>3</sup> /sec |
| Mg <sup>+</sup> +Mg                                                          | 63.2                                                 | 51.0                                                         | 56.0                                                 | 63.9                                                         | 50.2                                                 | 81.0                                                         |
| N <sup>+</sup> +Mg                                                           | 14.3                                                 | 12.2                                                         | 14.4                                                 | 17.3                                                         | 14.1                                                 | 24.0                                                         |
| O <sub>2</sub> <sup>+</sup> (composite)+Mg                                   | 27.4                                                 | 20.1                                                         | 21.5                                                 | 22.4                                                         | 17.7                                                 | 26.0                                                         |
| O <sub>2</sub> <sup>+</sup> (X <sup>2</sup> Σ <sub>g</sub> <sup>-</sup> )+Mg | 16.8                                                 | 12.3                                                         | 13.2                                                 | 13.8                                                         | 11.1                                                 | 16.3                                                         |
| N <sub>2</sub> <sup>+</sup> +Mg <sup>a</sup>                                 | 10.7                                                 | 7.24                                                         | 11.3                                                 | 10.8                                                         | 12.1                                                 | 16.3                                                         |
| NO <sup>+</sup> +Mg                                                          | 10.8                                                 | 8.11                                                         | 12.7                                                 | 13.4                                                         | 13.6                                                 | 20.4                                                         |
| N <sub>2</sub> O <sup>+</sup> +Mg                                            | 13.4                                                 | 21.7                                                         | 31.8                                                 | 31.1                                                         | 31.3                                                 | 43.2                                                         |

<sup>a</sup> The reliability of the N<sub>2</sub><sup>+</sup>+Mg extrapolation is not as high as for the other reactions shown.

For the excited oxygen molecular ion ( $\sigma^4\Pi_u$ ), sufficient excess energy exists to cause dissociation of the resultant oxygen molecule. Since many dissociative curves exist through which such a process might proceed, this may be a probable mechanism, and could help to explain why the excited state has a much larger cross section for charge transfer than the ground state.

The charge transfer processes described above may be broken into two groups, those involving molecular ions and those involving atomic ions. Consideration of the results shows that all the molecular species give cross sections for reaction whose energy dependence exhibits the behavior that might be expected for resonant or near resonant processes. Processes with a small energy defect can easily be realized with molecular species because of the multitude of vibration rotation levels which lie above every electronic state. From this point of view, molecules can be considered as possessing a near continuum of states available for reaction.

For the two atomic species studied, one case of near resonant behavior and one case of nonresonant behavior was observed. N<sup>+</sup> charge exchange with Mg has a large cross section and the mechanism proposed for this reaction shows that near resonance can be obtained by assuming both the N and Mg<sup>+</sup> are formed in excited states. For atomic oxygen no such combination of states exists and the cross section for the process is small.

It is interesting to note that low excited ionic states exist for magnesium. The presence of such a low-lying state allows the N<sup>+</sup> charge exchange to occur. Work similar to that described for magnesium has been done in our laboratory using sodium as the neutral target. In this case, the sodium ground-state ion, since it is devoid of loosely bound electrons, has no low-lying levels. As a consequence, near resonance cannot be obtained for either N<sup>+</sup> or O<sup>+</sup>. Our experiments have shown that the cross sections for N<sup>+</sup> and O<sup>+</sup> on Na

are small. These results will be the subject of a future publication.

#### A. Extrapolation

Using our experimental technique, interaction energies of less than 1 eV are difficult to obtain. Nevertheless, considerable interest in reactions of this nature lies in the energy range from thermal to 1 or 2 eV. In order to obtain cross-section values in this region, an extrapolation method developed in this laboratory has been used.<sup>15</sup> This extrapolation method combines the energy dependence of the Rapp-Francis<sup>2</sup> resonant charge transfer theory with the energy dependence of the Gioumousis-Stevenson<sup>16</sup> complex formation model.

The general formula developed for the total charge exchange cross section takes into account the probabilities for charge exchange to occur both when a complex is formed and when it is not, and also corrects for nonrectilinear orbit when complex formation does not occur. The method can be formulated as follows. The total charge exchange cross section  $\sigma$  will be given by

$$\sigma = f\sigma_2 \text{ when } 2\sigma_1 \leq \sigma_2 \quad (2)$$

or by

$$\sigma = (f - \frac{1}{2})\sigma_2 + \sigma_1 \text{ when } 2\sigma_1 > \sigma_2. \quad (3)$$

Here  $f$  is the fraction of collisions resulting in complex formation which decays into the charge exchange channel.  $\sigma_2$  is the Gioumousis-Stevenson complex formation model cross section and is represented by

$$\sigma_2 = \pi(2e^2\alpha/E)^{1/2}, \quad (4)$$

in which  $e$  is the electronic charge,  $\alpha$  is the polarizability of the neutral, and  $E$  is the barycentric interaction energy. Also,  $\sigma_1$ , given by

$$\sigma_1 = \sigma_0[1 + (\sigma_2/4\sigma_0)^2], \quad (5)$$

represents the Rapp-Francis resonant charge exchange formula modified to take account of the curved orbits of the reactants. The form of the Rapp-Francis formula is

$$\sigma_0^{1/2} = A - B \log E, \quad (6)$$

where  $A$  and  $B$  are constants.

The extrapolation is carried out by fitting the modified Rapp-Francis formula [Eq. (5)] to the high-energy portion of the measured data, that is, in the region where complex formation should be negligible. The calculated curve is then extended to lower energies using the test given with Eqs. (2) and (3) to evaluate when the measured data deviate from the form of Eq. (5). In this manner the contribution of complex formation is determined and the calculated curve can be extended to energies below those measured. A computer program has been developed to perform the calculations.

The extrapolation technique was developed by assuming that the relative abundance of the various products emerging from the capture-formed complex is independent of the relative kinetic energy of the reactants; that is,  $f$  remains constant. If this condition is not met, the technique will not give valid rate coefficients at near thermal energies. In general, whether or not the extrapolation technique is valid can be seen by observing if the calculated cross-section curve fits the experimental data to the lowest energy of measurement. In the present studies, the extrapolation is found to be valid for all systems measured except  $H_2O^+$  and  $H_2O^+$  on magnesium.

Table IV gives the results obtained for the extrapolation of the  $N^+$ ,  $N_2^+$ ,  $NO^+$ , and  $N_2O^+$  to thermal

energies. Cross sections and rate constants are given for three temperatures.

#### ACKNOWLEDGMENTS

The authors wish to acknowledge the benefit of discussions with our colleagues, particularly James K. Layton, Dr. R. F. Stebbings, and Dr. J. W. McGowan. Special recognition is due Dr. D. M. J. Compton for his suggestion that activation analysis be used to determine beam densities.

\* This work was supported by the Defense Atomic Support Agency under Contract DASA01-69-C-0044.

<sup>1</sup> D. R. Bates, in *Atomic and Molecular Processes*, edited by D. R. Bates (Academic, New York, 1962).

<sup>2</sup> D. Rapp and W. E. Francis, *J. Chem. Phys.* **37**, 2631 (1962).

<sup>3</sup> O. B. Firsov, *Zh. Eksp. Teor. Fiz.* **21**, 100 (1951).

<sup>4</sup> R. F. Stebbings and J. A. Rutherford, *J. Geophys. Res.* **73**, 1035 (1968).

<sup>5</sup> R. S. Narcisi and A. B. Bailey, *J. Geophys. Res.* **70**, 3687 (1965).

<sup>6</sup> R. A. Goldberg and L. J. Blumle, *J. Geophys. Res.* **75**, 133 (1970).

<sup>7</sup> R. F. Stebbings, B. R. Turner, and J. A. Rutherford, *J. Geophys. Res.* **71**, 771 (1966).

<sup>8</sup> B. R. Turner, J. A. Rutherford, and R. F. Stebbings, *J. Geophys. Res.* **71**, 4521 (1966).

<sup>9</sup> B. R. Turner and J. A. Rutherford, *J. Geophys. Res.* **73**, 6751 (1968).

<sup>10</sup> C. F. Geise, *Rev. Sci. Instr.* **30**, 260 (1959).

<sup>11</sup> M. Knudsen, *Ann. Physik* **28**, 75 (1909); **28**, 999 (1909).

<sup>12</sup> B. R. Turner, J. A. Rutherford, and D. M. J. Compton, *J. Chem. Phys.* **48**, 1602 (1968); R. F. Malhis, B. R. Turner, and J. A. Rutherford, *ibid.* **49**, 2051 (1968).

<sup>13</sup> D. C. Lorents, G. Black, and O. Heinz, *Phys. Rev.* **137**, 1049 (1965).

<sup>14</sup> L. L. Marino, A. C. H. Smith, and E. Caplinger, *Phys. Rev.* **128**, 2243 (1962).

<sup>15</sup> F. A. Wolf and B. R. Turner, *J. Chem. Phys.* **48**, 4226 (1968).

<sup>16</sup> G. Gioumoussis and D. P. Stevenson, *J. Chem. Phys.* **29**, 294 (1958).

APPENDIX B  
EFFECT OF METASTABLE  $O^+(^2D)$  ON REACTIONS  
OF  $O^+$  WITH NITROGEN MOLECULES

Preceding page blank

Effect of Metastable  $O^+(^2D)$  on Reactions of  $O^+$  with Nitrogen Molecules\*

J. A. RUTHERFORD AND D. A. VROOM

Gulf Radiation Technology, A Division of Gulf Energy and Environmental Systems Company, San Diego, California 92112

(Received 26 July 1971)

Laboratory measurements indicate that the metastable ions of  $O^+$  in reaction with  $N_2$  in the low-energy range (14 eV) react to form principally  $N_2^+$ , while the ion-molecule reaction to form  $NO^+$  has a very small probability. The ground-state  $O^+$  ion reacts mainly to form  $NO^+$ . The abundance of metastable  $O^+(^2D)$  ions was determined using the observation that  $O^+(^2D) + N_2$  has a small cross section for forming  $NO^+$ . The ion energy dependence for both reactions has been measured within the energy range 1.0–500 eV.

The ion-molecule reaction most widely dealt with by aeronomists has been that involving  $O^+$  in collision with  $N_2$  to form  $NO^+$ . The effect of excited states of  $O^+$  on the rate of this reaction has been open to question. Dalgarno<sup>1</sup> has pointed out that in the  $F$  region  $O^+(^2D)$  ions are lost principally by collisions with neutral  $O_2$  and  $N_2$ . An indication that the excited states may not be of importance in the formation of  $NO^+$  was reported by Stebbings *et al.*<sup>2</sup> who noted there was little change in the cross section for  $O^+ + N_2 \rightarrow NO^+ + N$  when excited states of  $O^+$  ions were introduced into the beam. The results reported here will show that the cross section for the reaction involving the excited atomic ion [ $O^+(^2D) + N_2 \rightarrow NO^+ + N$ ] is in fact very small. Furthermore, we will indicate that the principal channel for these reactants results in production of  $N_2^+$  which is probably formed in the ( $A\ ^2\Pi_u, v=1$ ) state.

The apparatus employed for the cross-section measurements has been described previously.<sup>2,3</sup> In this instrument, the primary ions are formed in an electron bombardment ion source, the electron energy of which can be carefully controlled. These ions are extracted from the source, mass analyzed, and accelerated or retarded to the desired energy. This ion beam then crosses a modulated neutral beam (modulated at 100 Hz), in this case  $N_2$ . The products of collisions between the ion and neutral beams are extracted along the direction of the primary ion beam, accelerated, focussed, and mass analyzed in a second mass spectrometer. The selected ions are then detected using an electron multiplier coupled with lock-in amplifier techniques.

The neutral beam is formed by effusion from a room-temperature orifice and modulated by mechanical chopping. The neutral beam density is determined by measuring the pressure in the neutral source with a differential pressure manometer and calculating the effusion from this source under known geometrical conditions.

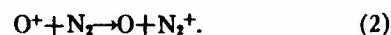
The ratio of the metastable electronic states to the ground state can be varied by careful control of the energy of the ionizing electrons in the primary ion source. When the electron energy is below the threshold for excited-state formation, no excited states can be formed and the resultant beam will be composed

entirely of ground-state ions. As the ionizing electron energy is increased metastable ions will appear in the beam.

Two reactions have been studied in detail here. These are



and



The effects of metastable  $O^+$  ions in the primary ion beam can be seen for Reaction (1) from Fig. 1. Here the relative probability for forming  $NO^+$  in collisions

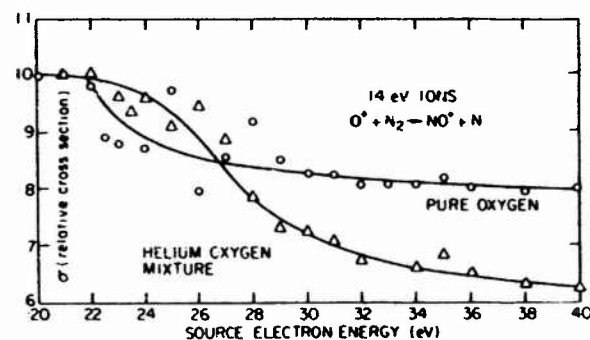


Fig. 1. Graphic representation of the decrease in the relative cross section for formation of  $NO^+$  ions from  $O^+$  impinging on  $N_2$  as a function of the ion source electron energy. The ion-neutral interaction energy is 14 eV. The open circles represent the case for pure  $O_2$  in the source while the open triangles represent the case for an  $O_2/He$  mixture.

between  $O^+$  and  $N_2$  is plotted as a function of the electron energy used to form the  $O^+$  ion. Two cases are shown: one where pure oxygen is used in the ion source and the other where the source contained 1%  $O_2$  in pure helium. The latter case has been included since it gives an enhancement in the number of metastable  $O^+$  ions in the beam and therefore better illustrates our conclusions. This enhancement arises because helium ions formed in the source will undergo a dissociative charge-transfer process with  $O_2$  to yield the metastable  $O^+(^2D)$ . Note that the  $NO^+$  data in Fig. 1 have been normalized to a value of 10 at 21 eV. This is below the threshold of 22 eV required for production of  $O^+(^2D)$  from molecular oxygen if the forma

tion of O<sup>+</sup>(<sup>2</sup>D) from pair production is neglected. This latter process is known to have a small cross section. Examination of the curves shows that for the formation of NO<sup>+</sup>, the relative cross section normalized on the total O<sup>+</sup> current starts to decrease

TABLE I. Cross section for O<sup>+</sup>+N<sub>2</sub>→NO<sup>+</sup>+N.

| Laboratory energy (eV) | Center-of-mass kinetic energy (eV) | Cross section (units of 10 <sup>-16</sup> cm <sup>2</sup> ) |
|------------------------|------------------------------------|-------------------------------------------------------------|
| 1.2                    | 0.76                               | 1.3                                                         |
| 1.4                    | 0.89                               | 1.2                                                         |
| 1.5                    | 0.95                               | 1.3                                                         |
| 1.7                    | 1.08                               | 1.6                                                         |
| 2.0                    | 1.27                               | 1.5                                                         |
| 2.2                    | 1.40                               | 1.7                                                         |
| 2.5                    | 1.59                               | 1.8                                                         |
| 2.7                    | 1.72                               | 2.0                                                         |
| 3.0                    | 1.91                               | 2.1                                                         |
| 3.2                    | 2.04                               | 2.2                                                         |
| 3.5                    | 2.23                               | 2.6                                                         |
| 4.0                    | 2.55                               | 2.8                                                         |
| 4.5                    | 2.86                               | 2.9                                                         |
| 5.0                    | 3.18                               | 3.0                                                         |
| 6.0                    | 3.82                               | 3.4                                                         |
| 7.0                    | 4.45                               | 3.6                                                         |
| 8.0                    | 5.09                               | 4.0                                                         |
| 9.0                    | 5.73                               | 3.8                                                         |
| 10.0                   | 6.36                               | 4.3                                                         |
| 11.0                   | 7.00                               | 4.6                                                         |
| 12.0                   | 7.64                               | 4.2                                                         |
| 13.5                   | 8.27                               | 4.4                                                         |
| 14.0                   | 8.91                               | 4.3                                                         |
| 15.0                   | 9.55                               | 4.0                                                         |
| 16.0                   | 10.18                              | 3.8                                                         |
| 17.0                   | 10.82                              | 3.5                                                         |
| 18.0                   | 11.45                              | 3.2                                                         |
| 19.0                   | 12.09                              | 2.7                                                         |
| 20.0                   | 12.73                              | 2.2                                                         |
| 21.0                   | 13.36                              | 1.8                                                         |
| 22.0                   | 14.00                              | 1.5                                                         |
| 23.0                   | 14.64                              | 1.3                                                         |
| 24.0                   | 15.27                              | 1.0                                                         |
| 25.0                   | 15.91                              | 0.80                                                        |
| 26.0                   | 16.55                              | 0.65                                                        |
| 27.0                   | 17.18                              | 0.53                                                        |
| 28.0                   | 17.82                              | 0.44                                                        |
| 30.0                   | 19.09                              | 0.34                                                        |
| 32.0                   | 20.36                              | 0.22                                                        |
| 34.0                   | 21.64                              | 0.15                                                        |
| 35.0                   | 22.27                              | 0.15                                                        |

in the case of pure oxygen above the threshold for O<sup>+</sup>(<sup>2</sup>D) indicating that the presence of this excited state depletes the number of ground-state particles available for reaction. This same result is seen for the helium oxygen mixture except that the effect is not seen until slightly higher in energy due to the

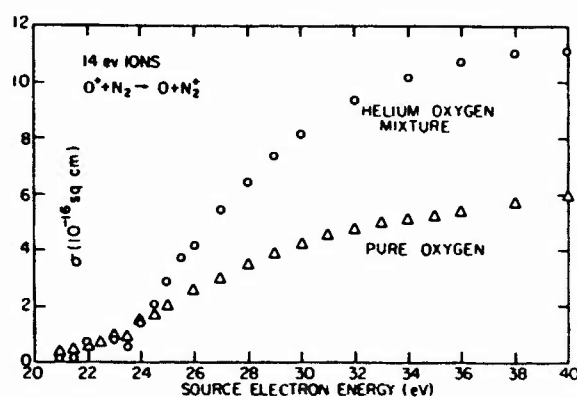


FIG. 2. Observed cross section for the charge-transfer reaction O<sup>+</sup>+N<sub>2</sub>→O+N<sub>2</sub><sup>+</sup> as a function for the ion source electron energy. The ion-neutral interaction energy is 14 eV. The open triangles represent the case for pure O<sub>2</sub> in the source while the open circles represent the case for an O<sub>2</sub>/He mixture.

excited state not being formed in significant concentration until above the ionization threshold for helium.

The electron energy dependence for the reaction O<sup>+</sup>+N<sub>2</sub>→O+N<sub>2</sub><sup>+</sup> is given in Fig. 2. The cross section shown in this figure (the observed cross section) is obtained using the total O<sup>+</sup> current. An effect opposite to that seen in Fig. 1 is observed here. In the curve for pure O<sub>2</sub> it is noted that the observed cross section for forming N<sub>2</sub><sup>+</sup> is very small for electron energies below the O<sup>+</sup>(<sup>2</sup>D) threshold and then increases as the number of excited states is increased. The effect is the same for the oxygen-helium mixtures below the threshold for ionization of helium but is more pronounced above this point as more excited states are then present. It must be noted that all the data shown in the figures are for a fixed ion-neutral interaction energy of 14 eV and illustrate the change which this cross section undergoes as the number of excited states in the beam is varied. An

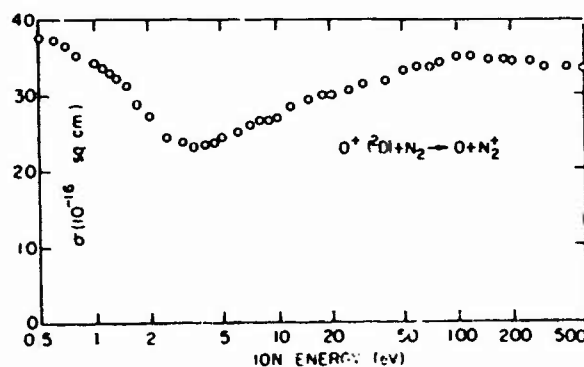
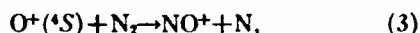


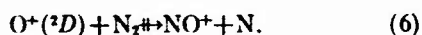
FIG. 3. Charge transfer cross section for O<sup>+</sup>(<sup>2</sup>D)+N<sub>2</sub>→O+N<sub>2</sub><sup>+</sup> as a function of the ion energy in the laboratory system.

interaction energy of 14 eV was chosen because the ion-molecule cross-section curve peaks at this value.

Examination of the figures allows the following conclusions to be drawn:



That is, Fig. 1 shows that  $\text{NO}^+$  is formed below the threshold for excited  $\text{O}^+$  ions [Reaction (3)]. Similarly, Fig. 2 shows that below the  $\text{O}^+(^2D)$  threshold very little  $\text{N}_2^+$  is formed [Reaction (4)], but above the onset of the excited state,  $\text{N}_2^+$  is readily formed [Reaction (5)]. Using the above information coupled with previously obtained results, we will show that



Assume that the cross section for this process is small compared to that for Reaction (3). Now since the observed cross section  $\sigma$  for any process can be written as

$$\sigma = \sum_n \sigma_n f_n, \quad (7)$$

where  $\sigma_n$  is the cross section for reactant ions in state  $n$  present in fractional abundance  $f_n$ , we can write our total cross section for formation of  $\text{NO}^+$  as

$$\sigma = \sigma(^4S, f(^4S)) + \sigma(^2D, f(^2D)). \quad (8)$$

Now since we have assumed that  $\sigma(^2D) \ll \sigma(^4S)$ , the presence of this species in the total  $\text{O}^+$  beam can be shown to lower the observed cross section by a percentage equal to its fractional abundance. Examination of Fig. 1 therefore indicates for electrons of 40 eV, that the excited-state concentration is 20% of the total beam for pure  $\text{O}_2$  and 37.5% for the oxygen/helium mixture. As discussed above, Fig. 2 shows that the charge-transfer process between  $\text{O}^+$  ions and  $\text{N}_2$  goes primarily with the excited state [Reactions (4) and (5)]. Using the fractional abundances determined above, it is therefore possible to correct the observed cross sections for Reactions (5) obtained using the total  $\text{O}^+$  beam intensity. For Reaction (5) [ $\text{O}^+(^2D) + \text{N}_2 \rightarrow \text{O} + \text{N}_2^+$ ] we get, for 14-eV ions colliding with the neutral particle, a cross section of  $29.5 \times 10^{-16} \text{ cm}^2$

for the pure  $\text{O}_2$  case and a cross section of  $30.6 \times 10^{-16} \text{ cm}^2$  for the  $\text{O}_2$ /helium mixture.

Using a totally different technique developed previously in this laboratory,<sup>4</sup> we have determined the fractional abundance of  $\text{O}^+(^2D)$  from the attenuation of an  $\text{O}^+$  beam in another gas to be 24%. This value was obtained using 40-eV electron energy in pure  $\text{O}_2$ . Using this value for the fractional abundance, we have obtained a cross section for Reaction (5) at 14 eV of  $26.8 \times 10^{-16} \text{ cm}^2$ . The difference between this value and those determined above is within experimental error and therefore indicates that our assumption of a small cross section for Reaction (6) is valid.

Using the above-determined fractional abundances, it is possible to obtain cross-section curves for the separate ion states for each reaction that is found to proceed with large probability. The charge-exchange cross section leading to production of  $\text{N}_2^+$  is given in Fig. 3. The values given by this figure are slightly lower at low energies than those reported previously.<sup>2</sup> Cross sections for the ion-molecule reaction producing  $\text{NO}^+$  are given in Table I.

Examination of Fig. 3 shows that the cross section for the reaction of  $\text{O}^+(^2D)$  with  $\text{N}_2$  remains large down to the lowest interaction energy studied. The energy available in charge transfer with  $\text{O}^+(^2D)$  is 16.1 eV. This energy is almost exactly that required for formation of the  $\text{N}_2^+$  in the ( $A^2\Pi_u, v=1$ ) state. This reaction is therefore a source of excited  $\text{N}_2^+$  ions in the  $F$  region where the  $\text{O}^+$  concentration is high. Decay of the  $\text{N}_2^+(A^2\Pi_u)$  state produces Meinel radiation. A discussion of how this reaction may lead to an enhancement of the Meinel radiation observed from airglow has been given by Wallace and Broadfoot.<sup>5</sup>

\* Work supported by the Defense Nuclear Agency under Contract DASA01-69-C-0044.

<sup>1</sup> A. Dalgarno and M. B. McElroy, *Planetary Space Sci.* **11**, 727 (1963).

<sup>2</sup> R. F. Stebbings, B. R. Turner, and J. A. Rutherford, *J. Geophys. Res.* **71**, 771 (1966).

<sup>3</sup> J. A. Rutherford, R. F. Mathis, B. R. Turner, and D. A. Vroom, *J. Chem. Phys.* **55**, 3785 (1971).

<sup>4</sup> B. R. Turner, J. A. Rutherford, and D. M. J. Compton, *J. Chem. Phys.* **48**, 1602 (1968).

<sup>5</sup> L. Wallace and A. L. Broadfoot, *Planetary Space Sci.* **17**, 975 (1969).



APPENDIX C

FORMATION OF SODIUM IONS BY CHARGE TRANSFER

Preceding page blank

## Formation of Sodium Ions by Charge Transfer\*

J. A. RUTHERFORD, R. F. MATHIS,<sup>†</sup> B. K. TURNER, AND D. A. VROOM

*Gulf Radiation Technology, A Division of Gulf Energy and Environmental Systems, San Diego, California 92112*

(Received 21 January 1971)

Cross sections have been measured in the energy range 1–500 eV for the charge transfer of several ions with neutral sodium. The ions studied are  $O^+$ ,  $N^+$ ,  $N_2^+$ ,  $NO^+$ ,  $O_2^+$ ,  $H_2O^+$ ,  $H_3O^+$ ,  $N_2O^+$ , and  $Na^+$ . The magnitude of these cross sections can be related to the availability of reaction paths which have a small internal energy defect. The smaller the energy defect the larger the cross section. Where possible the measured cross sections have been extrapolated to thermal energy. Comparison is made with other experiments.

### I. INTRODUCTION

Sodium ions have been shown in rocket studies to be one of the more prevalent metallic species in the upper atmosphere.<sup>1</sup> Since this ion is monatomic, recombination is slow. In addition its ionization potential (5.138 eV) is significantly below that of the more common atmospheric species, and it cannot therefore be readily destroyed by charge transfer. As a consequence, metallic ions of this type may be expected to be long lived in the upper atmosphere. Information on charge transfer reactions leading to formation of sodium ions from the neutral species may therefore be important to an understanding of atmospheric deionization.

The results presented in this paper represent the second part of an experimental program in which asymmetric charge transfer processes leading to production of metallic ions are being studied. In cases where the ionization potential of the metal is lower than or equal to that required to form the primary ion, charge transfer to the ground state will be either exothermic or resonant. In the first publication in this series<sup>2</sup> it was shown that even though several exothermic channels for reaction may be open at all interaction energies, the greatest contribution to the total cross section comes from the channel which results in closest energy resonance between reactant and product states. Similarly, if no channel allows near-energy resonance, then the charge transfer cross section is found to be small. The results to be presented here lead to the same conclusions.

### II. EXPERIMENTAL

A detailed description of the crossed beam apparatus employed for the charge transfer measurements between ions and metal vapors has been given previously.<sup>2</sup>

The neutral beam is generated in a resistively heated Knudsen cell. The major difficulty encountered in these experiments is the determination of the neutral beam density. Two methods were employed. First, the density was calculated from the system geometry, the size of the port of egress in the Knudsen cell, the temperature of the cell, and the vapor pressure of sodium.<sup>3</sup> This technique has been employed in our previous experiment and demands accurate values for the vapor pressures as a function of temperature. The second

method involved running the neutral beam for a known time and collecting all the sodium which passes through the collision region in a liquid nitrogen cooled vessel (liquid nitrogen cooling was required to ensure complete collection). The amount deposited was then determined using activation analysis.<sup>2</sup> For sodium the beam densities calculated from the two methods did not agree, the neutron activation analysis gave the higher density. This difference (a factor of 2) was attributed to inaccuracy in determination of the sodium vapor pressure due to oxide layer contamination in either our cell or that used to determine the published vapor pressure. The beam densities used here are therefore those determined by activation analysis.

The possible error which may exist in our absolute cross sections is greater than in the previously reported Mg results and arises due to uncertainty in the neutral beam density. For these experiments we estimate that our values may be in error by as much as 40% at high energy, increasing to 60% at the lowest energies. It should be noted that this is an error in the absolute magnitude. The reproducibility in the measured energy dependence was better than 15%.

### III. RESULTS

Charge transfer cross sections for reactions between nine ions and neutral sodium have been measured in the energy range 1–500 eV. The cross sections are presented in graphical form since this representation aids the interpretation and discussion of the data. Processes which exhibit similar structure and which have similar cross sections have been grouped, where possible, in the same figure.

The resonant charge transfer cross section for sodium ions on sodium is given in Fig. 1 together with the data for  $H_2O^+$ ,  $H_3O^+$ , and  $N_2O^+$ . All of the processes have cross sections, which are similar in magnitude and which show an increase in cross section with decreasing energy down to the lowest measured energies. The results for the symmetric resonant process,  $Na^+ + Na$ , could not be determined below about 30 eV primary ion energy as separation of the fast primary from the slow secondary ions could not be achieved at lower energies.

Figure 2 gives the charge transfer cross sections for  $N_2^+$  and  $NO^+$  ions impinging on neutral sodium. Here

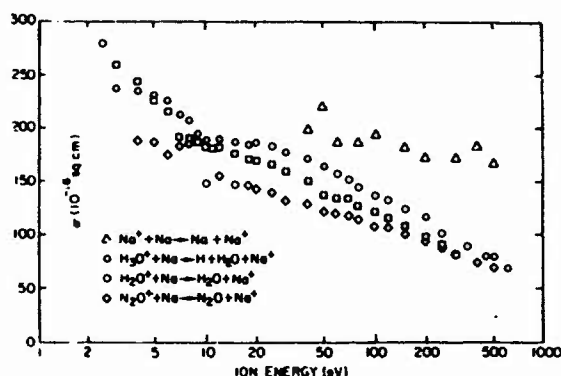


FIG. 1. Charge transfer cross sections for  $\text{Na}^+$ ,  $\text{H}_2\text{O}^+$ ,  $\text{H}_2\text{O}^+$ , and  $\text{N}_2\text{O}^+$  ions impinging on neutral Na as a function of the energy of the incident ion.

again the cross sections increase with decreasing ion energy. The magnitude of the cross sections for these two ions on neutral sodium are, however, considerably smaller than those for the three polyatomic species shown in Fig. 1. Possible reasons for this difference will be given in the following section.

As in the case of the magnesium results reported earlier,<sup>3</sup> the possible effects of metastable species in the primary ion beam were investigated. Figure 3 shows the variation in the charge transfer cross section for 50 eV  $\text{O}_2^+$  impinging on Na as the electron energy in the ion source was varied. For electron energies of less than 16 eV, no excited electronic states can exist in the beam and the cross sections measured are for the  $\text{O}_2^+$  ( $X^1\Pi_g$ ) ground state. Increasing the energy above 16 eV introduces some excited states and the cross section for  $\text{Na}^+$  production can be seen to increase. Above about 30 eV the ratio of ground to metastable ion states remains nearly constant, and the cross section therefore becomes a constant with respect to the electron energy.

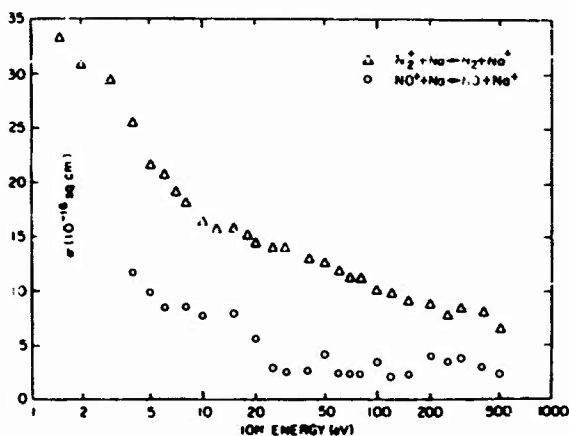


FIG. 2. Charge transfer cross sections for  $\text{N}_2^+$  and  $\text{NO}^+$  ions impinging on neutral Na as a function of the energy of the incident ion.

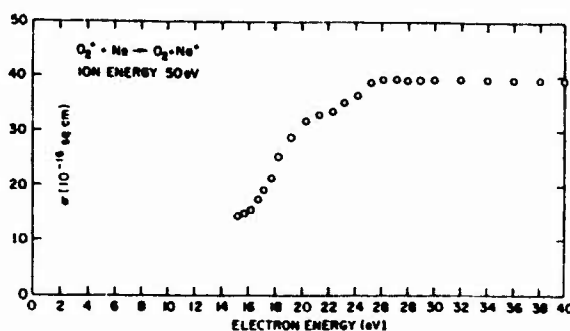


FIG. 3. Dependence of the charge transfer cross section upon the source electron energy for the reaction  $\text{O}_2^+ + \text{Na} \rightarrow \text{O}_2 + \text{Na}^+$ . The  $\text{O}_2^+$  had a kinetic energy of 100 eV.

By keeping the electron energy below 16 eV, the cross section for the ground state  $\text{O}_2^+$  alone can be determined. Using the data obtained from variation of the primary ion source energy it is possible to obtain cross sections for charge transfer from the metastable states provided the ratio of ground to metastable states is known. This information is obtained in a supplementary experiment. The technique employed here was developed previously in this laboratory.<sup>4</sup> The percentage of metastable states in a beam of  $\text{O}_2^+$  formed with 40 eV electrons (the energy used to determine the composite curve given in Fig. 4) was found to be 32%. Using this percentage, the composite curve, and the information given in Fig. 3, the metastable state charge transfer cross sections could be obtained. The results are given together with the ground state curve in Fig. 4.

The  $\text{NO}^+$  is also known to have a metastable state. In these experiments,  $\text{N}_2\text{O}$  was used to produce the  $\text{NO}^+$

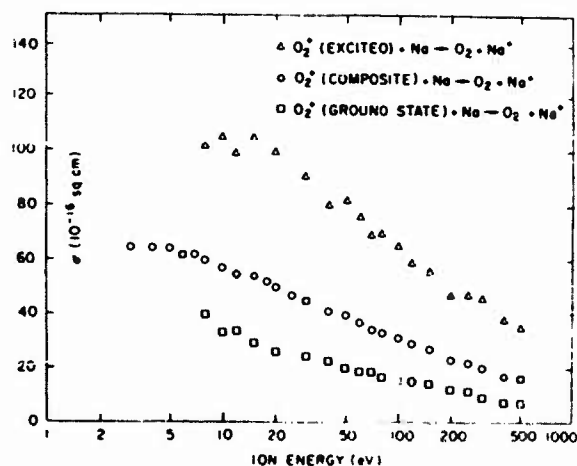


FIG. 4. Charge transfer cross sections for different states of excitation of the  $\text{O}_2^+$  ions with Na as a function of the incident ion energy. The cross section is shown for ground state  $\text{O}_2^+$  ions, for  $\text{O}_2^+$  ions in the mixture of states (composite) which results when 40 eV electrons impinging on  $\text{O}_2$  to form the  $\text{O}_2^+$ , and for the excited states alone.

TABLE I. Recombination energies and relevant energies of reactants and products cited in the text.\*

| Species and ground state              | Excited neutral states and energy above ground state (eV) | Ground ionic state and ionization potential (eV) | Ion state and energy above ionic ground state (eV) |
|---------------------------------------|-----------------------------------------------------------|--------------------------------------------------|----------------------------------------------------|
| Na ( $3s, {}^2S_{1/2}$ )              |                                                           | ( $2p^4, {}^1S_0$ ), 5.138                       |                                                    |
| N <sub>2</sub> ( $X {}^1\Sigma_g^+$ ) | ( $w {}^1\Delta_u$ ), 8.89                                | ( $X {}^2\Sigma_g^+$ ), 15.58                    |                                                    |
| NO ( $X {}^2\Pi$ )                    | ( $a {}^4\Pi$ ), ~4.7                                     | ( $X {}^1\Sigma^+$ ), 9.27                       |                                                    |
| O <sub>2</sub> ( $X {}^2\Sigma_g^-$ ) | ( $B {}^2\Sigma_u^-$ ), 6.12                              | ( $X {}^2\Pi_g$ ), 12.06                         | ( $a {}^4\Pi_u$ ), 4.04                            |

\* Atomic energy levels obtained from C. E. Moore, Natl. Bur. Std. (U.S.) Circ. No. 467 (1949), Vol. 1. Molecular levels obtained from F. R. Gilmore, "Basic Energy Level and Equilibrium Data for Atmospheric

Atoms and Molecules," The Rand Corp., Research Memorandum RM-5201-ARPA, March 1967.

primary beam. Previous experiments in this laboratory have shown that NO<sup>+</sup> ions produced from N<sub>2</sub>O contain a very low percentage of metastable ions.

Attempts were also made to measure the charge transfer between the atomic ions O<sup>+</sup> and N<sup>+</sup> and atomic sodium. The cross sections were found in both cases to be very small. A possible explanation for the absence of reaction will be given in the following section.

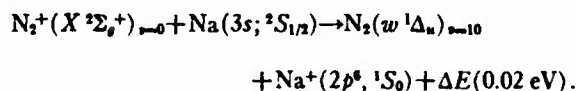
#### IV. DISCUSSION

All the charge transfer processes reported here are exothermic or energy resonant for transfer of an electron from the ground state of neutral sodium into the lowest available state of the neutralized ion. In interpreting the charge transfer results obtained, an attempt has been made to account for the excess energy available. In this regard a correlation between the size of the cross section, its energy dependence, and the final states of the products, has been made. Recombination energies and atomic and molecular energy levels used in the discussion are given in Table I.

The four largest cross sections measured for charge exchange with neutral sodium are given in Fig. 1. Of these the largest process, over the energy range considered, is the resonant charge transfer process Na and Na<sup>+</sup>. The energy dependence of the other three cross sections is essentially that which would be predicted for mechanisms with small energy defects.<sup>2</sup> With species such as H<sub>2</sub>O<sup>+</sup>, H<sub>2</sub>O<sup>+</sup>, and N<sub>2</sub>O<sup>+</sup>, it is not possible to say in what final states the polyatomic species will be produced due to a lack of information on these states. The possibility of the excess energy residing as internal energy in the sodium ion produced can be discounted as the lowest excited state of Na<sup>+</sup> lies approximately 23 eV above the ground state.

The charge transfer cross section for N<sub>2</sub><sup>+</sup> on sodium, shown in Fig. 2, is much smaller than that for Na with the polyatomic ions. The excess energy available in the reaction, 10.44 eV, is sufficient to dissociate the N<sub>2</sub> into two ground state nitrogen atoms. Another possible mechanism involves formation of the N<sub>2</sub> molecule in a highly excited state such as the  $w {}^1\Delta_u$ .

Either reaction path leads to a near-resonant mechanism. Since the dissociation energy of N<sub>2</sub>, 9.76 eV, is very nearly equal to that available from the reaction, 10.44 eV, dissociation of the molecule would not be expected to be probable without a large shift in the bond length of the neutral prior to forming the dissociative state, i.e., the repulsive curves leading to the dissociation limit at 9.76 eV will pass through the Franck-Condon region at an energy greater than 10.44 eV. As a consequence, dissociation can only occur through violation of the Franck-Condon principle. This violation of the Franck-Condon principle tends to favor the second mechanism outlined above for the N<sub>2</sub><sup>+</sup>+Na reaction. This process can be represented as



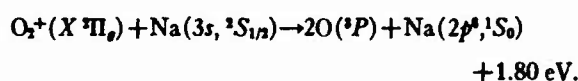
The charge transfer cross section between NO<sup>+</sup> and Na is also small, see Fig. 2. The excess energy, in this case, 4.13 eV, is not sufficient to dissociate the molecule and in fact lies about 0.6 eV, below the first molecular excited state. The only possible reaction mechanisms which lead to near resonance here are formation of the ground molecular state in a high vibrational level or formation of the  $a {}^4\Pi$  excited state. The latter process is endothermic by approximately 0.6 eV and also involves a large shift in internuclear distance between the ionic state and the final state. The formation of the highly excited vibrational ground state does not involve as large a change in internuclear distance and is therefore the more probable reaction mechanism.

In Fig. 4, the charge transfer cross sections for the ground and excited oxygen ions are shown. Again the shape of both curves is consistent with a mechanism having a small energy defect. The excess energy available from reaction of sodium with both the ground O<sub>2</sub><sup>+</sup> state, 6.92 eV, and the excited state 10.96 eV, is sufficient to dissociate the resultant oxygen molecules ( $D_0=5.12$  eV). For the ground state O<sub>2</sub><sup>+</sup> ion, the

TABLE II. Calculated cross sections and rate coefficients.

| Reaction               | 300°K                                             |                                                           | 600°K                                             |                                                           | 1200°K                                            |                                                           |
|------------------------|---------------------------------------------------|-----------------------------------------------------------|---------------------------------------------------|-----------------------------------------------------------|---------------------------------------------------|-----------------------------------------------------------|
|                        | Cross section<br>$\times 10^{16}$ cm <sup>2</sup> | Rate coefficient<br>$\times 10^{10}$ cm <sup>3</sup> /sec | Cross section<br>$\times 10^{16}$ cm <sup>2</sup> | Rate coefficient<br>$\times 10^{10}$ cm <sup>3</sup> /sec | Cross section<br>$\times 10^{16}$ cm <sup>2</sup> | Rate coefficient<br>$\times 10^{10}$ cm <sup>3</sup> /sec |
| $N_2^+ + Na$           | 24.5                                              | 18.9                                                      | 13.9                                              | 15.2                                                      | 8.33                                              | 12.8                                                      |
| $O_2^+(X^1\Pi_g) + Na$ | 18.5                                              | 13.8                                                      | 13.1                                              | 13.9                                                      | 9.78                                              | 14.7                                                      |
| $O_2^+(a^1\Pi_g) + Na$ | 26.2                                              | 19.6                                                      | 23.6                                              | 24.9                                                      | 21.2                                              | 31.8                                                      |
| $H_2O^+ + Na$          | 31.9                                              | 27.4                                                      | 32.1                                              | 39.1                                                      | 31.4                                              | 54.1                                                      |
| $N_2O^+ + Na$          | 28.7                                              | 20.2                                                      | 27.1                                              | 26.9                                                      | 25.2                                              | 35.6                                                      |

dissociation products resulting from charge transfer must both be in the ground state. This process can be represented as



The two oxygen atoms would be expected to carry away equal amounts of the excess energy.

For the metastable  $O_2^+$  more energy is available and as a consequence the products of a dissociative process may be in excited states. Oxygen atoms in the excited  $^1D$  and  $^1S$  states as well as the ground  $^3P$  state are possible products. This density of reaction channels is greater than for the ground state process and may explain the greater cross section for this species.

The charge exchange cross sections for  $O^+ + Na$  and  $N^+ + Na$  are as stated above, very small, and no data were obtained for these processes. This result may be attributed to the lack of energy levels available in either product to make near resonance possible. A similar result was found previously for the reaction of  $O^+$  with magnesium.<sup>3</sup> For  $N^+$  on magnesium, energy levels allowing a near-resonance mechanism exist, and the cross section was found to be significantly larger.

In general, when molecular species are being considered, the possibility of near resonance will generally exist for an exothermic process. The multitude of bound electronic states with their associated vibrational and rotational levels coupled with dissociation continuum makes near resonance possible for all exothermic processes. This general conclusion is well demonstrated here and in previously reported charge transfer processes.<sup>2,5</sup>

Other measurements of charge transfer cross sections between atmospheric ions and sodium have been reported. Henderson *et al.*<sup>6</sup> have obtained results for  $N_2^+$  and  $O_2^+$  on sodium in the energy range 25–200 eV. The energy dependence of their cross sections is similar to ours, but the absolute values tend to be about an order of magnitude lower. Peterson<sup>7</sup> has also measured  $N_2^+ - Na$  charge exchange. Once again, the energy dependence is similar in the two experiments but his absolute values are about a factor of 2 larger

than ours. It should be noted that both Henderson *et al.* and Peterson used hot wire detectors to obtain their beam densities.

The results reported here have been obtained for primary ion energies ranging from about 1 to 500 eV energy. Much of the interest in charge transfer cross sections between atmospheric ions and metallic species is in the energy range from thermal to 1 or 2 eV. In order to extend our measured charge transfer cross sections to lower energies, an extrapolation technique has been developed and has been described fully in a previous publication.<sup>8</sup>

One assumption inherent in the extrapolation procedure is that the relative abundances of the various products emerging from the capture-formed complex are independent of the relative kinetic energy of the reactants. Failure of this criterion invalidates the derived rate coefficients. In general, whether or not the extrapolation technique is valid can be seen by observing if the calculated cross section fits the experimental data to the lowest energies considered. A computer program has been developed to perform the calculations. Results for the five ion species which were found to extrapolate are given in Table II. Both cross sections and rate coefficients are presented.

Thermal energy rate coefficients have been obtained for charge transfer from  $N_2^+$ ,  $O_2^+$ , and  $NO^+$  to Na by Farragher *et al.*<sup>9</sup> using a flowing afterglow technique. For  $N_2^+$  and  $O_2^+$  they obtained values of  $5.8 \times 10^{-10}$  cm<sup>3</sup>/sec and  $6.7 \times 10^{-10}$  cm<sup>3</sup>/sec, respectively, while for  $NO^+$ , values of about an order of magnitude less were obtained. The value for  $N_2^+$  and  $O_2^+$  are between a factor of 2 and 3 lower than those given in Table II.

#### ACKNOWLEDGMENTS

The authors would like to thank both Dr. R. H. Neynaber and Professor R. F. Stebbings for their interest in the experiments and their helpful comments on the manuscript.

\* This work was supported by the Defense Nuclear Agency under Contract No. DASA01-69-C-0044.

† Present address: Dept. of Physics, University of Missouri at Rolla, Rolla, Mo.

- <sup>1</sup> R. S. Narcisi and A. B. Bailey, *J. Geophys. Res.* **70**, 3687 (1965).
- <sup>2</sup> J. A. Rutherford, R. F. Mathis, B. R. Turner, and D. A. Vroom, *J. Chem. Phys.* **55**, 3785 (1971).
- <sup>3</sup> R. E. Honig, *RCA Rev.* **23**, 567 (1962).
- <sup>4</sup> B. R. Turner, J. A. Rutherford, and D. M. J. Compton, *J. Chem. Phys.* **48**, 1602 (1968); R. F. Mathis, B. R. Turner, and J. A. Rutherford, *ibid.* **49**, 2051 (1968).
- <sup>5</sup> See, for example, Ref. 2, R. F. Stebbings, B. R. Turner, and J. A. Rutherford, *J. Geophys. Res.* **71**, 771 (1966) and B. R. Turner, J. A. Rutherford, and R. F. Stebbings, *ibid.* **71**, 4521 (1966).
- <sup>6</sup> W. R. Henderson, J. E. Mentall, and W. L. Fite, *J. Chem. Phys.* **46**, 3447 (1967).
- <sup>7</sup> J. R. Peterson (private communication).
- <sup>8</sup> F. A. Wolf and B. R. Turner, *J. Chem. Phys.* **48**, 4226 (1968).
- <sup>9</sup> A. L. Farragher, J. A. Peden, and W. L. Fite, *J. Chem. Phys.* **50**, 287 (1969).

**APPENDIX D**

**FORMATION OF CALCIUM IONS BY CHARGE TRANSFER**

**Preceding page blank**

## FORMATION OF CALCIUM IONS BY CHARGE TRANSFER\*

J. A. Rutherford, R. F. Mathis,<sup>†</sup> B. R. Turner, and D. A. Vroom

Gulf Radiation Technology  
A Division of Gulf Energy & Environmental Systems  
San Diego, California 92112

### ABSTRACT

Charge transfer cross sections have been measured in the energy range from 1 to 500 eV for nine common atmospheric ions in collision with neutral calcium atoms. The ions studied are  $O^+$ ,  $N^+$ ,  $N_2^+$ ,  $NO^+$ ,  $O_2^+$ ,  $H_2O^+$ ,  $H_3O^+$ ,  $N_2O^+$ , and  $Ca^+$ . In all cases the cross sections are found to be large indicating near resonant processes. Mechanisms consistent with this observation are given. Extrapolation of the measured cross sections to thermal energies has also been carried out.

---

\* This work was supported by the Defense Nuclear Agency under Contract No. DASA01-69-C-0044.

Preceding page blank



## I. INTRODUCTION

The experiments discussed represent the third in a series of studies undertaken to investigate the importance of charge transfer as a method of producing metallic ions in processes related to aeronomy and the low energy aspects of asymmetric charge transfer. Studies involving magnesium<sup>1</sup> and sodium<sup>2</sup> have been reported previously.

Calcium is one of the more dominant metallic species present in the upper atmosphere. Its presence has been observed in rocket experiments<sup>3</sup> and in studies of optical emissions from the atmosphere.<sup>4, 5</sup> The low ionization potential of this species (6.113 eV) coupled with the fact that it is atomic, make the normal processes for deionization in the atmosphere (dissociative recombination and charge transfer) ineffective. As a consequence, calcium ions will be long-lived and therefore may have an influence on the chemistry of the upper atmosphere greater than the concentration of this species would suggest.

## II. EXPERIMENTAL

The experiments were performed using the tandem mass spectrometer apparatus described in detail previously.<sup>1</sup> In this instrument, a modulated neutral beam of the metallic species is interposed between two mass spectrometers. The first of these spectrometers produces the primary ion beam while the second is used to analyze the products of reaction. The primary ion source is constructed in such a manner that the energy of the electron beam can be regulated with enough precision to allow control of the state

of excitation of the ions in the beam.

The neutral beam was formed in a heated cell as described in reference 1. The vapor pressure in the cell was generally of the order 50 microns. At the pressures used in the metal vapor cell, dimerization of the metal atoms is not expected to be a problem. In spite of this, during the course of the experimental investigations attempts were made to see charge-transfer to dimers in the beam. No evidence of such species was found. As in the previous experiments, both activation analysis and molecular effusion techniques were used to determine the neutral beam density. For calcium, these two methods agreed to within 1%.

Other possible experimental errors have been discussed in reference 1. The total error is expected to be similar here, that is  $\pm 30\%$  at high impact energies rising to a factor of  $\pm 2$  at the lowest energies.

### III. RESULTS

Charge transfer cross sections have been measured for collisions between nine ions and neutral calcium in the energy range from 1 to 500 eV. These cross sections are presented here in graphical form. Unless otherwise noted, the primary ions were formed using 40 eV electrons.

In Fig. 1 are shown the charge transfer cross sections for  $\text{Ca}^+$ ,  $\text{H}_2\text{O}^+$ ,  $\text{N}_2\text{O}^+$  and  $\text{N}_2^+$  incident on Ca atoms. The results for the symmetric  $\text{Ca}^+$  on Ca are shown only for interaction energies above 30 eV since the fast primary and slow secondary calcium ions cannot be separated below this energy.

Cross sections for  $\text{H}_3\text{O}^+$  and  $\text{NO}^+$  on Ca are given in Fig. 2 while those for  $\text{N}^+$  and  $\text{O}^+$  are given in Fig. 3. It should be noted that the  $\text{O}^+$  cross section is for the ground state of the primary ion only. A beam of pure

ground state  $O^+$  is obtained by keeping the electron energy in the primary ion source below the threshold energy for formation of metastable states. When the electron energy was raised above the threshold for metastable state production, only a small change in the charge transfer cross sections was observed. The  $NO^+$  ion is also known to possess metastable states. In these experiments the concentration of metastables was kept low. As a consequence, the cross section curve for  $NO^+$  on Ca in Fig. 2 may be taken to be that for the ground state of the ion.

For  $O_2^+$  a large effect due to metastable states was observed. In Fig. 4 the results obtained for the charge transfer cross section at one ion energy (100 eV) are given as a function of the number of metastable ions in the beam. The number of metastables is varied by changing the primary ion source electron energy. Below 16 eV, no metastable  $O_2^+$  ions may be formed and Fig. 4 shows a cross section of about  $55 \times 10^{-16} \text{ cm}^2$ . As the electron energy is increased the cross section is seen to rise reaching a limiting value above 30 eV. This rise is due to the metastables in the beam. In Fig. 5 the charge transfer cross section for ground state  $O_2^+$  on Ca is shown. This curve is obtained using  $O_2^+$  ions formed by electrons with energies less than 16 eV. The composite curve, also shown in Fig. 5 is obtained using  $O_2^+$  ions formed with 40 eV electrons. In order to obtain the curve for the excited state alone it is necessary to have the ground state cross section, the composite curve and the percentage of metastable ions in the beam. This latter value is determined in a subsidiary experiment.<sup>6</sup> The cross section for the excited state alone is also shown in Fig. 5.

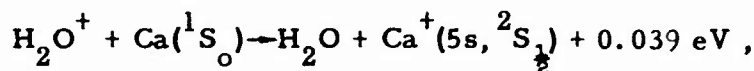
#### IV. DISCUSSION

Mechanisms postulated to explain the experimental results obtained must in some manner account for all the energy released in the reaction. Previous experiments in this series<sup>1,2</sup> have shown that where excited

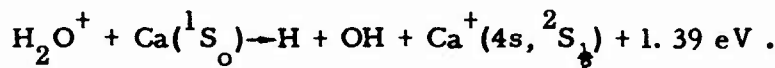
states of the products allow near resonant reactions, the cross section for the process is largest at low energies and decreases as the energy of the ions increases. When no excited states can give a resonant condition, the cross section was found to be small.

For calcium, all the cross sections were found to be large and product states giving resonant channels are therefore postulated to be the main reaction paths. Table I contains the states of the reactant and products used in the discussion together with their energies. The reaction paths suggested below are to be considered only as possible explanations for the results.

Figure 1 gives the results obtained for the symmetric charge transfer process of  $\text{Ca}^+ + \text{Ca}$ . This reaction must have exact energy resonant for ground state  $\text{Ca}^+$  and as a consequence a large cross section could be expected. The charge transfer cross sections for  $\text{H}_3\text{O}^+$ ,  $\text{N}_2\text{O}^+$  (Fig. 1) and  $\text{H}_3\text{O}^+$  (Fig. 2) on Ca are of comparable size to the symmetric case. The energy dependence and magnitude of these cross sections is that which would be predicted for reaction channels having small energy defect. For these polyatomic species it is difficult to ascertain what the states of the products might be. For  $\text{H}_2\text{O}^+$  two possible mechanisms are suggested, however. One of these involves production of the  $\text{Ca}^+$  in an excited state and the other leads to dissociation of the polyatomic molecule. These reactions can be written as



and



The excess energy in the last reaction could go into kinetic energy of the neutral products.

TABLE I. Recombination energies and relevant energies of reactants and products cited in the equations in the text.<sup>a</sup>

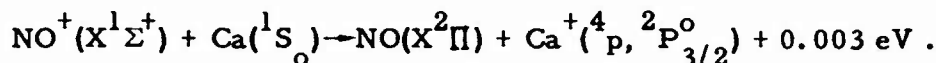
| Species and ground state    | Excited neutral state and energy above ground state (eV) | Ground ionic state and Ionization potential (eV) | Ion excited state and energy above ionic ground state                                                        |
|-----------------------------|----------------------------------------------------------|--------------------------------------------------|--------------------------------------------------------------------------------------------------------------|
| $\text{Ca}(4s^2, ^1S_0)$    |                                                          | $(4s, ^2S_{1/2}), 6.113$                         | $(4p, ^2P_{3/2}^o), 3.151$<br>$(5s, ^2S_{1/2}), 6.467$<br>$(5p, ^2P_{3/2}^o), 7.504$<br>$(4f, ^2F^o), 8.437$ |
| $\text{O}(2p^3, ^3P)$       |                                                          | $(2p^3, ^4S^o), 13.618$                          |                                                                                                              |
| $\text{N}(2p^3, ^4S^o)$     |                                                          | $(2p^2, ^3P), 14.534$                            |                                                                                                              |
| $\text{NO}(X^2\Pi)$         |                                                          | $(X^1\Sigma^+), 9.267$                           |                                                                                                              |
| $\text{O}_2(X^3\Sigma_g^-)$ | $(B^3\Sigma_u^-), \sim 6.1$                              | $(X^2\Pi_g), 12.063$                             | $(a^4\Pi_u), 4.038$                                                                                          |
| $\text{H}_2\text{O}$        |                                                          | 12.619                                           |                                                                                                              |

<sup>a</sup> Atomic energy levels obtained from "Atomic Energy Levels," C. Moore, ed., N. B. S. Circular 467, 1949, Vol. 1. Atomic Ionization Potentials obtained from "Ionization Potentials and Ionization Limits Derived from the Analysis of Optical Spectra," C. Moore, NSRDS-NBS 34, 1970. Molecular levels obtained from "Basic Energy Level and Equilibrium Data for Atmospheric Atoms and Molecules," F. R. Gilmore, The Rand Corporation, Research Memorandum, R.M.-5201-ARPA, March 1967.

The reaction of Ca with  $N_2O^+$  is probably dissociative in nature since the exothermicity of the reaction (6.78 eV) is much greater than the dissociation energy (1.68 eV). The  $H_3O^+$  reaction will also be dissociative since this species exist only as an ion.

The charge transfer cross section for  $N_2^+$  on calcium, shown in Fig. 1, is somewhat smaller than that for the polyatomic species but is still large. The excess energy available in this reaction (9.47 eV) can go to producing  $N_2$  in an excited state. Several  $N_2$  states lie in the correct energy region.<sup>7</sup> Among these are the  $a^1\Pi_g$ ,  $a'^1\Sigma_u^-$ ,  $B'^3\Sigma_u^-$  and the  $W^1\Delta_u$  states. The several reaction paths available may account for the large charge transfer cross section for  $N_2^+$  on calcium.

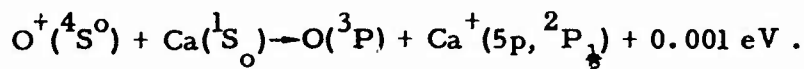
The charge transfer cross section for  $NO^+$  on calcium is smaller than that for  $N_2^+$  on calcium. Consideration of the energies of the possible states available in the products shows that a near resonant channel exists if the  $Ca^+$  is formed in the ( $4p, ^2P_{3/2}^0$ ) state. This reaction may be written as



The energies of the states involved are given in Table I. The fact that there is only one possible near resonant channel may account for this cross section being smaller than that for the  $N_2^+$  case. It is of interest to note that for this reaction, where only one reaction path may exist, the experimental scatter in the data is less than for the case of  $N_2^+$  where many paths may exist. Although no concrete evidence of how the presence of these different paths leads to increased scatter in the results exists, one can postulate that the different possible channels have different reaction probabilities as a function of interaction energy thereby leading to structure in the curve. This structure appears in our data as scatter.

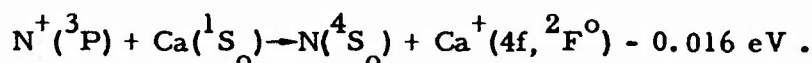
For  $O^+$  in the ground state charge exchanging with calcium, the cross section values are similar, at low energies, to those for the  $NO^+$  reaction.

Here again a single reaction path, leading to very close energy resonance, exists. The reaction is represented as

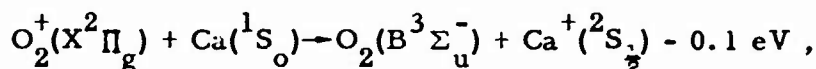


In previous studies involving reactions of  $\text{O}^+$  with  $\text{Mg}^1$  and  $\text{Na}^2$  the charge transfer cross sections were small. In these former cases no set of product states allowed a near resonant mechanism.

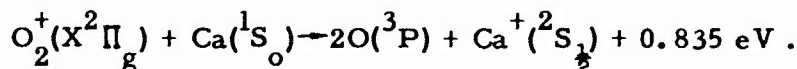
Near resonance also exists for the reaction of  $\text{N}^+$  with calcium. In this case the energy defect is larger than for the  $\text{O}^+$  reaction and this may be one of the factors which causes the  $\text{N}^+$  cross section to be smaller than that for  $\text{O}^+$  at low energies. The reaction may be written as



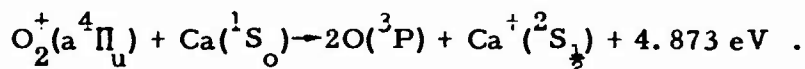
The results for  $\text{O}_2^+$  on Ca, seen in Fig. 5 again indicate that near resonant processes may be important. For the ground state two near resonant processes are given



and



Of these two the second is the more probable since the excess energy can easily be absorbed by the two ground state O atoms. For the excited state of  $\text{O}_2^+$  only a dissociative process is suggested. If both the O atoms are produced in the ground state the reaction may be written as



The excess energy here is great enough that one of the O atoms may be produced in an excited state such as  $^1\text{D}$  or possibly even  $^1\text{S}$ . It should be noted that if dissociation does occur in these reactions, oxygen atoms with kinetic energies well above thermal are produced.

Using our experimental technique, interaction energies of less than 1 eV are difficult to obtain. In many applications the interest in charge transfer reactions lies in the energy range from thermal to 1 or 2 eV. In order to obtain cross section values in this region, an extrapolation

method developed in this laboratory has been used.<sup>8</sup> This technique assumes that the relative abundance of the various products emerging from the interaction complex remains fixed. If this condition is not met, the technique will not give valid rate coefficients near thermal energies. In general, whether or not the extrapolation procedure is valid can be seen by observing if the calculated cross section fits the experimental data to the lowest energy of measurement. In this regard, we have arbitrarily set an average limit on this deviation of  $\pm 10\%$  for the fit of the experimental and calculated cross sections at the lowest measured energies. We also require that no deviations larger than this occur over the intermediate energy range between the lowest energy points and the high energy region where the calculation is normalized to the measured cross sections. In the present studies, the extrapolation procedure is found to be valid for all systems. The cross sections and rate coefficients obtained for three different temperatures are given in Table II.

#### ACKNOWLEDGEMENT

The authors would like to thank both Dr. R. H. Neynaber and Professor R. F. Stebbings for their interest in the experiments and their helpful comments on the manuscript.



TABLE II. Calculated cross sections and rate coefficients.

| Reaction                                    | 300°K                                          |                                                              |                                                | 600°K                                                        |                                                |                                                              | 1200°K                                         |                                                              |                                                |
|---------------------------------------------|------------------------------------------------|--------------------------------------------------------------|------------------------------------------------|--------------------------------------------------------------|------------------------------------------------|--------------------------------------------------------------|------------------------------------------------|--------------------------------------------------------------|------------------------------------------------|
|                                             | Cross Section<br>$\times 10^{15} \text{ cm}^2$ | Rate Coefficient<br>$\times 10^{10} \text{ cm}^3/\text{sec}$ | Cross Section<br>$\times 10^{15} \text{ cm}^2$ | Rate Coefficient<br>$\times 10^{10} \text{ cm}^3/\text{sec}$ | Cross Section<br>$\times 10^{15} \text{ cm}^2$ | Rate Coefficient<br>$\times 10^{10} \text{ cm}^3/\text{sec}$ | Cross Section<br>$\times 10^{15} \text{ cm}^2$ | Rate Coefficient<br>$\times 10^{10} \text{ cm}^3/\text{sec}$ | Cross Section<br>$\times 10^{15} \text{ cm}^2$ |
| $\text{N}^+ + \text{Ca}$                    | 13.3                                           | 11.3                                                         | 7.82                                           | 9.39                                                         | 5.53                                           | 9.39                                                         | 5.53                                           | 9.39                                                         | 5.53                                           |
| $\text{O}^+(^4\text{S}^0) + \text{Ca}$      | 9.35                                           | 7.56                                                         | 11.5                                           | 13.2                                                         | 12.9                                           | 20.9                                                         | 12.9                                           | 20.9                                                         | 12.9                                           |
| $\text{N}_2^+ + \text{Ca}$                  | 26.3                                           | 17.7                                                         | 29.1                                           | 27.8                                                         | 30.5                                           | 41.1                                                         | 30.5                                           | 41.1                                                         | 30.5                                           |
| $\text{O}_2^+(\text{X}^2\Pi_g) + \text{Ca}$ | 27.4                                           | 17.8                                                         | 21.3                                           | 19.6                                                         | 17.3                                           | 22.5                                                         | 17.3                                           | 22.5                                                         | 17.3                                           |
| $\text{O}_2^+(\text{a}^4\Pi_g) + \text{Ca}$ | 54.1                                           | 35.1                                                         | 42.7                                           | 39.2                                                         | 35.2                                           | 45.7                                                         | 35.2                                           | 45.7                                                         | 35.2                                           |
| $\text{NO}^+ + \text{Ca}$                   | 59.9                                           | 39.5                                                         | 43.6                                           | 40.7                                                         | 33.3                                           | 44.0                                                         | 33.3                                           | 44.0                                                         | 33.3                                           |
| $\text{H}_2\text{O}^+ + \text{Ca}$          | 51.7                                           | 40.1                                                         | 54.2                                           | 59.5                                                         | 55.2                                           | 85.7                                                         | 55.2                                           | 85.7                                                         | 55.2                                           |
| $\text{H}_3\text{O}^+ + \text{Ca}$          | 58.4                                           | 44.4                                                         | 48.9                                           | 52.6                                                         | 42.5                                           | 64.7                                                         | 42.5                                           | 64.7                                                         | 42.5                                           |
| $\text{N}_2\text{O}^+ + \text{Ca}$          | 62.5                                           | 37.3                                                         | 58.9                                           | 49.7                                                         | 55.4                                           | 66.2                                                         | 55.4                                           | 66.2                                                         | 55.4                                           |

## REFERENCES

<sup>†</sup>Present address: Dept. of Physics, University of Missouri at Rolla, Rolla, Missouri.

1. J. A. Rutherford, R. F. Mathis, B. R. Turner, and D. A. Vroom, J. Chem. Phys. 55, 3785 (1971).
2. J. A. Rutherford, R. F. Mathis, B. R. Turner, and D. A. Vroom, J. Chem. Phys. 56, 4654 (1972).
3. R. S. Narcisi and A. B. Bailey, J. Geophys. Res. 70, 3687 (1965).
4. A. L. Broadfoot, Planet. Space Sci. 15, 503 (1967).
5. H. S. Hoffman and M. S. Longmire, Nature 218, 858 (1968).
6. B. R. Turner, J. A. Rutherford and D. M. J. Compton, J. Chem. Phys. 48, 1602 (1968), and R. F. Mathis, B. R. Turner and J. A. Rutherford, J. Chem. Phys. 49, 2051 (1968).
7. F. R. Gilmore, J. Quant. Spectry. Radiative Transfer 5, 369 (1965).
8. F. A. Wolf and B. R. Turner, J. Chem. Phys. 48, 4226 (1968).

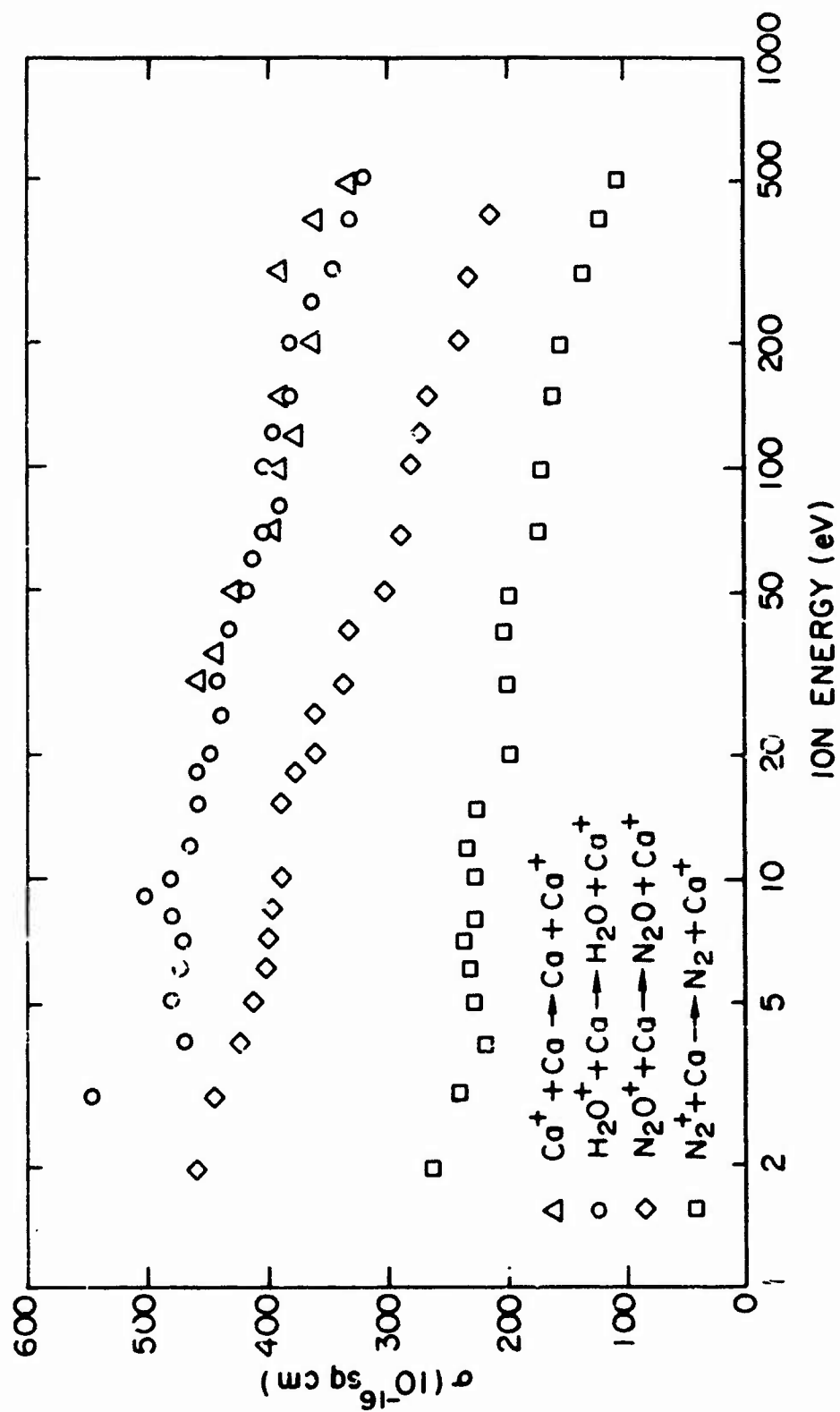


Figure 1. Charge-transfer cross sections for  $\text{Ca}^+$ ,  $\text{H}_2\text{O}^+$ ,  $\text{N}_2\text{O}^+$ , and  $\text{N}_2^+$  ions impinging on neutral Ca as a function of the energy of the incident ions.

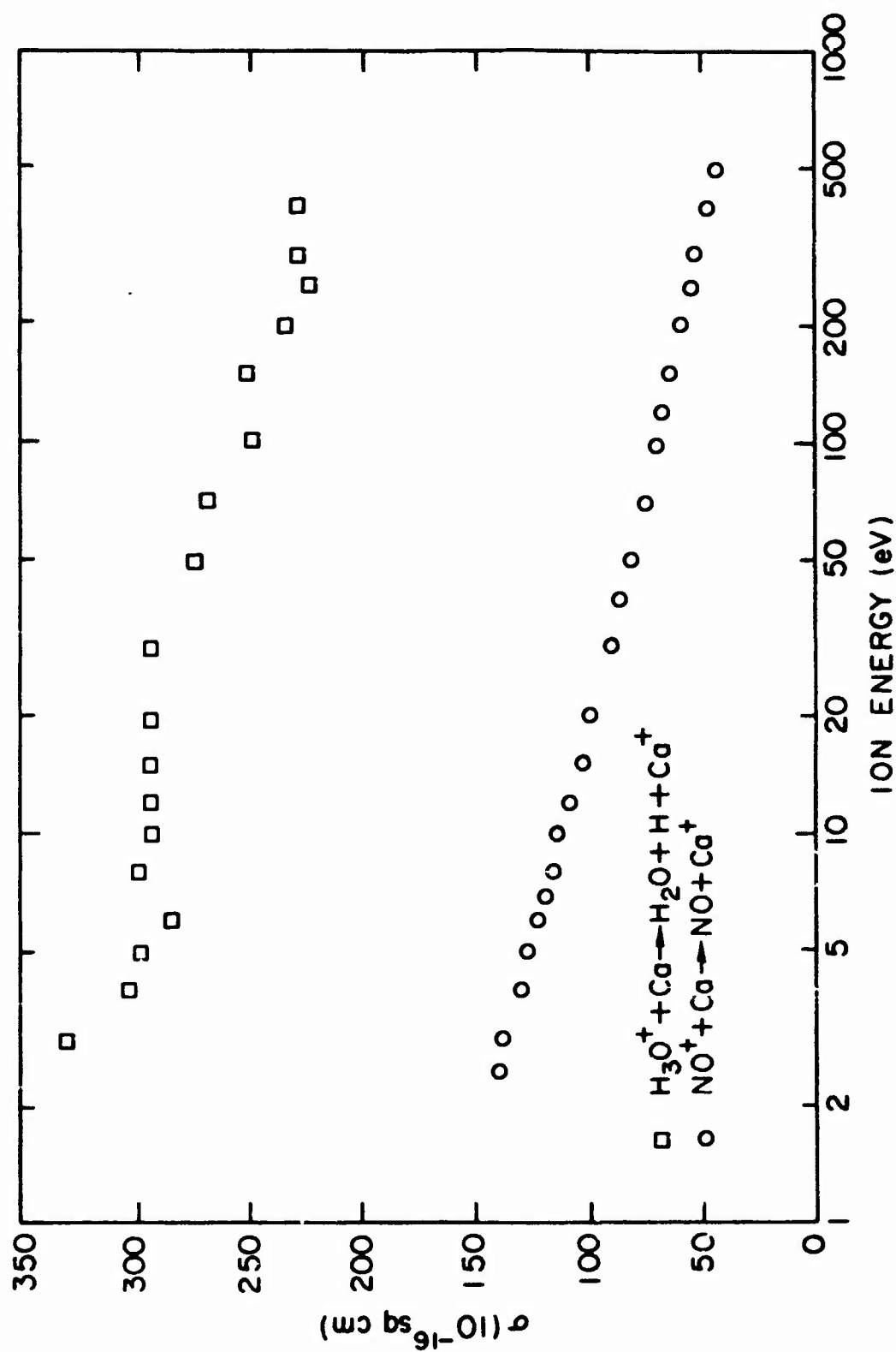


Figure 2. Charge-transfer cross sections for  $\text{H}_3\text{O}^+$  and  $\text{NO}^+$  ions impinging on neutral Ca as a function of the energy of the incident ions.

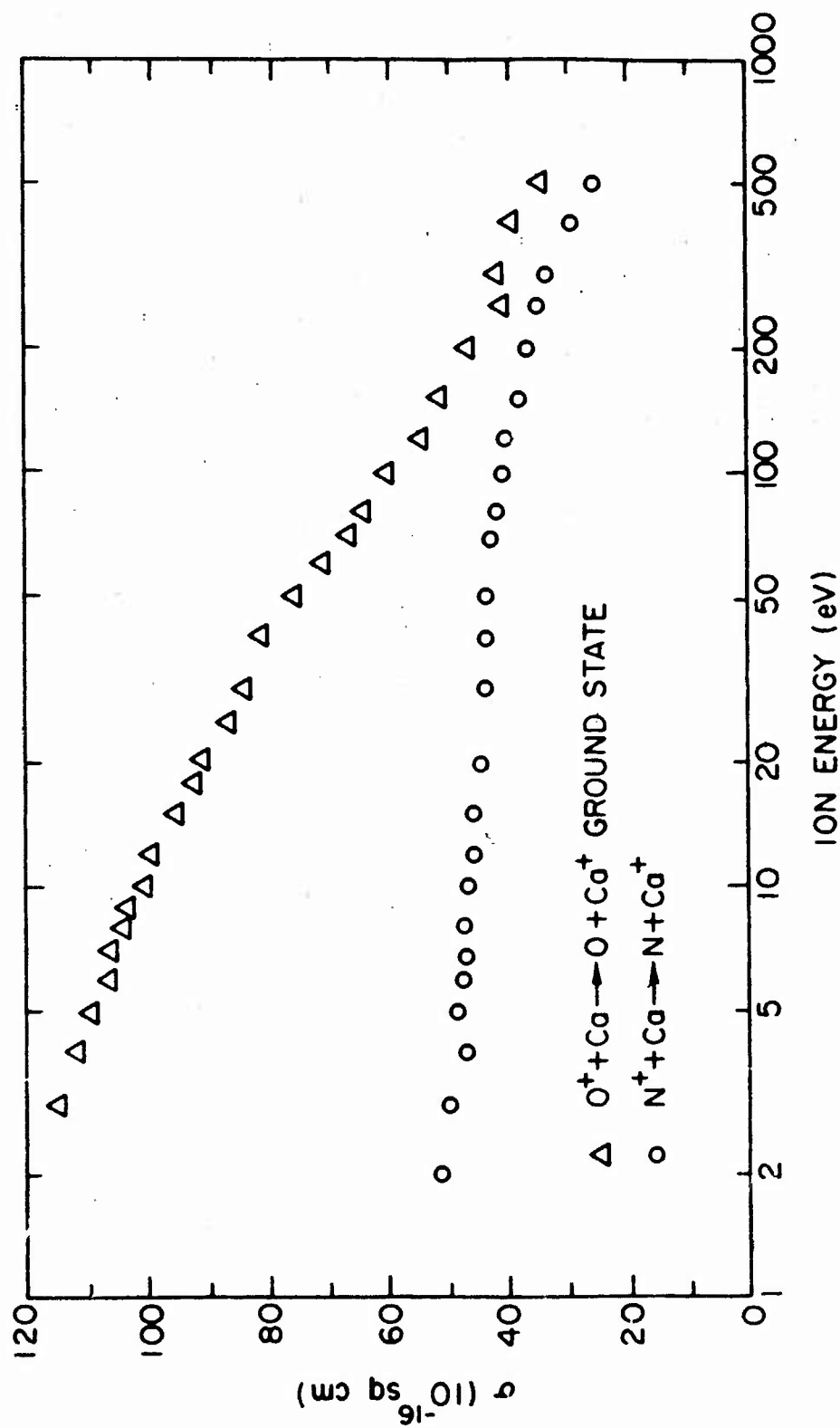


Figure 3. Charge-transfer cross sections for the atomic ions  $N^+$  and  $O^+$  impinging on neutral Ca as a function of the energy of the incident ions.

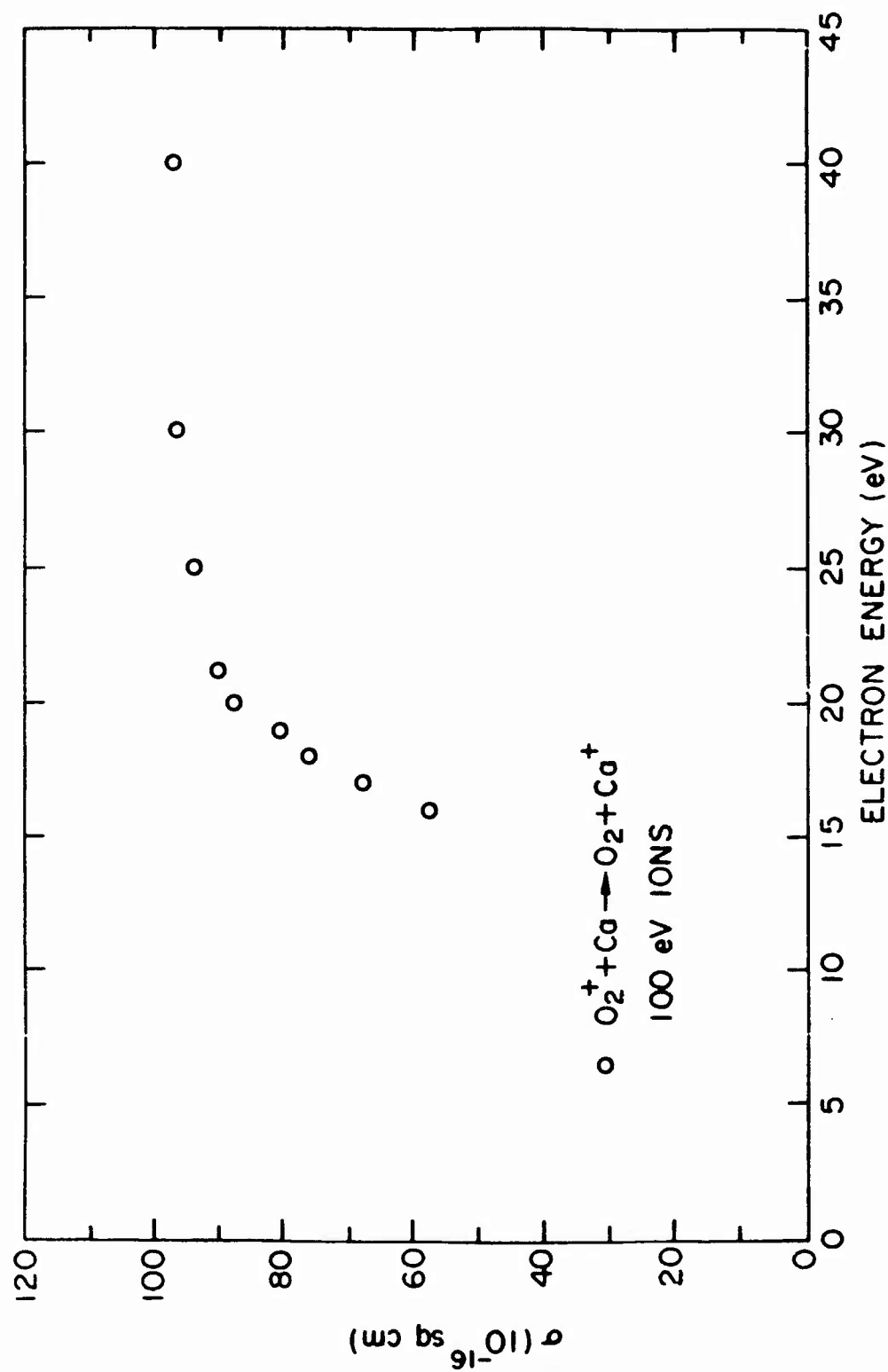


Figure 4. Dependence of the charge-transfer cross section upon the primary ion source electron energy for the reaction  $\text{O}_2^+ + \text{Ca} \rightarrow \text{O}_2 + \text{Ca}^+$ . The  $\text{O}_2^+$  had a kinetic energy of 100 eV.

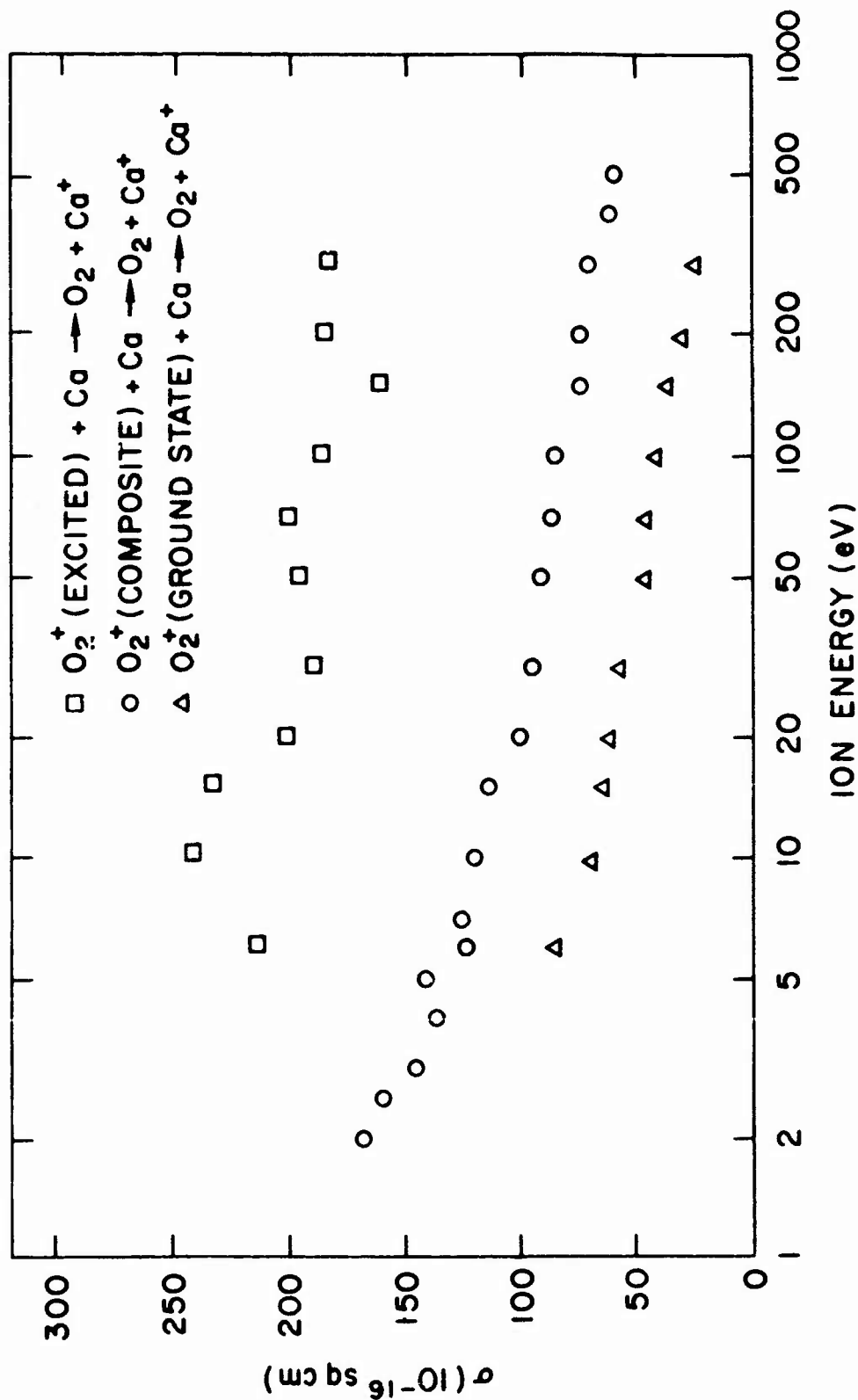


Figure 5. Charge-exchange cross sections for different states of excitation of the  $O_2^+$  ions with  $Ca^+$  as a function of the incident ion energy. The cross section is shown for ground-state  $O_2$  ions, for  $O_2^+$  ions in the mixture of states (composite) which results when 40 eV electrons impinged on  $O_2$  to form the  $O_2^+$ , and for the excited states.

APPENDIX E

FORMATION OF IRON IONS BY CHARGE TRANSFER



## FORMATION OF IRON IONS BY CHARGE TRANSFER<sup>\*</sup>

J. A. Rutherford and D. A. Vroom

Gulf Radiation Technology  
A Division of Gulf Energy & Environmental Systems  
San Diego, California 92112

### ABSTRACT

Reactions of iron atoms with common atmospheric ions have been studied in the energy range from 2 to 500 eV. The ions considered are  $H^+$ ,  $O^+$ ,  $N^+$ ,  $N_2^+$ ,  $NO^+$ ,  $O_2^+$ ,  $H_2O^+$  and  $H_3O^+$ . With the exception of one proton transfer reaction, all of the processes studied involved charge transfer. All but one of the charge transfer reactions were found to have large cross sections over the total energy range and probably proceed by near resonant energy paths. Where possible the measured cross sections have been extrapolated to thermal energies.

### INTRODUCTION

Iron is known to be an important minor constituent of the upper atmosphere;<sup>1,2</sup> its presence being accounted for by the ablation of meteors. Even though this species is in low concentration, it can have an important effect on the chemistry of the upper atmosphere. Its low ionization potential (7.870 eV)<sup>3</sup> allows it to undergo charge exchange with all common atmospheric ions. Iron ions, once formed in the

---

<sup>\*</sup>This work was supported by the Defense Nuclear Agency under Contract No. DASA01-69-C-0044.

upper atmosphere, should have a long lifetime since radiative recombination (a process known to have small cross sections) is probably the only significant loss mechanism.

The results reported here represent the fourth part in a series of experiments to look at asymmetric charge transfer processes involving metal atoms. Previous sections have dealt with reactions of magnesium,<sup>4</sup> sodium<sup>5</sup> and calcium<sup>6</sup> interacting with common atmospheric ions. These previous studies have shown the importance of near resonant reaction paths in low energy charge transfer. The results in this present publication support this observation.

## EXPERIMENTAL

The apparatus and experimental techniques employed for measurement of charge transfer processes between ions and metal vapor have been described previously.<sup>4</sup> Briefly the apparatus consists of two mass spectrometers operating in tandem. The modulated beam of metal vapor is interposed between the two spectrometers. The first mass spectrometer is used to analyze the primary ion beam while the second analyzes the modulated beam of secondary ions produced by collisions between the primary ion beam and the metal vapor.

The low vapor pressure of iron compared with the previously studied metal vapors required a molecular effusion source capable of withstanding high temperatures. This cell was constructed from a high purity alumina crucible surrounded by tungsten foil. Passage of current through the foil served to heat the crucible. The temperature was monitored using an optical pyrometer. Pure iron wire placed in the crucible was used as the source of iron vapor. Pressures of the order of 50 microns were generally used in the heated crucible. The neutral beam was formed by effusion of the iron vapor from a small hole in the side of the crucible.

At the pressures used in the metal vapor cell, dimerization of the metal atoms is not expected to be a problem. In spite of this, during the course of the experimental investigations, attempts were made to see charge-transfer to dimers in the beam. No evidence of such species was found.

As in the previous metal atom studies,<sup>4-6</sup> two methods were used to obtain the neutral beam density; molecular effusion calculations and activation analysis. The errors in both methods are larger here than in the previous studies. The molecular effusion method suffers from errors in temperature measurement due to use of the optical pyrometer while the neutron activation technique is troubled by trace quantities of manganese. Errors of up to  $\pm 30\%$  can exist for both methods. The two methods gave, however, iron beam densities that agreed to within 1.5%. The possibility of a larger systematic error in the absolute cross sections than that reported for the other metal atoms data<sup>4-6</sup> exists here because of the increased uncertainty in the neutral beam density. The maximum possible error here is  $\pm 50\%$  at high impact energies increasing to as much as a factor of 2.2 at the lowest energies.

## RESULTS AND DISCUSSION

The cross sections for charge transfer, and in one case, proton transfer, between neutral iron atoms and several ions were determined over the energy range from 2 to 500 eV. An electron energy of 40 eV was used to form the primary ions. These cross sections are presented here in graphical form since this type of presentation aids in the discussion of the data.

The cross sections for the charge transfer of neutral iron with the ions  $\text{H}_2\text{O}^+$ ,  $\text{O}_2^+$ ,  $\text{O}^+$  and  $\text{H}^+$  are shown in Fig. 1, while those for charge transfer with  $\text{N}_2^+$ ,  $\text{NO}^+$  and  $\text{N}^+$  are shown in Fig. 2. The charge transfer

and proton transfer reactions involving  $\text{H}_3\text{O}^+$  are shown in Fig. 3.

The cross section curves shown in Figs. 1 and 2 are all very similar in that they show an increase in magnitude with decreasing ion energy. This increase is similar for all seven species shown. In addition to this, the absolute magnitudes of the cross section curves are all quite large and do not show a large variation from species to species. For example, at 10 eV all the cross sections lie between 10 and  $35 \times 10^{-16} \text{ cm}^2$  while at 500 eV the total range of cross sections is between 5 and  $30 \times 10^{-16} \text{ cm}^2$ . It is interesting to note in this regard, that  $\text{H}^+$  and  $\text{O}^+$  (see Fig. 1) which have similar ionization potentials, have cross section curves that are essentially the same.

The explanation for the similarity in the magnitude of the cross sections for all species in Fig. 1 and 2 probably arises due to the multiplicity of states in which the iron ion may be formed by the charge transfer process. Previous studies of charge transfer with metal atoms in this laboratory<sup>4-6</sup> have shown that only for cases of very near resonance are the cross sections large at low energies. That is, in cases where formation of the product particles in specific states can result in a small energy defect, the cross section is large. Iron, with its multitude of excited ion states allows a near resonance situation to exist for all the reactions shown in Figs. 1 and 2. Near resonance can, in some cases, also arise when the resultant neutral particle is left in an excited state. In our experiment, the state of excitation of the products could not be determined.

The cross section curves for the reaction of iron with  $\text{H}_3\text{O}^+$  (see Fig. 3) differ from those discussed above. The charge transfer process leading to production of the neutral product  $\text{H}_2\text{O}$  and  $\text{H}$  can be seen from the figure to reach a maximum at about 7 eV ion energy and then decrease to lower energies. Such behavior is indicative of a non-resonant process.

The recombination energy of  $\text{H}_2\text{O}^+$  is thought to be about 7 eV<sup>7</sup> and the reaction is therefore endothermic by about 0.87 eV. The cross section curve is therefore what would be expected in this case.

The proton-transfer cross section shown in Fig. 3 decreases rapidly with increasing ion energy over the whole range considered. This behavior is what would be expected for an exothermic ion-molecule reaction. The excess energy for this reaction can come from the  $\text{FeH}^+$  bond formed. As a consequence, when one considers both the charge transfer and proton transfer processes, it can be seen that a large cross section for destruction of  $\text{H}_3\text{O}^+$  exist over the entire energy range studies.

The effects of long-lived excited states in the primary ion beam were investigated for cases where these species are known to exist ( $\text{O}^+$ ,  $\text{O}_2^+$  and  $\text{NO}^+$ ). In all cases very little change was observed in the cross section curve when excited states were introduced into the primary ion beam. The relative independence of the cross section on the state of excitation of the incident ion is not surprising since the multitude of states available in the iron ion makes near resonance possible for these species also.

Considerable interest in charge transfer cross sections for the energy range from thermal to 1 or 2 eV exists. Our measurements cover only the top end of the range. In order to obtain values for lower interaction energies an extrapolation procedure has been developed. This procedure, which is described fully in another publication<sup>8</sup> has been used to extend the iron charge transfer cross sections to lower energies.

The extrapolation procedure operates on the assumption that the relative abundance of the various products emerging from the reaction stays constant over the total energy range from thermal to 500 eV. Failure of this condition invalidates the rate coefficients obtained at low energies from the calculation. In general, whether or not the extrapolation procedure is valid can be seen by observing if the calculated cross section fits the

experimental data to the lowest energy of measurement. In this regard, we arbitrarily have set an average limit on this deviation of  $\pm 10\%$  for the fit of the experimental and calculated cross sections over the lowest measured energy points. We also require that no deviations larger than this occur over the intermediate energy range between the lowest energy points and the high energy region where the calculation is normalized to the measured cross sections. Results for the charge transfer reactions between iron and the ions studied for which the extrapolation is valid are given in Table I. Both cross sections and rate coefficients are given.

#### ACKNOWLEDGEMENT

The authors would like to thank Dr. R. H. Neynaber for his continuing contributions to the research and for his comments on the manuscript.

TABLE I. Calculated Cross Sections and Rate Coefficients

| Reaction                           | 300°K                                   |                                                              |                                         | 600°K                                                        |                                         |                                                              | 1200°K                                  |                                                              |                                                              |
|------------------------------------|-----------------------------------------|--------------------------------------------------------------|-----------------------------------------|--------------------------------------------------------------|-----------------------------------------|--------------------------------------------------------------|-----------------------------------------|--------------------------------------------------------------|--------------------------------------------------------------|
|                                    | Cross Section<br>$10^{15} \text{ cm}^2$ | Rate Coefficient<br>$\times 10^{10} \text{ cm}^3/\text{sec}$ | Cross Section<br>$10^{15} \text{ cm}^2$ | Rate Coefficient<br>$\times 10^{10} \text{ cm}^3/\text{sec}$ | Cross Section<br>$10^{15} \text{ cm}^2$ | Rate Coefficient<br>$\times 10^{10} \text{ cm}^3/\text{sec}$ | Cross Section<br>$10^{15} \text{ cm}^2$ | Rate Coefficient<br>$\times 10^{10} \text{ cm}^3/\text{sec}$ | Rate Coefficient<br>$\times 10^{10} \text{ cm}^3/\text{sec}$ |
| $\text{H}^+ + \text{Fe}$           | 26.6                                    | 73.5                                                         | 13.7                                    | 53.4                                                         | 7.19                                    | 39.7                                                         |                                         |                                                              |                                                              |
| $\text{N}^+ + \text{Fe}$           | 18.0                                    | 14.7                                                         | 9.92                                    | 11.4                                                         | 5.79                                    | 9.46                                                         |                                         |                                                              |                                                              |
| $\text{O}^+ + \text{Fe}$           | 37.8                                    | 29.4                                                         | 20.2                                    | 22.2                                                         | 11.0                                    | 17.1                                                         |                                         |                                                              |                                                              |
| $\text{N}_2^+ + \text{Fe}$         | 6.78                                    | 4.29                                                         | 4.05                                    | 3.63                                                         | 3.02                                    | 3.83                                                         |                                         |                                                              |                                                              |
| $\text{NO}^+ + \text{Fe}$          | 14.8                                    | 9.16                                                         | 8.48                                    | 7.42                                                         | 5.35                                    | 6.61                                                         |                                         |                                                              |                                                              |
| $\text{O}_2^+ + \text{Fe}$         | 18.8                                    | 11.4                                                         | 11.5                                    | 9.87                                                         | 7.46                                    | 9.05                                                         |                                         |                                                              |                                                              |
| $\text{H}_2\text{O}^+ + \text{Fe}$ | 20.4                                    | 15.1                                                         | 13.2                                    | 13.8                                                         | 9.07                                    | 1.34                                                         |                                         |                                                              |                                                              |

## REFERENCES

1. R. S. Narcisi and A. D. Bailey, *J. Geophys. Res.* 70, 3670 (1965).
2. W. Swider, Jr., *Planet. Space Sci.* 17, 1233 (1969).
3. C. E. Moore, *Nat. Std. Ref. Data Ser.*, Nat. Bur. Stds. (US), 34, 1970.
4. J. A. Rutherford, R. F. Mathis, B. R. Turner and D. A. Vroom, *J. Chem. Phys.* 55, 3785 (1971).
5. J. A. Rutherford, R. F. Mathis, B. R. Turner and D. A. Vroom, *J. Chem. Phys.* 56, 4654 (1972).
6. J. A. Rutherford, R. F. Mathis, B. R. Turner, and D. A. Vroom, submitted for publication in *J. Chem. Phys.*
7. B. R. Turner and J. A. Rutherford, *J. Geophys. Res.* 73, 6751 (1968).
8. F. A. Wolf and B. R. Turner, *J. Chem. Phys.* 48, 4226 (1968).



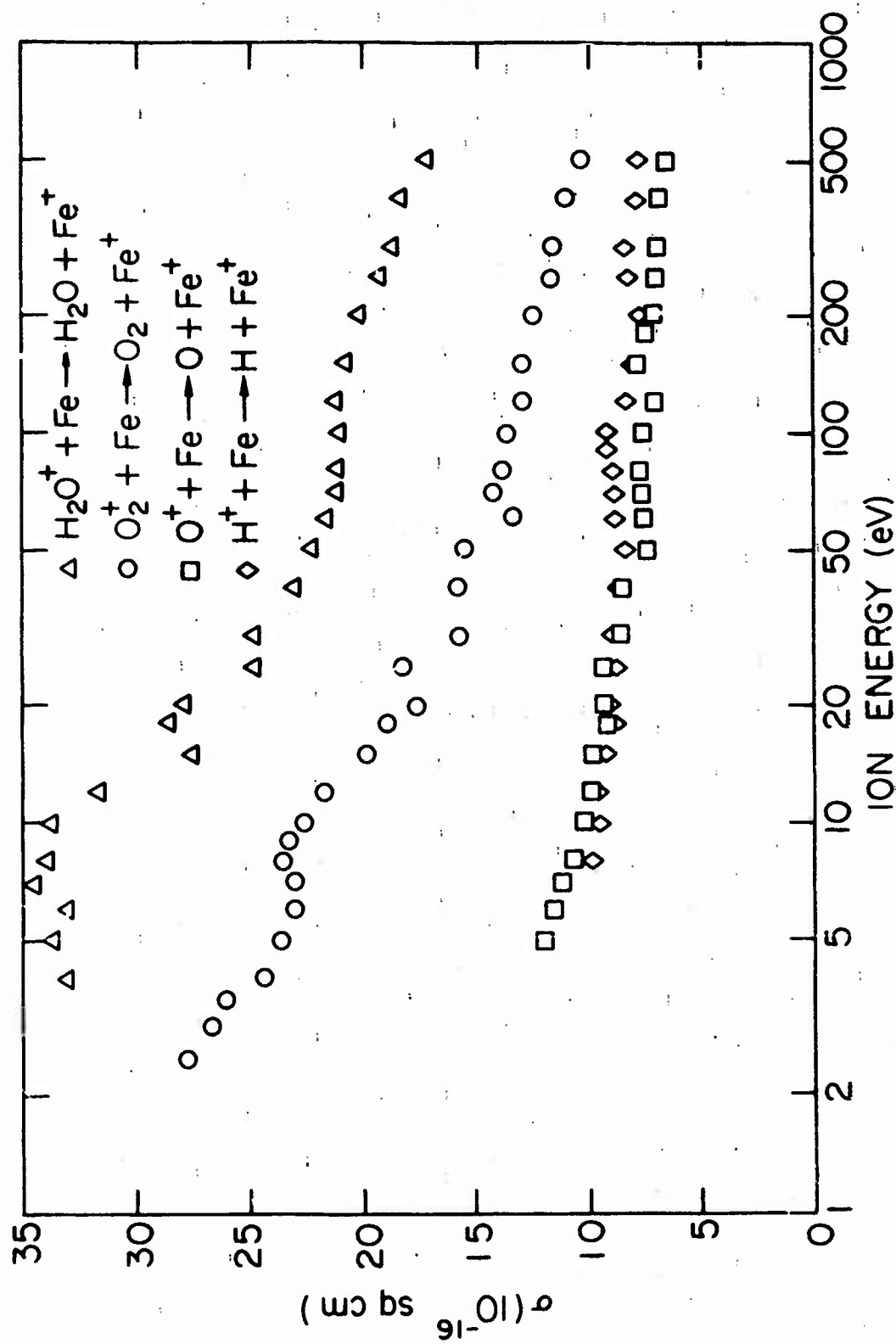


Figure 1. Charge-transfer cross sections for  $\text{H}_2\text{O}^+$ ,  $\text{O}_2^+$ ,  $\text{O}^+$ , and  $\text{H}^+$  ions impinging on neutral iron as a function of the energy of the incident ion.

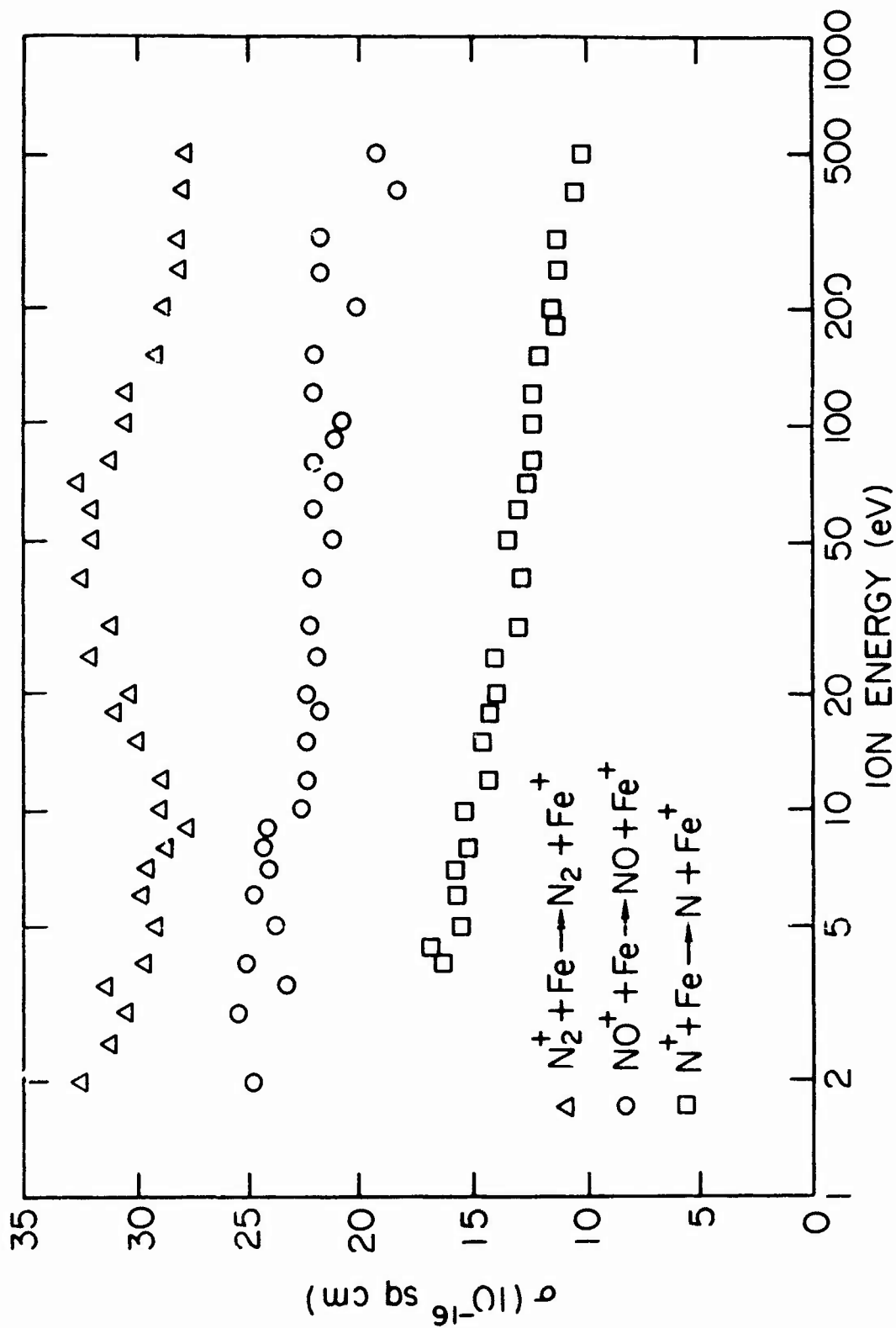


Figure 2. Charge-transfer cross sections for  $N_2^+$ ,  $NO^+$ , and  $N^+$  ions impinging on neutral iron as a function of the energy of the incident ion.

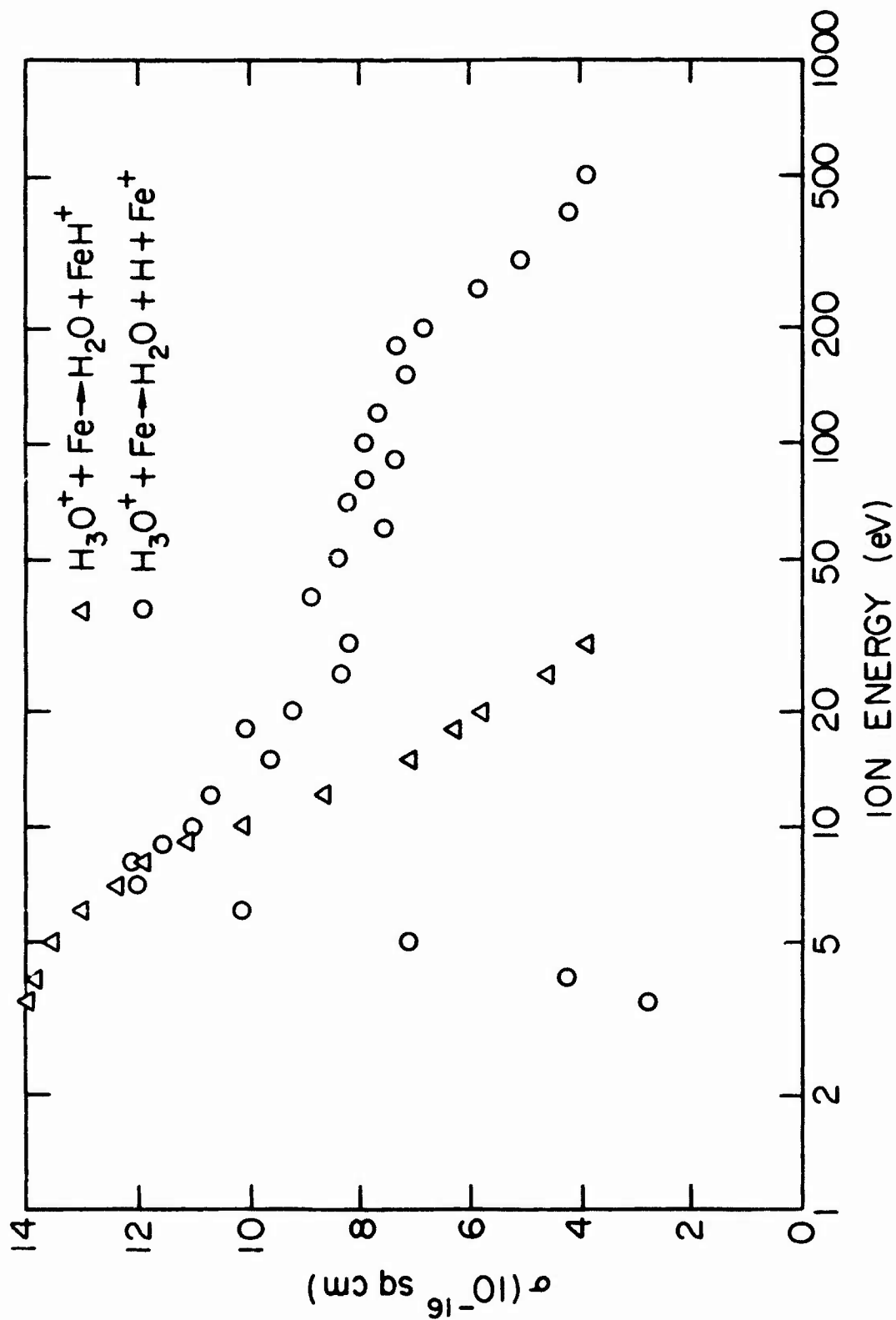


Figure 3. Charge-transfer and proton-transfer cross sections for  $\text{H}_3\text{O}^+$  ions impinging on neutral iron as a function of the energy of the incident ion.

**APPENDIX F**  
**NEGATIVE ION REACTIONS WITH NEUTRAL OZONE**

**Preceding page blank**

## NEGATIVE ION REACTIONS WITH NEUTRAL OZONE\*

J. A. Rutherford, B. R. Turner, and D. A. Vroom

Gulf Radiation Technology  
A Division of Gulf Energy & Environmental Systems  
San Diego, California 92112

### ABSTRACT

Charge transfer reactions between  $O^-$ ,  $O_2^-$ ,  $OH^-$  and  $NO_2^-$  and  $O_3$  have been studied to obtain cross sections for formation of  $O_3^-$ . The energy range of the ions extended from 1 eV - 500 eV. The accepted value for the electron affinity of  $O_3$  has been checked by looking at the above charge transfer process as well as  $F^-$ ,  $Cl^-$ , and  $CO_3^-$  with  $O_3$ . The results show that the electron affinity of  $O_3$  must be close to accepted value of approximately 2 eV. A further result of this study is that the electron affinity of  $NO_2$  must be similar to that of  $O_3$ .

Preceding page blank

---

\*This work was supported by the Defense Nuclear Agency under Contract No. DASA01-69-C-0044.

## INTRODUCTION

Ozone is known to be an important constituent of the lower atmosphere and, as a consequence, its chemistry is of interest. One aspect of the problem is the conjecture that the negative ion of this species is an important intermediate in the formation of long-lived negative ions in the D region.<sup>1</sup> Previous investigations of reactions of ions with this species have been restricted to thermal energy studies with  $O^-$  and  $O_2^-$  using flowing afterglow techniques.<sup>2</sup> The study of negative ion reactions is always hampered by the lack of knowledge of the electron affinity of many of the species. One aspect of the present study has been to try and establish with more reliability these important constants.

The present investigation has also pointed out the importance of near resonance in low energy negative ion charge transfer processes. As in previous studies<sup>3,4</sup> using positive ions the results obtained indicate that unless a reaction channel which allows all the excess energy in the reaction to be absorbed by the products the charge transfer cross section will be small at low energies.

## APPARATUS

A detailed description of the apparatus in the configuration employed for positive ion-neutral metal vapor charge transfer reactions has been given in a previous publication.<sup>3</sup> The reactions investigated here involve

the formation of negative ions. In general the only apparatus changes required for such studies are a reversal of the magnetic and electric fields employed. The major experimental modification here was the construction of an ozone generator capable of producing pure ozone and the installation of a sample handling system which did not lead to decomposition of this unstable species. The generation and handling system will be described in detail after a brief outline of the apparatus.

The instrument consists of tandem mass spectrometers with the neutral beam interposed at right angles. Primary ions are generated by electron impact in the ion source of the first mass spectrometer, a 180-deg magnetic sector. After mass analysis, the primary ions are accelerated or retarded to the desired interaction energy and allowed to interact with the neutral beam. Product ions formed due to reaction between the primary ions and the neutral beam are extracted from the interaction region along the direction of the primary beam by a weak electric field. Collection efficiencies of about 70% are usually obtained. These ions are then accelerated, focused and mass analyzed in a 60-deg magnetic sector, and finally detected with a Be-Cu electron multiplier. The neutral beam effuses from a small hole in a room-temperature iridium tube located in a separately pumped chamber of the apparatus. The beam passes from this source chamber, through an intermediate chamber which serves to collimate the beam and into the experimental region. There it is mechanically chopped and allowed to interact with the primary ion beam. The modulation of the

neutral beam allows selective amplification and phase-sensitive detection.

The neutral beam density is determined from the pressure of ozone in the tube, and the geometry of the apparatus. The ozone pressure was determined using a differential pressure measurement. This method which assures that the pressure measured is that at the point of effusion from the tube, requires that the gas be pure. As is shown below, our beam was composed of pure  $O_3$ .

Ozone was produced using an electric discharge in a low-pressure flow of pure oxygen. A schematic representation of the generation system which is similar to that employed by Griggs and Kaye<sup>5</sup> is given in Fig. 1. Pure oxygen (Linde ultrahigh purity dry) at a pressure of about 0.1 Torr flowed from a leak valve through a stainless steel tube and into a liquid-nitrogen-cooled glass U-tube. This U-tube had a collector protruding from the bottom to accumulate the liquid ozone. The U-tube was connected to a silica-gel filled ozone storage container, also constructed of glass. The connection between the U-tube and the storage container is made using stainless steel fittings. The ac potential required to produce the discharge in the U-tube was applied using a neon sign transformer between this fitting and ground potential (stainless steel inlet tube and fitting used for connecting the U-tube and inlet).

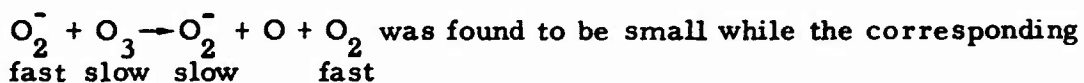
Ozone trapped at the bottom of the U-tube was allowed to collect until a sufficient supply for a day's experiments was obtained. The discharge and oxygen flow were then terminated and, after evacuation of system, the U-tube



warmed to room temperature. During the warming period, the ozone vaporized and transferred to the dry-ice-cooled silica gel in the storage container.<sup>6</sup> The ozone was stored until needed in the cooled silica gel. To obtain ozone at a pressure sufficient to produce an adequate beam in the crossed beam apparatus, the silica gel was warmed slightly by replacing the dry ice with an alcohol slush bath. Ozone from the storage container was allowed into the neutral beam source through a stainless steel leak valve and stainless steel tube.

Care was taken to keep impurities in the ozone beam to a minimum. Apart from the use of pure O<sub>2</sub> gas for formation of ozone, the generation system including the silica gel storage vessel was pumped and outgassed before the oxygen discharge was initiated. After sufficient ozone was formed, the generator was again pumped to remove any excess O<sub>2</sub>. This last operation was performed prior to transfer of the ozone to the silica gel.

To test the purity of the ozone prepared in this manner, the resultant beam was probed using O<sub>2</sub><sup>-</sup> ions. The cross section for the reaction



was found to be small while the corresponding process  $\underset{\text{fast}}{\text{O}_2^-} + \underset{\text{slow}}{\text{O}_2} \rightarrow \underset{\text{fast}}{\text{O}_2} + \underset{\text{slow}}{\text{O}_2^-}$  is known to be large. Fast O<sub>2</sub><sup>-</sup> ions crossing our ozone beam did not produce an appreciable quantity of slow O<sub>2</sub><sup>-</sup> ions.

Since O<sub>2</sub> is the most probable impurity in our ozone beam, the dearth of O<sub>2</sub><sup>-</sup> ions produced in the above reaction indicates an absence of this species.

## RESULTS

Reactions of ozone with  $O^-$ ,  $O_2^-$ ,  $OH^-$ ,  $NO_2^-$ ,  $F^-$ ,  $Cl^-$ ,  $O_3^-$  and  $CO_3^-$  have been investigated. Those processes which were found to have readily measurable cross sections have been studied in detail while for those for which the reaction probability is small, only upper limits on the cross sections are given.

The ions for which reactions with ozone have been studied in detail are  $O^-$ ,  $O_2^-$ ,  $OH^-$  and  $NO_2^-$ . In all cases the major reaction channel is non-dissociative charge transfer to form  $O_3^-$ . The cross section data obtained for the first three of these reactions are given in Fig. 2 while those for  $NO_2^-$  on ozone are presented in Fig. 3.

The symmetric charge transfer reaction  $O_3^-$  on  $O_3$  has only been studied at high interaction energies. Experimental limitations, arising from the inability of our secondary mass spectrometer to distinguish between fast primary and slow secondary  $O_3^-$ , prevented low-energy values being obtained. The resonant charge transfer cross section was found to vary between 6 and  $4 \times 10^{-16} \text{ cm}^2$  in the range between 150 and 400 eV.

The upper limits for charge transfer reactions of the ions  $F^-$ ,  $Cl^-$  and  $CO_3^-$  with ozone are given in Table I.

The charge exchange cross section for the process  $O_3^- + NO_2 \rightarrow O_3 + NO_2^-$  was remeasured here. The results which agree with our previous measurements<sup>7</sup> are given in Fig. 3.

The nature of the errors present in our experiment have been discussed previously.<sup>3</sup> The magnitude of the error in absolute cross sections given here depend upon the species being studied. For  $O^-$ ,  $O_2^-$ ,  $OH^-$  and  $O_3^-$  charge exchange with ozone, the possible error on the values reported are  $\pm 25\%$  at impact energies above 30 eV and may increase to as much as  $\pm 40\%$  at the lowest ion energies. For  $F^-$ ,  $Cl^-$  and  $CO_3^-$  charge exchange with ozone, only upper limits on the cross section are given. For these measurements the primary beams of  $F^-$ ,  $Cl^-$  and  $CO_3^-$  used were small, and no detectable signal could be found at only impact energy. The actual cross sections for these charge exchange processes may be much lower than the upper limits given.

For  $NO_2^-$  charge transfer with neutral ozone and the reverse reaction of  $O_3^-$  on  $NO_2$ , experimental difficulties were encountered due to the similarity in mass of the primary and secondary ions ( $NO_2^-$  is 46 amu and  $O_3^-$  48 amu). In our apparatus, the secondary ions are extracted in the same direction as the primary ions and both beams therefore enter the secondary mass spectrometer. These two beams will have, in general, different masses and different energies (i.e., the primary ions will have the energy with which they passed through the collision region plus the energy due to the accelerating lenses after the collision region, while the secondary ions have only the energy due to the accelerating region). Under these conditions if the primary ion has a mass similar to but slightly less than that of the secondary ion, there will be a range of primary ion energies

when both the primary ion and the secondary ions are in focus in the secondary mass spectrometer. Under these conditions the DC signal due to the primary ion beam overloads the amplifier system to such an extent that the secondary ion signal cannot be measured. This situation occurs for the reaction of  $\text{NO}_2^-$  on  $\text{O}_3$  in the primary ion energy range from 10 to 100 eV. For  $\text{O}_3^-$  on  $\text{NO}_2$ , a related but less severe problem occurs in the ion energy range from 12 to 30 eV. Here, the resolution of the primary mass spectrometer is such that above 12 eV a small amount of  $\text{NO}_2^-$  is present in the  $\text{O}_3^-$  beam making measurement impossible up to an energy of 30 eV where the secondary mass spectrometer is able to separate the fast from the slow  $\text{NO}_2^-$  particles. The amount of  $\text{NO}_2^-$  present in the primary ion beam above 12 eV is large compared to the secondary ion signal but is very small compared to the  $\text{O}_3^-$  and as a consequence does not interfere with measurement of the  $\text{O}_3^-$  charge transfer with  $\text{NO}_2$ .

## DISCUSSION

Table II lists the electron affinities used to calculate the energetics of the reactions studied. The electron affinity of  $\text{O}_3$  is listed at 1.9 eV. This value which was first obtained by Wood and D'Orazio<sup>8</sup> is in good agreement with the recent photodetachment value of 2.09 eV given by Sinnott and Beaty<sup>9</sup> but is lower than earlier accepted values which placed this constant at about 3 eV.<sup>10</sup> The choice of approximately 2 for the electron affinity of  $\text{O}_3$  can be justified by considering the magnitude of

the charge transfer cross sections measured here for reactions where the other component has a known electron affinity.

A possible reason for the uncertainty which has existed and still in some instances does exist concerning the value of the adiabatic electron affinity of species such as  $O_3$  and  $NO_2$  may be that triatomic molecules can undergo changes in geometry between the negative ion and neutral ground state. A significant change in geometry can lead to a vertical electron affinity which is appreciably higher than the adiabatic value since the product will be formed in a high vibrational level. In many cases, earlier experimental values reported for electron affinities have been high and have tended to become lower as measurements have improved. The values for the molecular species listed in Table II are the currently accepted values and, in general, tend to be lower than those reported in earlier publications.

If changes in geometry take place when going from the neutral to negative ion of such a molecule as  $O_3$ , they would tend to lower the symmetric charge transfer cross section. The cross section values measured for  $O_3^-$  on  $O_3$  here are lower than one would normally expect for symmetric charge transfer between two atomic species where geometry is not a consideration.  $H^- + H$  has a cross section of approximately  $4 \times 10^{-15} \text{ cm}^2$  at 200 eV as opposed to approximately  $4 \times 10^{-16} \text{ cm}^2$  for  $O_3^-$  on  $O_3$ . The structure of  $O_3$  in the gas phase is known with considerable accuracy the 0-0-0 bond angle being  $116^\circ 47' \pm 2'$ .<sup>15</sup> For the negative ion, the bond angle

is less well known, the value being predicted to be  $110^\circ \pm 5^\circ$  by Smith.<sup>16</sup>

This prediction has been supported by the solid phase ESR results of Tagaya and Takeshi.<sup>17</sup> The low value of the  $O_3^-$  on  $O_3$  cross section obtained here may indicate the difference in angle may be greater than  $6^\circ$  but may also be the result of the fact that the  $O_3^-$  primary ion is formed in high vibrational levels which would tend to make this cross section smaller than one would expect for a resonant process.

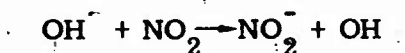
In Fig. 2, the data for the three species in Table II which have electron affinities lower than that of  $O_3$ , namely,  $O^-$ ,  $O_2^-$  and  $OH^-$ , are presented. All three cross sections are large, the one for  $OH^-$  on  $O_3$  being the largest. This latter case has the closest energy balance (see Table II). All three reactions are exothermic and it is probable that the excess energy in the reactions may be absorbed into vibrational energy of the products. For  $O_2^-$  on ozone the excess energy is approximately 1.5 eV which is equal to the  $O_3^-$  bond energy ( $D_0(O_2-O^-) = 1.5$  eV).<sup>11</sup> Here the energy may be taken up by vibrationally excitation of both the  $O_2$  and  $O_3^-$  products or partially by formation of the  $O_2$  in the excited ( $a^1\Delta_g$ ). This latter state lies 0.98 eV above the neutral ground state.

For the reactions  $O^- + O_3$  and  $O_2^- + O_3$ , thermal energy values of the rate coefficients have been measured previously.<sup>2</sup> The measured points are included in our figure and a smooth interpolation of our data to these results is shown. For  $OH^- + O_3$ , no thermal energy values has been determined. The extension of our data was made using the extrapolation procedure

previously employed.<sup>12</sup> It is of interest to note that for  $O^- + O_3$  and  $O_2^- + O_3$  the extrapolation procedure gave thermal energy rate constants that were higher by approximately a factor of 2 compared to the measured values shown in the figure.

The electron affinities of  $F^-$  and  $Cl^-$  are greater than that for  $O_3$  and as a consequence the processes are endothermic. The cross sections for charge exchange with these species is therefore small as indicated in Table I.

The reaction of  $NO_2^-$  with  $O_3$  is of interest since the electron affinity of  $NO_2$  is in doubt. Fehsenfeld et al. have established that the  $NO_2$  electron affinity should be greater than 1.8 eV since the reaction



is known to proceed at thermal energies with a large rate coefficient.<sup>13</sup>

Our results here indicate that the electron affinity of this species must be close to that of ozone since both the forward and reverse negative reactions with these two species are found to proceed (see Fig. 3) with nearly equal cross section at the lowest energies measured.

In the above reactions, the cross sections are seen to be appreciable when the reaction is exothermic. The largest cross section at low energies is for the  $OH^-$  on  $O_3$  which has the smallest energy defect. This result is consistent with previous positive ion charge transfer<sup>3,4</sup> reactions which show that if near energy resonance exists, the process proceeds with a high probability.

## REFERENCES

1. E. E. Ferguson, Rev. of Geophys. 5, 305 (1967).
2. F. C. Fehsenfeld, A. L. Schmeltekopf, H. I. Schiff, and E. E. Ferguson, Planet. Space Sci. 15, 373 (1967).
3. J. A. Rutherford, R. F. Mathis, B. R. Turner and D. A. Vroom, J. Chem. Phys. 55, 3785 (1971).
4. J. A. Rutherford, R. F. Mathis, B. R. Turner, and D. A. Vroom, J. Chem. Phys., May 1, 1972.
5. M. Griggs and S. Kaye, Rev. Sci. Instr. 39, 1658 (1968).
6. H. I. Schiff, private communication.
7. J. A. Rutherford and B. R. Turner, J. Geophys. Res. 72, 3795 (1967).
8. R. H. Wood and L. A. D'Orazio, J. Phys. Chem. 69, 2562 (1965).
9. G. Sinnott and E. C. Beaty, in the "Abstracts of Papers of the VIIth International Conference on the Physics of Electronic and Atomic Collisions," Amsterdam, July, 1971, North Holland Publishing Co., p. 176.
10. See, for example, R. C. Curran, J. Chem. Phys. 35, 1849 (1961), H. O. Pritchard, Chem. Rev. 52, 529 (1953), and N. S. Buchel'nikova Usp. fiz. nauk. 65, 531 (1958).
11. F. R. Gilmore, "Basic Energy-Level and Equilibrium Data for Atmospheric Atoms and Molecules," Rand Corp. Memorandum RM-5201-ARPA, March 1967.
12. F. A. Wolf, and B. R. Turner, J. Chem. Phys. 48, 4226 (1968).
13. F. C. Fehsenfeld, E. E. Ferguson and D. K. Bohme, Planet. Space Sci. 17, 1759 (1969).
14. D. G. Hummer, R. F. Stebbings and W. L. Fite, Phys. Rev. 119, 668 (1960).



REFERENCES (contd)

15. T. Tanaka and Y. Morino, J. Mol. Spectrosc. 33, 538 (1970).
16. P. Smith, J. Phys. Chem. 60, 1471 (1956).
17. K. Tagaya and M. Takeshi, J. Phys. Soc. Japan 23, 70 (1967).

TABLE I

Cross section upper limits for some negative ion  
charge transfer reactions with ozone in the  
impact energy range from 1 to 10 eV.

| Reaction                                    | Cross section<br>upper limit<br>(cm <sup>2</sup> ) |
|---------------------------------------------|----------------------------------------------------|
| $F^- + O_3 \rightarrow F + O_3^-$           | $2 \times 10^{-17}$                                |
| $Cl^- + O_3 \rightarrow Cl + O_3^-$         | $2 \times 10^{-17}$                                |
| $CO_3^- + O_3 \rightarrow CO_2 + O + O_3^-$ | $2 \times 10^{-16}$                                |

TABLE II

Electron affinities of the atoms and molecules studied.

| <u>Species</u>  | <u>Electron Affinity<br/>(eV)</u> |
|-----------------|-----------------------------------|
| O               | 1.478 <sup>a</sup>                |
| F               | 3.5 <sup>b</sup>                  |
| Cl              | 3.7 <sup>b</sup>                  |
| OH              | 1.83 <sup>c</sup>                 |
| O <sub>2</sub>  | 0.43 <sup>d</sup>                 |
| NO <sub>2</sub> | ~2.0 <sup>e</sup>                 |
| O <sub>3</sub>  | 1.9 <sup>f</sup>                  |

<sup>a</sup>R. S. Berry, J. E. Mackie, R. L. Taylor, and R. Lynch.  
J. Chem. Phys. 43, 3067 (1965).

<sup>b</sup>"Bond Energies, Ionization Potentials and Electron Affinities,"  
V. I. Vedeneyev, L. V. Gurvich, V. N. Kondrat'yev, V. A.  
Medvedev and Ye. L. Frankevich, eds., St. Marten's Press,  
New York (1966).

<sup>c</sup>L. M. Branscomb, Phys. Rev. 148, 11 (1966).

<sup>d</sup>R. Celotta, R. Bennett, J. Hall, J. Levine, and M. W.  
Siegel, Bull. Am. Phys. Soc. 16, 212 (1971).

<sup>e</sup>This work.

<sup>f</sup>Ref. 8.

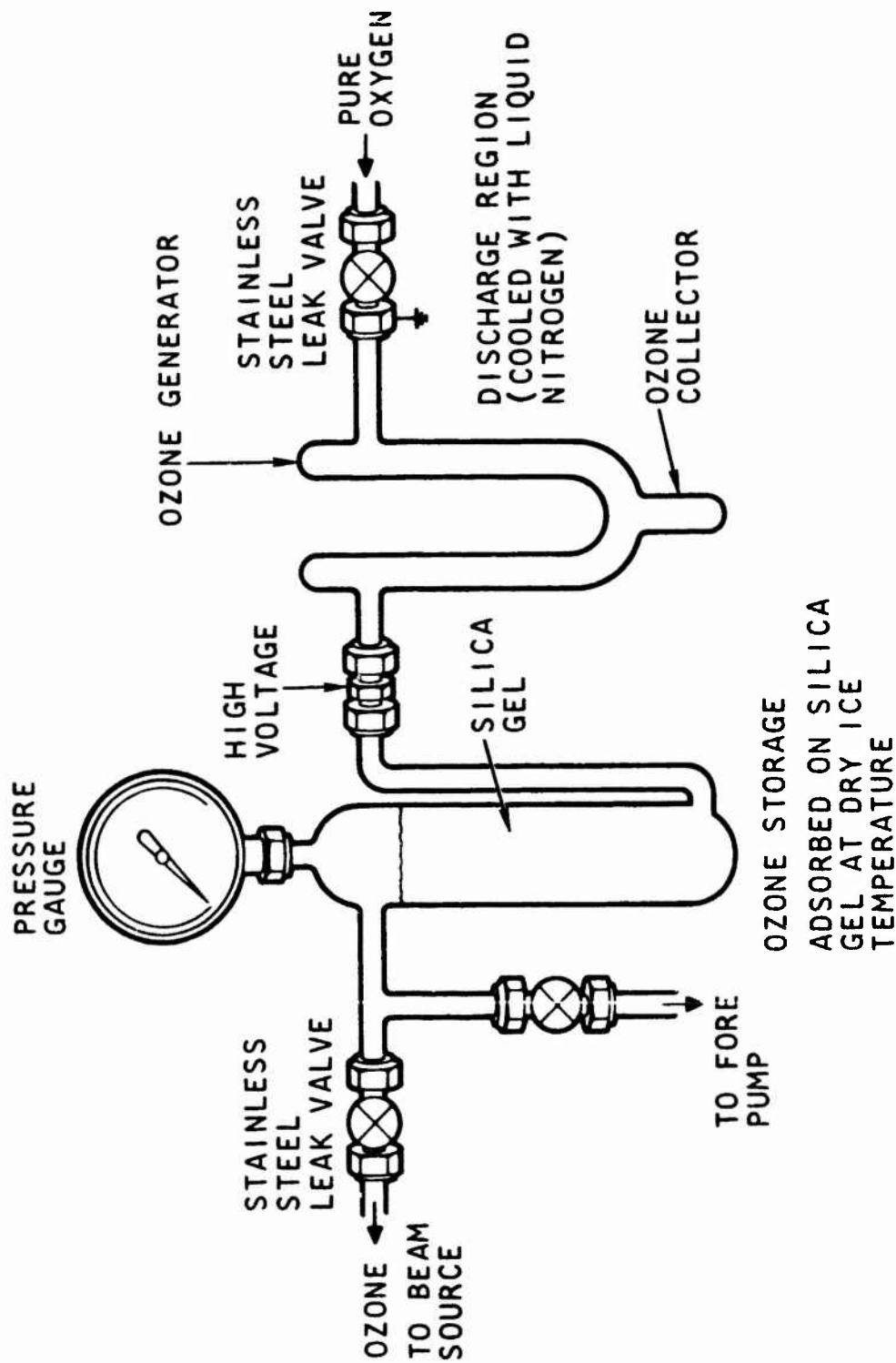


Figure 1. Ozone generator.

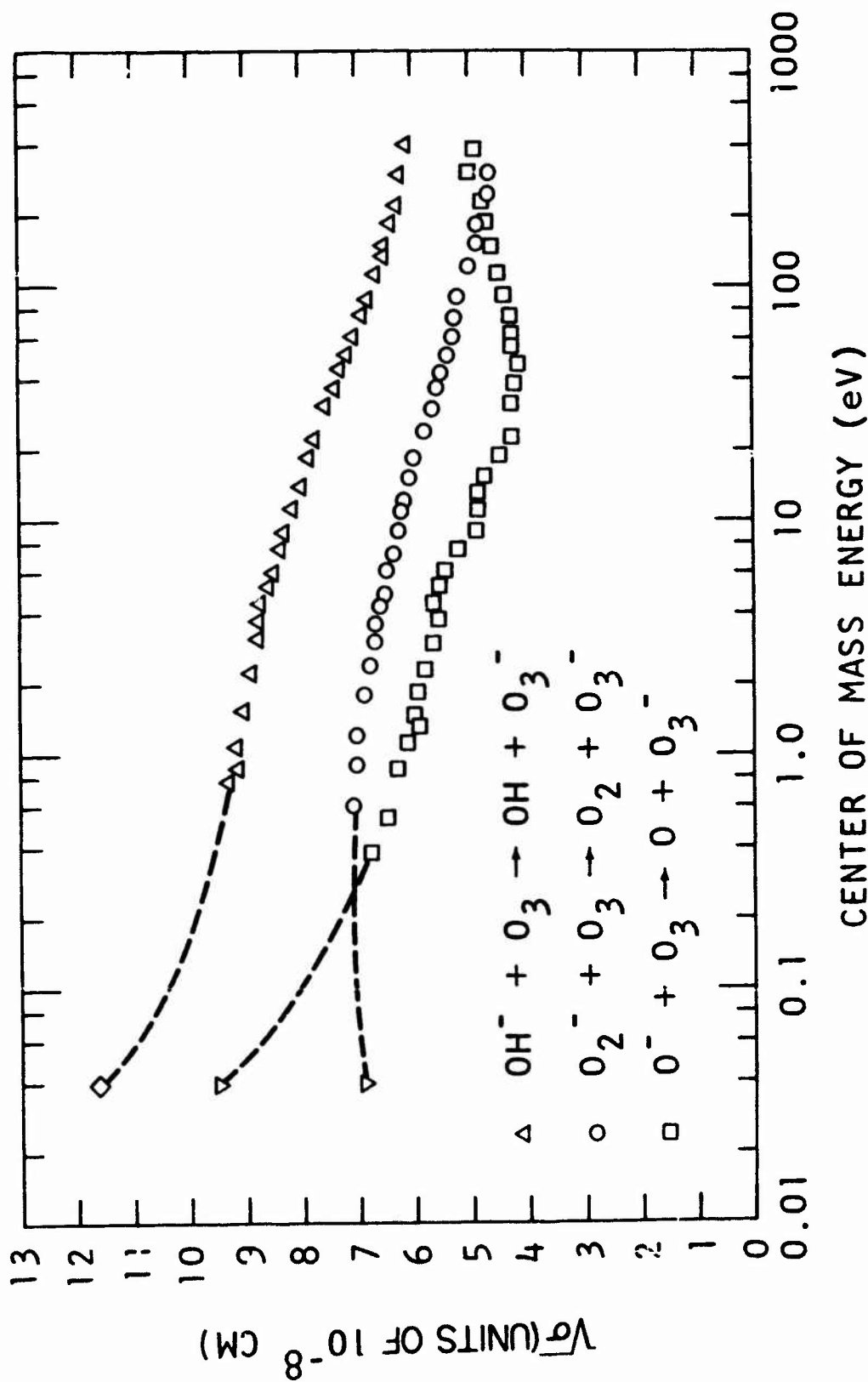


Figure 2. Square root of the cross sections for the indicated reactions for  $\text{OH}^-$ ,  $\text{O}_2^-$ , and  $\text{O}^-$  impinging on neutral as a function of the center of mass energy. The measured data for  $\text{OH}^-$  have been extended to thermal energies using an extrapolation technique. The thermal energy rate coefficient for  $\text{OH}^-$  ( $\diamond$ ) is  $1.1 \times 10^{-9} \text{ cm}^3 \text{ sec}^{-1}$ . For  $\text{O}_2^-$  and  $\text{O}^-$ , the thermal rate coefficients of reference 2 are shown ( $\nabla$ ). These values are  $3 \times 10^{-10} \text{ cm}^3 \text{ sec}^{-1}$  for  $\text{O}_2$  and  $7 \times 10^{-10}$  for  $\text{O}^-$ . A smooth extension of our data to the equivalent thermal cross sections is given.

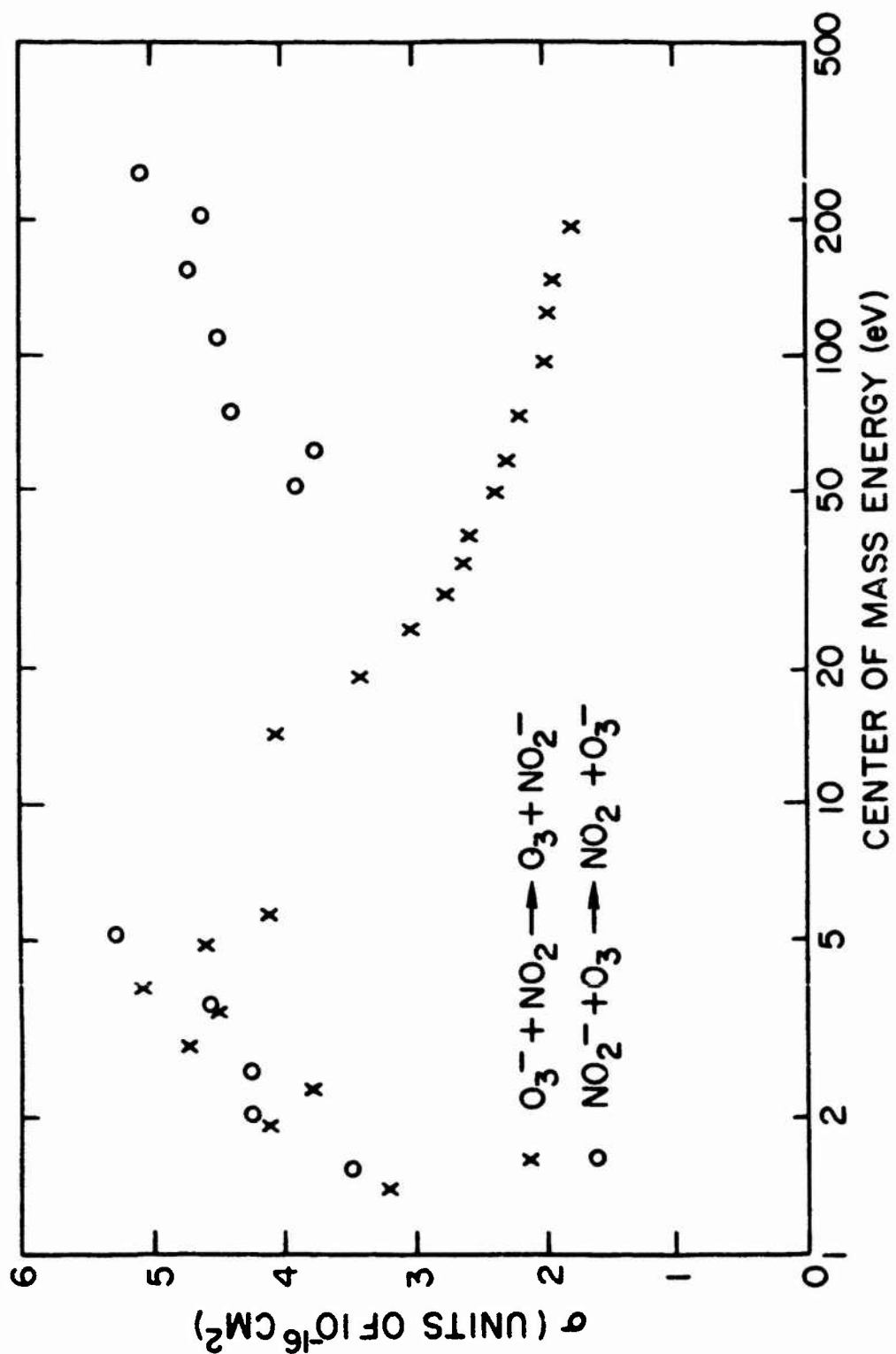


Figure 3. Cross sections for the indicated reactions between  $\text{NO}_2$  and  $\text{O}_3$  and their negative ions as function of the center of mass energy.